APPLICATION OF
ECCENTRICITY CONCEPT
TO
MULTISTORY BUILDINGS

By

© VICTOR WAI-TO CHEUNG, B.A.Sc., M.A.Sc.

A Thesis

Submitted to the School of Graduate Studies

in Partial Fulfilment of the Requirements

for the Degree

Doctor of Philosophy

McMaster University

September 1986

ISBN 0-315-35873-4

ECCENTRICITY CONCEPT FOR MULTISTORY BUILDINGS

DOCTOR OF PHILOSOPHY (1986)
(Civil Engineering and
Engineering Mechanics)

McMaster University
Hamilton, Ontario

TITLE: Application of Eccentricity Concept to Multistory Buildings

AUTHOR: Victor Wai-To Cheung

B.A.Sc. (University of Toronto)

M.A.Sc. (University of Toronto)

SUPERVISOR: Dr. W. K. Tso

NUMBER OF PAGES: xii, 222

ABSTRACT

This thesis presents a study in extending the eccentricity concept to multistory buildings to evaluate their torsional behaviour under static and dynamic lateral loads. The eccentricity concept enables the separation of horizontal loadings into lateral and torsional components thereby enhancing the understanding of the structural behaviour of multistory buildings.

To acheive this, formal definition for the center of rigidity is established for eccentric and irregular multistory buildings in general. The centers of rigidity are shown to be load centers at the floors and they should be reference points from which eccentricities are measured. A procedure is given to locate the rigidity centers with the aid of a plane frame program.

The centers of twist are then defined. They are convenient points of reference for the generalized floor displacements and will lead to uncoupled equations of lateral and torsional equilibrium. The centers of rigidity and centers of twist are in general load dependent and not the same set of points for multistory buildings. Only for buildings with proportional framing that they become the same set of points.

A method for lateral load analysis of symmetric and eccentric setback structures is presented next. The eccentricity concept and the displacement compatible load concept are employed by the proposed method. This is a non-trivial application of the eccentricity concept in analysis of irregular multistory buildings.

Finally, an analytical investigation into the static and dynamic behaviour of uniform eccentric wall-frame buildings is carried out to examine the complexities of wall-frame interaction under eccentric loadings. A class of uniform eccentric wall-frame buildings had been identified which will have centers of rigidity along a vertical line, thereby satisfied the seismic provision requirement of NBCC 1985. The adequacy of the code procedures is evaluated for this class of structures. It is shown that for other classes of eccentric wall-frame multistory buildings, it is difficult to apply the concept of eccentricity and code procedures to obtain reasonable estimates of the torsional effect. For eccentric wall-frame structures in general, therefore, dynamic analysis remains to be the most reliable method to distribute the torsional effect at the present time.

ACKNOWLEDGEMENTS

The author wishes to express his sincere gratitude to Dr. W. K. Tso for his guidance, advice and interest during the course of this study.

Special thanks are due to Dr. A. C. Heidebrecht, Dr. F. A. Mirza and Dr. W. Weaver for their guidance and encouragement.

The author also wishes to record his appreciation to Miss Pauline Koh and Miss Connie Lam for their very skillful typing of this thesis and production of the drawings.

Particular acknowledgement is due to the Natural Sciences and Engineering Research Council for providing financial support for the research work.

TABLE OF CONTENTS

LIST OF FIGURES

LIST OF TABLES

CHAPTER 1

INTRODUCTION

1.1 General

In highrise building design, one important aspect is the ability of the building to perform in a satisfactory manner under lateral loads. These lateral loads can be caused by wind, and/or seismic ground motions. A building becomes asymmetric if there exists irregularity in geometry, or uneven distribution of stiffness or mass in the plan of the structure. For asymmetric buildings, lateral loadings will lead to torsional responses, in addition to lateral responses. Torsional responses will induce additional shear forces (torsional shears) to the lateral resisting elements of the building. Further, additional deformations and motions are also induced, the effect of which is especially pronounced at the perimeter and corners of the building. The additional torsional shears demand extra strength requirements for the lateral resisting elements. The additional deformations may cause non-structural damage to windows and curtain walls, while the additional motions may lead to human discomfort. Therefore, from a designer's point of view, asymmetry usually implies additional strength

and/or stiffness requirements for the lateral load resisting system.

Given the architectural building plan layout, it is necessary for designers to have an appreciation of the torsional load effect on the building. This enables the required strengths and stiffnesses of the different lateral resisting elements to be estimated in the preliminary design stage. The usual types of lateral resisting elements employed in highrise design are shear walls and moment resisting frames. It is also possible to combine these elements to form a resisting system, resulting in buildings commonly known as wall-frame structures.

In many seismic building codes [1,3,6,12,21,27,31,38], allowance is made for the torsional effect. The buildings are required to design for additional torques applied simultaneously with the required lateral forces. The applied torque at any floor is computed as the product of the lateral load and a quantity known as design eccentricity at that floor. The design eccentricity is in turn expressed as a function of the structural eccentricity at the particular floor. The structural eccentricity is defined as the distance between the center of rigidity at a level and the resultant of all applied lateral forces at the same level. Therefore, in order to evaluate the floor torques, it is necessary to establish the

structural eccentricities at the different floors of the eccentric building.

Two important questions come up if one adopts the building code approach to allow for the torsional effect. First, how can one in general determine the structural eccentricities, and hence the design torques as specified in the codes? This question arises since the determination of the structural eccentricities requires a knowledge of the rigidity centers of the building. However, there is no accepted procedure to locate the rigidity centers in general. The building codes leave the problem of locating the rigidity centers of a building to the discretion of the designers. Thus the eccentricity concept for torsional response computation can not readily be applied in design.

Second, the seismic load effects are often treated by building codes as sets of prescribed statically equivalent loads. So, how adequate is the quasi-static code procedures in representing the torsional effect caused by lateral loads which are dynamic in nature?

Different seismic building codes use different approaches to approximate the effect of torsion in buildings. Special attention will be paid to the torsional provisions of the National Building Code of Canada 1985 (NBCC 1985) [3].

NBCC 1985 appears to recognize the fact that the static seismic provisions can not be applied to all irregular multistory buildings [14]. . A new clause (4.1.9.24) had been introduced in NBCC 1985 which directs attention to the limitations of the applicability of the torsional provisions :

"Where the centroids of mass and centers of stiffness of the different floors do not lie approximately on vertical lines, a dynamic analysis shall be carried out to determine the torsional effects...".

The centers of stiffness as specified in clause (4.1.9.24) can be interpreted as having the same meaning as centers of rigidity in defining structural eccentricities. Thus in applying specifically the torsional provisions of NBCC 1985, a designer has to have a knowledge of the rigidity centers of the building in order to

(i) determine whether the provisions are applicable; and assuming the provisions are applicable, to

(ii) determine the structural eccentricities, thus the design eccentricities and finally the design torque at each story of the building.

It is the purpose of this research to provide answers concerning the application of the eccentricity concept to evaluate the torsional effect on multistory buildings in general. Specifically, it is concerned in (i) to provide a framework such that eccentricities in

multistory buildings are defined, (ii) to study the limitation of using the eccentricity concept in dealing with torsional problems, and (iii) to evaluate the accuracy of the Canadian torsional code provisions as applied to multistory buildings.

1.2 Review of Past Works

The torsional behaviour of buildings due to static eccentric lateral loads had been investigated in past years. The eccentricity concept as derived from the field of mechanics of elastic materials is extended for torsional analysis of multistory buildings. With the aid of the eccentricity concept, the lateral and torsional component of the applied eccentric loads can be identified.

In mechanics of materials, the eccentricity of the applied loads on an uniform section will be the distance between its shear center and the resultant load. The shear center is defined as the point when the resultant lateral load acts through will result in no twisting of the section. Its location will be a function of the geometric properties of the section and independent of the applied loadings.

Wilbur [39] first extended the eccentricity concept to the torsional analysis of eccentric regular frame buildings with orthogonal framing. The frame behaviour was modelled as a shear beam in his analysis. A paper on the

torsional behaviour of eccentric single story buildings was presented by Lin [19]. The eccentricity concept was used to analyse a single reinforced concrete story. Elastic behaviour of concrete was assumed and the structural layout was not restricted to orthogonal framing. The center of rigidity was introduced as an alternative term for the center of stiffness and since then it became a more accepted terminology in highrise design. The intermixing of the two terms "center of stiffness" and "center of rigidity" can be found in many later published materials on the topic, eg. NBCC 1985. From then on it was believed that the eccentricity concept for single story buildings can be extended directly to multistory structures without modification. Based on this belief, the rigidity centers of a multistory building are computed on a per floor basis, assuming that the effect of adjacent floors above and below is negligible. Later researchers recognized that the torsional behaviour of multistory buildings was more complicated. The complexity in the distribution of torsional effect can not be predicted by single story models in general. Poole [26] determined that the rigidity centers of multistory buildings will be in general a function of the applied loads. He suggested to identify the shear center at a story as the rigidity center. A computer

model was proposed to obtain the lateral shears in the resisting elements and use the resultant of the lateral shears at a story to provide the location of the shear center at that story. Tso [33] pointed out that in current seismic codes, difficulties arise in defining the centers of rigidity for irregular buildings. There is generally no accepted procedure for estimating the structural eccentricity quantity for multistory buildings. The same problem was also raised by Humar [16]. Humar interpreted the center of rigidity (referred to as the center of resistance in [16]) differently from the conventional concept. Conventionally, the rigidity centers are interpreted as points at floor levels, when the resultant lateral forces act through them will result in no rotational movement of all floors. Humar defined the rigidity center at a floor as the point when the resultant lateral force is applied through it, the level under consideration does not undergo any rotation. It is permitted to have twisting to occur at other floor levels. However, no formal procedure for determining the centers of rigidity was given in his discussion.

It was about fifty years ago that the idea of applying the eccentricity concept for torsional analysis of multistory buildings was initiated. However, two fundamental questions still remain unanswered. First there does not

appear to be any accepted definition (the conceptual definition) for the rigidity centers of multistory buildings. Second, for any given definition of the center of rigidity, researchers often failed to provide a convenient computational procedure for the designer to locate the rigidity centers.

The torsional provisions of many seismic codes also utilized the eccentricity concept for building design. Some investigations into the accuracy of the different seismic code procedures as applied to single story buildings had been conducted. The modal spectrum technique [29] was used as the standard for comparison of solution obtained. Bustamante and Rosenblueth [7] analytically investigated the dynamic magnification of the torsional effect in single story buildings. Kan and Chopra [17] also studied the dynamic responses of a torsionally coupled single story building. It was found that the dynamic behaviour of a torsionally coupled system is related to that of a corresponding uncoupled system. The uncoupled system will have coincident mass and rigidity centers, but with other properties identical to the actual system. The effect of modal coupling was also investigated in their study. The German seismic code [6] introduced supplementary eccentricity term in the design eccentricity calculation.

This is intended to provide approximation of the modal coupling effect [22]. Tso and Dempsey [36] carried out a dynamic analysis study on monosymmetric single story buildings to assess the accuracy of the torsional provisions of a number of seismic codes. It was found that most seismic codes underestimate the torsional effect in special circumstances when cross modal coupling effect is significant.

In dealing with multistory buildings, Newmark [24] developed a simple estimate of the equivalent eccentricity for symmetrical structures to account for the torsional component of ground motion. Base on the continuous method, an analysis of the elastic earthquake response of asymmetric multistory structures on elastic foundations was presented by Mendelson and Baruch [20]. Kan and Chopra [18] investigated the dynamic behaviour of a class of uniform frame building. The frames were modelled as shear beams and the building had mass and rigidity centers falling on two vertical lines. The dynamic responses of such a class of torsionally coupled system can again be related to responses of the corresponding uncoupled system. Pekau and Gordon [25] studied the cross modal coupling effect on multistory frame buildings. Rutenberg, Tso and Heidebrecht [30], Glück, Reinhorn and Rutenberg [13] suggested approximate dynamic analysis method for uniform eccentric wall-frame buildings.

Tso and Meng [37] studied the dynamic behaviour of shear beam buildings to assess the accuracy of the torsional provisions of NBCC 1977. It was found that the code procedures provided reasonable approximation for shear beam buildings with mass and rigidity centers falling on two vertical lines. This finding was incorporated as an additional clause in NBCC 1985 stating the limitations on the applicability of the torsional provisions.

It can be seen that most researchers evaluate the accuracy of the seismic codes using either single story building models or shear beam models; for the reason that the rigidity centers of these models can easily be located.

1.3 Scope and Objectives

The purpose of the present research is to extend the concept of eccentricity to multistory buildings to study their torsional behaviour under static and dynamic lateral loads.

In chapter 2, a formal definition of the center of rigidity will be given and mathematical expressions established for multistory buildings. A practical procedure for determining the locations of the rigidity centers in multistory buildings is then suggested. The intermixing use of the terms "shear center", "center of rigidity", "center

of stiffness" and "center of twist" has been a general practice in highrise building design. The conditions under which each term can be strictly applied will be classified. With the rigidity centers defined, the structural eccentricity at a floor can then be determined. Once established, the eccentricity concept can be employed in the torsional analysis of multistory buildings.

It is shown that employing the eccentricity concept in lateral load analysis will lead to an efficient solution of the problem, computationwise. More importantly, it enables the identification of the lateral and torsional component of the applied loads. Thus designers will have a better appreciation of the torsional characteristics of the building in design.

In chapter 3, a non-trivial example of employing the eccentricity concept is given in the study of behaviour of buildings with eccentric setback under lateral loads. In the preliminary design stage of such buildings, it is desirable to have hand calculation procedures for determining the distribution of resisting forces in the lateral elements. The concept of "displacement compatible" load will be introduced. This together with the eccentricity concept enables a hand calculation method to be used for analysis of a special class of eccentric setback buildings. This proposed procedure will also provide a better understanding

of the load transfer mechanisms involved in such buildings.

With the centers of rigidity properly defined, the accuracy and applicability of current seismic code of NBCC 1985 in predicting the torsional behaviour of multistory buildings is studied in chapter 4. The class of uniform eccentric wall-frame buildings with mass and rigidity centers falling on two vertical lines to which the code procedures are applicable is identified. Investigation into the interaction between the walls and frames under eccentric lateral loads is then conducted. The dynamic responses of this class of eccentric wall-frame buildings are studied to provide a base of reference for assessing the accuracy of code procedures as applied to such structures. The limitations of using the eccentricity concept to study the torsional behaviour of eccentric multistory buildings are also presented.

Finally, the conclusions of this study are summarized in chapter 5. It is the hope of this study to clarify the difficulties and applicability of the eccentricity concept in the study of torsional behaviour of multistory buildings under lateral loadings.

Chapter 2

ECCENTRICITY CONCEPT FOR MULTISTORY BUILDINGS

2.1 Introduction

In highrise building design, one important aspect is the ability of the building to perform in a satisfactory manner under lateral loads caused by wind, or seismic ground motions. If there exists asymmetry in geometry, stiffness or mass distribution in the plan of the building, lateral loadings lead to torsional responses, in addition to lateral responses. From a design viewpoint, it is necessary to know the magnitude of such torsional effect so that the required strengths and stiffnesses of the different lateral resisting elements (frames and/or walls) can be estimated. In many seismic building codes, allowance for the torsional effect is made by requiring buildings to be designed for additional torques applied simultaneously with the required lateral forces. The applied torque at any floor is computed as the product of the lateral load resultant and the design eccentricity at that floor. The design eccentricity is a function of the structural eccentricity which is defined as the distance between the center of rigidity at a level and the resultant of all lateral forces at that level. Therefore, in order to calculate the floor torques using

code provisions, it is necessary to establish the structural eccentricities at the different floors of the building. Assuming the line of action of the resultant lateral load at each floor is known, the problem of determining the structural eccentricity then reduces to locating the center of rigidity at each floor. Thus the eccentricity concept plays an important role both in the understanding and in the design of eccentric buildings.

The concept of eccentricity arose from considering the behaviour of a single story building with a roof slab which provides the diaphragm action to mobilize the resistance of different lateral resisting elements [19]. For such buildings, it can be shown that the center of rigidity can be located by requiring the first moments of the stiffnesses of the lateral resisting elements about the center of rigidity being zero. This gives rise to the interchanging use of the terms "center of rigidity" and "center of stiffness", since they represent the same point on the roof slab. Acting through the center of rigidity, the resultant of lateral loadings gives rise to translational deformation only. Since each resisting element experiences the same displacement, the center of rigidity can also be determined by considering the first moments of the shear forces instead of the first moments of the stiffnesses of the elements. As a result, the center

of rigidity is also identified with the "shear center" of the single story building.

The extension of this concept to eccentric multistory buildings is not trivial. There are different definitions for the centers of rigidity. One interpretation [16] defines the center of rigidity at a floor being the point when the resultant lateral force at that floor passes through it, the floor will not undergo any rotation. The other floors may or may not have rotation. Another suggestion [26] is to identify the shear center at each floor as the center of rigidity in order to obtain the structural eccentricity at that floor. In this thesis, the centers of rigidity of a multistory building are defined as the set of points located at floor levels such that when the given distribution of lateral loadings pass through them, no rotational movement of the building about a vertical axis will occur [34]. This last definition is a direct extension of the concept of eccentricity to multistory buildings. Even for buildings with identical floor layouts, the centers of rigidity may not be determined based on examination of a typical floor plan. An example of such a situation is an uniform eccentric wall-frame structure. Due to the wall-frame interaction effect, the relative stiffnesses between the walls and frames joined by the rigid floor diaphragms

change from floor to floor. As a result, the common interpretation that the centers of rigidity of an uniform building can be obtained by examination of a typical floor plan does not apply in such a case.

With the centers of rigidity defined, it is necessary to derive a procedure to determine the locations of these centers for eccentric buildings. The purpose for the determination of such centers are three fold: First, having located the centers of rigidity, the floor torques caused by the lateral loads at each floor can be determined by replacing the resultant lateral force at each floor by a force and a torque acting at the center of rigidity at that floor. The floor torque distribution provides an useful measure of the torsional effect caused by the lateral loadings on the building. Second, the design eccentricities as given in most seismic codes are expressed in terms of the structural eccentricity. Thus a knowledge of the eccentricity of the building is required for the aseismic design of buildings with allowance for the torsional effect. Third, recent changes in the seismic provisions of NBCC 1985 stated that the torsional provisions are strictly applicable to eccentric buildings with centers of mass and centers of rigidity located on two vertical lines. For eccentric buildings that do not satisfy such condition, the code provisions may or may not be valid to estimate the torsional

effect induced by seismic ground motions. The code suggests to use the more reliable approach of dynamic analysis [4] to estimate the torsional effect under such circumstances. Therefore, in order to determine whether the torsional provisions can be applied with confidence, there is a need for the designer to locate the centers of rigidity of the building. Currently, there does not appear to be any accepted procedure to determine the centers of rigidity for eccentric multistory buildings. Without such a procedure, the eccentricity value at each floor level remains ill-defined. As a result, designers of such buildings are left to their own interpretation of the torsional provisions in the seismic codes.

While the rigidity centers are important in identifying the lateral and torsional load effect, there exists another set of points - the centers of twist, which also plays an important role in the lateral analysis process. For single story buildings, the center of twist is used to obtain the torsional deformation under applied torque. Defined as the point on the roof slab which experiences no translational displacement when the loading consists of applied torque only, the deformation of a single story building subjected to lateral loading can be solved readily if the deformations are referred to the center of

twist. For a single story building, the center of twist coincides with the center of rigidity. Again, there does not appear to be any procedure available for locating the positions of the centers of twist for multistory buildings.

The purpose of this chapter is to clarify the concept of "center of rigidity" and "center of twist" for multistory buildings, and extend the concept of eccentricity and its role in multistory building design. The centers of rigidity and centers of twist will be defined mathematically for multistory buildings. The purpose to use each set of centers in the design and analysis of eccentric buildings will be discussed. A practical procedure to locate the centers of rigidity will then be presented. This procedure involves the use of a standard plane frame program only. Therefore, it is a procedure well suited for use in design offices. Finally, three examples of eccentric buildings subjected to seismic lateral loadings are presented. The results are computed based on static code procedures and are compared to that from dynamic spectrum analysis to illustrate the accuracy of the code procedures of NBCC 1985 in estimating the torsion effect on the buildings.

In the development of the theory, the following assumptions will be made:

(1) Material behaviour is linear elastic;

(2) Deformations are small;

(3) Floor slabs act as rigid diaphragms to transmit lateral loads; and

(4) For simplicity, only orthogonal framing arrangements are considered. All resisting elements will have their principal axes parallel to the reference axes of the structure.

2.2 Eccentric Single Story Buildings

Before considering the behaviour of multistory buildings, it is useful to trace the development of the center of rigidity and center of twist concept for single story buildings first.

2.2.1 Center of Rigidity

For single story buildings, the equation of equilibrium for the roof diaphragm about some reference axis z (Fig. 2.1) can be written as

$$\begin{bmatrix} k_{xx} & 0 & k_{x\theta} \\ 0 & k_{yy} & k_{y\theta} \\ k_{\theta x} & k_{\theta y} & k_{\theta\theta} \end{bmatrix} \begin{Bmatrix} \delta_x \\ \delta_y \\ \delta_\theta \end{Bmatrix} = \begin{Bmatrix} P_x \\ P_y \\ P_\theta \end{Bmatrix} \qquad (2.1)$$

where

$$k_{xx} = \sum_i (k_x)_i \qquad (2.2a)$$

$$k_{yy} = \sum_j (k_y)_j \qquad (2.2b)$$

$$k_{\theta x} = k_{x\theta} = -\sum_i (k_x)_i Y_i \qquad (2.2c)$$

$$k_{\theta y} = k_{y\theta} = \sum_j (k_y)_j X_j \qquad (2.2d)$$

$$k_{\theta\theta} = \sum_i (k_x)_i Y_i^2 + \sum_j (k_y)_j X_j^2 \qquad (2.2e)$$

$(k_x)_i$ and $(k_y)_j$ represent the stiffnesses of the individual resisting elements in the x and y global direction and Y_i and X_j represent the distances of these elements from the reference axis z. The lateral loads applied to the building are represented by P_x and P_y respectively. P_θ will be the torque on the building as caused by P_x and P_y about the z axis. Denoting the x and y coordinate of the line of action of the applied loads as X_m and Y_m respectively, then the torque loading P_θ will be given by

$$P_\theta = P_y X_m - P_x Y_m \qquad (2.3)$$

Let the coordinates of the center of rigidity be represented by X_R and Y_R. Then, by definition, if the load resultants act through the center of rigidity, δ_θ will be equal to zero. Eqn. (2.1) becomes

$$k_{xx}\delta_x = P_x \qquad (2.4a)$$

$$k_{yy}\delta_y = P_y \tag{2.4b}$$

$$k_{\theta x}\delta_x + k_{\theta y}\delta_y = - Y_R P_x + X_R P_y \tag{2.4c}$$

Using eqns. (2.4a) and (2.4b), eqn. (2.4c) can be written as

$$\frac{k_{\theta x}}{k_{xx}} P_x + \frac{k_{\theta y}}{k_{yy}} P_y = - Y_R P_x + X_R P_y \tag{2.5}$$

Since P_x and P_y are independent, eqn. (2.5) leads to

$$X_R = \frac{k_{\theta y}}{k_{yy}} = \frac{\Sigma(k_y)_j X_j}{\Sigma(k_y)_j} \tag{2.6a}$$

$$Y_R = - \frac{k_{\theta x}}{k_{xx}} = \frac{\Sigma(k_x)_i Y_i}{\Sigma(k_x)_i} \tag{2.6b}$$

Therefore, the location of the center of rigidity is determined by the ratio of first moments of stiffnesses to total lateral stiffness. In other words, its location can be computed as the center of stiffness.

Once the lateral displacements δ_x and δ_y were determined, the resisting forces in each individual element can then be computed. For frame i in the x direction, the lateral resisting force $(f_x^L)_i$ is given by

$$(f_x^L)_i = \frac{(k_x)_i}{\Sigma(k_x)_i} P_x \tag{2.7a}$$

in which the superscript "L" denotes response associated with the lateral load effect. Eqn. (2.7a) shows that the applied force P_x can be distributed among the resisting elements according to their relative stiffnesses.

Similarly, for elements in the y direction, the lateral resisting force will be given by

$$(f_y^L)_j = \frac{(k_y)_j}{\Sigma(k_y)_j} P_y \qquad (2.7b)$$

Thus the resultant of the resisting forces in each direction will pass through the center of rigidity of the building. Since the resisting forces will also be the resisting shears in the elements, the center of rigidity is often identified as the shear center for single story buildings.

The above analysis leads to the interchanging use of the terms "center of rigidity", "center of stiffness" and "shear center" for single story buildings. As shown in eqn. (2.6), the rigidity center will only be a function of the stiffness properties of the building and does not depend on the applied loads.

2.2.2 Center of Twist

The center of twist is defined as the point on the roof slab which does not undergo any translational displacement when the structure is subjected to applied

torque only. Assuming that the coordinates of the center of twist are represented by X_T and Y_T. Subjected to applied torque, the center of twist will have no translational displacement and the displacements of other points on the roof slab can be computed treating the center of twist as a stationary point. A rotation of the roof slab by an amount δ_θ will induce displacements δ_{xi} and δ_{yj} along the plane of stiffness of element i and j respectively. For small displacements, then

$$\delta_{xi} = -(Y_i - Y_T)\ \delta_\theta \qquad (2.8a)$$

$$\delta_{yj} = (X_j - X_T)\ \delta_\theta \qquad (2.8b)$$

The torsional shear developed in an element is given by

$$(f_x^T)_i = (k_x)_i \delta_{xi} \qquad (2.9a)$$

$$(f_y^T)_j = (k_y)_j \delta_{yj} \qquad (2.9b)$$

in which the superscript "T" denotes response associated with the torsional load effect.

Since the applied torque loading results in no net resultant force on the structure, the summation of all resisting forces in the x and y direction will be equal to zero. Thus,

$$\sum_i (k_x)_i (Y_i - Y_T)\delta_\theta = 0 \qquad (2.10a)$$

$$\sum_j (k_y)_j (X_j - X_T)\delta_\theta = 0 \qquad (2.10b)$$

and from which X_T and Y_T can be determined. From eqn. (2.10), the x and y coordinate of the center of twist will be given by

$$X_T = \frac{\Sigma(k_y)_j X_j}{\Sigma(k_y)_j} \qquad (2.11a)$$

$$Y_T = \frac{\Sigma(k_x)_i Y_i}{\Sigma(k_x)_i} \qquad (2.11b)$$

Comparing eqn. (2.11) with eqn. (2.6) shows that the center of twist coincides with the center of rigidity for single story buildings. The location of the center of twist will again be a function of the stiffness properties of the structure only and independent of the applied torque.

An alternate proof that the center of rigidity and the center of twist necessarily be the same point for single story buildings can be given using the work-energy principle in mechanics.

Consider a single story building acted upon by a torque P_θ and a point load P_y whose line of action passes through the center of rigidity. When load P_y is applied first, the floor diaphragm will move, as a rigid body, without rotation by an amount δ_y. The work done by P_y will be

$$W = P_y\delta_y/2 \tag{2.12}$$

Next, the torque P_θ is applied, resulting in an angle of rotation δ_θ. This rotation will take place about the center of twist. Assuming that the center of rigidity does not coincide with the center of twist, but is located at a distance "c" from it, then the center of rigidity will be displaced a further distance equal to $c\delta_\theta$. The total work done by all forces is now

$$W = P_y\delta_y/2 + P_\theta\delta_\theta/2 + P_y c\delta_\theta \tag{2.13}$$

If the load sequence is reversed, i.e. P_θ is applied first, and followed by P_y, the total work done will be given by

$$W = P_\theta\delta_\theta/2 + P_y\delta_y/2 \tag{2.14}$$

For a linear elastic structure to which the principle of superposition holds, the total strain energy in the structure will be independent of the sequence of load application. Thus, the total work done should be the same for both cases. Equating eqns. (2.13) and (2.14) leads to the condition of

$$P_y c\delta_\theta = 0 \tag{2.15}$$

Since $P_y \neq 0$ and $\delta_\theta \neq 0$, this leads to

$$c = 0 \tag{2.16}$$

Thus, the "center of rigidity" must coincide with the "center of twist" for a single story structure.

Thus far, a procedure to locate the center of rigidity and center of twist for single story buildings is

given. In the next section, the role played by each of the two centers in the lateral load analysis process will be presented.

2.2.3 Uncoupling the Equation of Equilibrium

If the center of twist is taken as the origin of reference, then the equilibrium equation as expressed by eqn. (2.1) can be reduced to three independent equations:

$$k_{xx}\,\delta_x = P_x \tag{2.17a}$$

$$k_{yy}\,\delta_y = P_y \tag{2.17b}$$

$$k_{\theta\theta}\delta_\theta = -P_x e_y + P_y e_x \tag{2.17c}$$

in which

$$k_{\theta\theta} = \Sigma(k_x)_I\,(Y_I - Y_T)^2 + \Sigma(k_y)_J\,(X_J - X_T)^2 \tag{2.2f}$$

$$e_x = X_m - X_R \tag{2.18a}$$

$$e_y = Y_m - Y_R \tag{2.18b}$$

Though mathematically X_T and X_R represent the same quantity (so is Y_T and Y_R), X_R is preferred over X_T (Y_R over Y_T) in eqn. (2.18) for defining the eccentricities. This follows directly as a straight interpretation of the definition of

structural eccentricity as stated earlier in this chapter.

Eqn. (2.17) represents three uncoupled equilibrium equations. The first two equations govern the lateral equilibrium of the building in the x and y direction respectively. The last equation, on the other hand, governs the torsional equilibrium of the structure. The torque loading represented in eqn. (2.17c) is expressed as the sum of the product of the lateral loads and the corresponding eccentricity (e_x or e_y).

Thus in lateral load analysis of single story structures, the rigidity center is useful in identifying the lateral and torsional load component. The center of twist, on the other hand, is a convenient point of reference for obtaining the solution to the problem.

The lateral shear as given by eqn. (2.7) and torsional shear as given by eqn. (2.9) in an element can be computed once the displacements δ_x, δ_y and δ_θ are determined from solving eqn. (2.17). The total design shear $(F_x)_i$ or $(F_y)_j$ of an element will be the sum of the lateral and torsional shears.

$$(F_x)_i = (k_x)_i [\delta_x - (Y_i - Y_T) \delta_\theta] \qquad (2.19a)$$

$$(F_y)_j = (k_y)_j [\delta_y + (X_j - X_T) \delta_\theta] \qquad (2.19b)$$

From eqn. (2.19), it can be seen that the element furthest

away from the center of twist will be most susceptible to the torsional effect. Thus an edge element will be a critical element in single story buildings as far as torsional effect is concerned.

2.2.4 Torsional Provisions in Seismic Codes as Applied to Single Story Buildings

Most seismic building codes formulate the design torsional moment at each story as a product of the story shear and a quantity termed "design eccentricity - e_n". As tabulated in Table 2.1, most building codes, except the German Code, define the design eccentricity in two parts. The first part is expressed as some magnification factor times the structural eccentricity. This part deals with the complex nature of torsion and the effect of the simultaneous action of the two horizontal ground disturbance. The second term is called accidental eccentricity to account for the possible additional torsion arising from variations in the estimates of the relative rigidities, uncertain estimates of dead and live loads at the floor levels, addition of wall panels and partitions after completion of the building, variation of the stiffness with time, and inelastic or plastic action. The effects of possible torsional motion of the ground are also considered to be included in this term. This term is in general a function of the plan dimension D_n

of the building in the direction of the computed eccentricity.

Take the case of the National Building Code of Canada 1985 [3] for discussion. The torsional moment M_{tn} in the horizontal plane of floor n can be interpreted as

$$M_{tn} = V_n e_n \tag{2.20}$$

in which V_n is the interstory shear at floor n. V_n will be equal to the design base shear V for single story buildings. The design eccentricity e_n shall be computed by one of the following equations, whichever provides the greater stresses:

$$e_n = 1.5e + 0.10D_n \tag{2.21a}$$

$$e_n = 0.5e - 0.10D_n \tag{2.21b}$$

in which "e" is the structural eccentricity.

Eqn. (2.21a) is intended for elements lying on the same side as the mass center, as measured from the center of rigidity, or more appropriately, the center of twist of the structure. For elements on opposite side of the mass center, eqn. (2.21b) will be applicable. The structural eccentricity "e" in eqn. (2.21) shall take on values as expressed by eqn. (2.18).

With eccentricity defined for single story buildings, the application of code procedures for aseismic design of such structures will be a straight forward task.

2.2.5 Summary

The center of rigidity and center of twist are two important points of reference in the torsional analysis of buildings. The severity of the torsional effect is commonly measured by the eccentricity of the building. It is defined as the distance between the center of rigidity and the resultant of all lateral forces at the roof. For single story buildings, the center of rigidity can be identified as the center of stiffness or as the shear center of the building. Though the center of twist can be proved to be the same point as the center of rigidity, it plays a different role in the lateral load analysis process. Formulation of the problem with reference to the center of twist as origin will lead to an uncoupling of the equation of equilibrium. The lateral and torsional responses can then be determined separately. For single story buildings, the location of both the center of rigidity and center of twist will depend on the configuration of the resisting system, and independent of the nature of the applied loads. With eccentricity defined for single story buildings, the torsional provisions of building codes can then be applied for aseismic design of such structures.

2.3 Eccentric Multistory Buildings

Complications in behaviour of a multistory building

are often caused by the variation in geometry and/or structural properties along the height. As a result, the extension of the eccentricity concept to multistory buildings will not be a trivial task. For multistory buildings, the centers of rigidity and centers of twist will not necessary be the same set of points. The two centers being different sets of points in general can be proved again using the work-energy principle in mechanics.

As for single story buildings, the work done expressions for two load sequences will be compared. Let the building be acted upon by a set of torques $\{P_\theta\}$ and a set of lateral loads $\{P_y\}$ at floor levels. The line of action of the floor loads $\{P_y\}$ will pass through the rigidity centers of the building having coordinate vector $\{X_L\}$. If the lateral loads $\{P_y\}$ are applied first, the floor diaphragms will undergo translational displacements $\{\delta_y\}$. The work done by $\{P_y\}$ will be

$$W = \frac{1}{2} \{P_y\}^T \{\delta_y\} \qquad (2.22)$$

If the torques $\{P_\theta\}$ are next applied, the floor diaphragms will further undergo rotational deformations represented by the vector $\{\delta_\theta\}$. The rotation of a floor slab will take place about the center of twist of the particular floor. Let the locations of the centers of twist at the different floors be represented by the coordinate vector $\{X_T\}$, then

the total work done by all forces will be

$$W = \frac{1}{2}\{P_y\}^T\{\delta_y\} + \frac{1}{2}\{P_\theta\}^T\{\delta_\theta\} + \{P_y\}^T([X_L] - [X_T])\{\delta_\theta\} \quad (2.23)$$

in which

$[X_L]$ and $[X_T]$ are diagonal matrices with diagonal elements equal to elements in the vectors $\{X_L\}$ and $\{X_T\}$ respectively. If the load sequence is reversed with the torques $\{P_\theta\}$ being applied first followed by the lateral loads $\{P_y\}$, then the work done expression will be given by

$$W = \frac{1}{2}\{P_\theta\}^T\{\delta_\theta\} + \frac{1}{2}\{P_y\}^T\{\delta_y\} \quad (2.24)$$

Since the total work done is independent of the sequence of load application for linear elastic structures, equating the work done expressions as represented by eqns.(2.23) and (2.24) results in

$$\{P_y\}^T([X_L] - [X_T])\{\delta_\theta\} = 0 \quad (2.25)$$

Unlike working with scalar quantities, the condition that

$$[X_L] - [X_T] = [0] \quad (2.26)$$

is a sufficient but not a necessary condition that eqn. (2.25) be satisfied. It is a special solution to eqn. (2.25) that represents the situation when the centers of rigidity and the centers of twist are the same set of points.

Detailed study of the centers of rigidity and centers of twist for multistory buildings will be presented in the following sections.

2.3.1 Centers of Rigidity

In the following, the development of the center of rigidity concept is for orthogonal framing buildings only. Non-orthogonal framing structures will be dealt with in Appendix A.

To obtain the locations of the centers of rigidity for a N story building with rigid floor diaphragms, consider the following matrix equation of equilibrium written for two orthogonal horizontal directions x and y, and for moment equilibrium about the vertical z axis.

$$\begin{bmatrix} [K_{xx}] & [0] & [K_{x\theta}] \\ [0] & [K_{yy}] & [K_{y\theta}] \\ [K_{\theta x}] & [K_{\theta y}] & [K_{\theta\theta}] \end{bmatrix} \begin{Bmatrix} \{\delta_x\} \\ \{\delta_y\} \\ \{\delta_\theta\} \end{Bmatrix} = \begin{Bmatrix} \{P_x\} \\ \{P_y\} \\ \{P_\theta\} \end{Bmatrix} \qquad (2.27a)$$

or

$$[K]\{\delta\} = \{P\} \qquad (2.27b)$$

Eqn. (2.27) gives rise to a set of 3N equations for the displacement variables $\{\delta_x\}$, $\{\delta_y\}$ and $\{\delta_\theta\}$ about the arbitrary z axis. Each submatrix is of order N by N and each subvector is of order N by 1. For buildings with orthogonal framing, the stiffness submatrices are

expressible in terms of individual frame stiffness matrix $[K_x]_i$ or $[K_y]_j$ by the following relations:

$$[K_{xx}] = \sum_i [K_x]_i \tag{2.28a}$$

$$[K_{yy}] = \sum_j [K_y]_j \tag{2.28b}$$

$$[K_{x\theta}] = [K_{\theta x}]^T = -\sum_i [K_x]_i [Y]_i \tag{2.28c}$$

$$[K_{y\theta}] = [K_{\theta y}]^T = \sum_j [K_y]_j [X]_j \tag{2.28d}$$

$$[K_{\theta\theta}] = \sum_i [Y]_i [K_x]_i [Y]_i + \sum_j [X]_j [K_y]_j [X]_j \tag{2.28e}$$

where

$[K_x]_i$ is the stiffness matrix of resisting element i whose plane of orientation is parallel to the x reference axis.

$[K_y]_j$ is the stiffness matrix of resisting element j whose plane of orientation is parallel to the y reference axis.

$[X]_j$ is the diagonal coordinate matrix of element j. The diagonal elements in the matrix being equal to the x distance of the j^{th} element from the y reference axis.

$[Y]_i$ is the diagonal coordinate matrix of element i. The diagonal elements in the matrix being equal to the y distance of the i^{th} element from the x reference axis.

Let the x and y coordinates of the centers of rigidity be represented by $\{X_L\}$ and $\{Y_L\}$ respectively. When the lateral loads act at the centers of rigidity, the structure will have no rotational deformation, or $\{\delta_\theta\} = \{0\}$. Rewriting eqn. (2.27) will lead to the following sets of equations:

$$[K_{xx}]\{\delta_x\} = \{P_x\} \tag{2.29a}$$

$$[K_{yy}]\{\delta_y\} = \{P_y\} \tag{2.29b}$$

$$[K_{\theta x}]\{\delta_x\} + [K_{\theta y}]\{\delta_y\} = \{P_\theta\} = -[P_x]\{Y_L\} + [P_y]\{X_L\} \tag{2.29c}$$

in which $[P_x]$ and $[P_y]$ are diagonal matrices with diagonal elements equal to elements in $\{P_x\}$ and $\{P_y\}$ respectively. Substituting eqns. (2.29a) and (2.29b) into eqn. (2.29c) results in

$$\begin{aligned}&[K_{\theta x}][K_{xx}]^{-1}\{P_x\} + [K_{\theta y}][K_{yy}]^{-1}\{P_y\}\\ &= -[P_x]\{Y_L\} + [P_y]\{X_L\}\\ &= -[Y_L]\{P_x\} + [X_L]\{P_y\}\end{aligned} \tag{2.30}$$

in which $[X_L]$ and $[Y_L]$ are diagonal coordinate matrices with diagonal elements equal to elements in $\{X_L\}$ and $\{Y_L\}$ respectively.

Since load vectors $\{P_x\}$ and $\{P_y\}$ are independent, eqn. (2.30) implies that

$$[K_{\theta x}][K_{xx}]^{-1}\{P_x\} = -[Y_L]\{P_x\} \tag{2.31a}$$

$$[K_{\theta y}][K_{yy}]^{-1}\{P_y\} = [X_L]\{P_y\} \tag{2.31b}$$

from which $\{X_L\}$ and $\{Y_L\}$ can be solved. Hence,

$$\{X_L\} = [P_y]^{-1}[K_{\theta y}]\,[K_{yy}]^{-1}\,\{P_y\}$$
$$= [P_y]^{-1}[K_{\theta y}]\,\{\delta_y\} \tag{2.32a}$$

$$\{Y_L\} = -[P_x]^{-1}[K_{\theta x}]\,[K_{xx}]^{-1}\,\{P_x\}$$
$$= -[P_x]^{-1}[K_{\theta x}]\,\{\delta_x\} \tag{2.32b}$$

It can be seen that the centers of rigidity are in general both a function of the lateral load distribution and stiffness properties of the structure. Thus, for multistory buildings, the centers of rigidity can no longer be identified as the stiffness centers of the structure in general. Also, they do not necessarily fall on a vertical line.

Once the lateral displacements $\{\delta_x\}$ and $\{\delta_y\}$ were determined by solving eqns. (2.29a) and (2.29b), the lateral resisting forces in the elements can then be computed.

$$\{f_x^L\}_i = [K_x]_i\,\{\delta_x\} \tag{2.33a}$$

$$\{f_y^L\}_j = [K_y]_j\,\{\delta_y\} \tag{2.33b}$$

Considering the definition of $[K_{\theta y}]$ as given in eqn. (2.28d), eqn. (2.32a) can be written as

$$[P_y]\{X_L\} = \sum_j [X]_j [K_y]_j \{\delta_y\} \qquad (2.34)$$

The product $[K_y]_j \{\delta_y\}$ represents the lateral floor loads on the j^{th} element due to deflection $\{\delta_y\}$. Therefore, the right hand side of eqn. (2.34) can be interpreted as the first moments of the floor loads of all elements about the z axis due to displacement $\{\delta_y\}$. Finally, the x coordinate of the center of rigidity at each floor is then given by the first moments of the floor loads divided by the total applied load at that floor. A similar argument can be used to interpret eqn. (2.32b) in determining the y coordinates of the centers of rigidity. Therefore, $\{X_L\}$ and $\{Y_L\}$ as defined in eqn. (2.32) can be interpreted as the "load centers" and thus the centers of rigidity of a multistory building should be identified with the "load centers" of the building.

Great care should be exercised in distinguishing the floor loads from the interstory shear forces. If one computes the ratio of the first moments of the interstory shear forces of all elements to the total interstory shears, one obtains the locations of the shear centers. Poole [26] suggested the use of plane frame programs to determine the shear centers and use the shear centers as reference points to measure floor eccentricities. It can be shown that if the resultant of the applied loads at each floor passes

through the shear center at that floor, both translational and rotational displacements will occur. Therefore, it is incorrect to measure eccentricity with respect to shear center for multistory buildings.

The load center concept represents a generalized way of interpreting the center of rigidity in building design. For single story buildings, no attempt had been made to differentiate between resisting force and resisting shear in an element since they represent the same quantity. This has a misleading effect on designers. Most people overlooked the fact that lateral floor loads and lateral floor shears are different quantities as far as multistory buildings are concerned.

2.3.2 Centers of Twist

The centers of twist are defined as points in the planes of the floors which do not undergo any translational displacement when the structure is subjected to applied torques only. Under applied torques, there will be rotation of the floor slabs. Let the rotational displacements be represented by the vector $\{\delta_\theta\}$. Then the torsional resisting forces in the elements will be given by

$$\{f^T_x\}_i = - [K_x]_i([Y]_i - [Y_T])\{\delta_\theta\} \qquad (2.35a)$$

$$\{f^T_y\}_j = [K_y]_j([X]_j - [X_T])\{\delta_\theta\}. \qquad (2.35b)$$

in which $[X_T]$ and $[Y_T]$ are diagonal matrices with elements denoting the x and y coordinates of the centers of twist.

For lateral equilibrium, the summation of all resisting forces in the x and y direction at each floor needs to be zero. Thus,

$$\sum_i [K_x]_i([Y]_i - [Y_T])\{\delta_\theta\} = \{0\} \qquad (2.36a)$$

$$\sum_j [K_y]_j([X]_j - [X_T])\{\delta_\theta\} = \{0\} \qquad (2.36b)$$

Defining the coordinate vectors of the centers of twist as $\{X_T\}$ and $\{Y_T\}$ with elements being equal to the diagonal elements of $[X_T]$ and $[Y_T]$ respectively, then the vectors $\{X_T\}$ and $\{Y_T\}$ can be obtained by solving eqn. (2.36).

$$\{X_T\} = [\delta_\theta]^{-1}[K_{yy}]^{-1}[K_{y\theta}]\{\delta_\theta\} \qquad (2.37a)$$

$$\{Y_T\} = -[\delta_\theta]^{-1}[K_{xx}]^{-1}[K_{x\theta}]\{\delta_\theta\} \qquad (2.37b)$$

where $[\delta_\theta]$ is a diagonal matrix with diagonal elements equal to elements in $\{\delta_\theta\}$. $\{X_T\}$ and $\{Y_T\}$ are thus in general a function of the resulting rotations, or implicitly a function of the applied torque distribution. The centers of twist will not necessarily fall on a vertical line and they are in general different from the centers of rigidity.

2.3.3 Special Class of Multistory Buildings

As shown in previous sections, the centers of rigidity and centers of twist of multistory buildings are in general (i) load distribution dependent; (ii) not necessarily the same set of points; and (iii) not lined up vertically above one another. In this section, the conditions under which the structure needs to satisfy in order to have the centers of rigidity and centers of twist load independent, coincide with one another and lie on a vertical axis will be discussed.

Consider the coordinate vector of the centers of rigidity in the x direction as given by eqn. (2.32a):

$$\{X_L\} = [P_y]^{-1}[K_{\theta y}][K_{yy}]^{-1}\{P_y\} \qquad (2.32a)$$

Defining the product of the matrices $[K_{\theta y}]\ [K_{yy}]^{-1}$ as

$$[a] = [K_{\theta y}][K_{yy}]^{-1} \qquad (2.38)$$

and express [a] as sum of two matrices $[\bar{a}]$ and $[a^*]$ by the relation

$$[a] = [\bar{a}] + [a^*] \qquad (2.39)$$

$[\bar{a}]$ is a diagonal matrix containing the diagonal elements of [a]. Making use of eqns. (2.38) and (2.39), eqn. (2.32a) can be written as

$$\{X_L\} = [\bar{a}]\{I\} + [P_y]^{-1}[a^*]\{P_y\} \qquad (2.40)$$

where {I} is the unity vector with all elements equal to unity. For $\{X_L\}$ to be load independent, it is necessary to have

$$[P_y]^{-1}[a^*]\{P_y\} = \{0\} \tag{2.41}$$

Since $\{P_y\}$ is an arbitrary load vector, eqn. (2.41) can only be satisfied if $[a^*]$ is a null matrix, or referring to eqn. (2.39), matrix [a] is a diagonal matrix.

Similarly, writing the product of the matrices $[K_{\theta x}]$ and $[K_{xx}]^{-1}$ as

$$[b] = [K_{\theta x}][K_{xx}]^{-1} \tag{2.42}$$

and express [b] as

$$[b] = [\bar{b}] + [b^*] \tag{2.43}$$

where $[\bar{b}]$ is a diagonal matrix containing the diagonal elements of [b], the necessary condition for the y coordinates of the centers of rigidity to be load independent is when [b] is a diagonal matrix.

The conditions under which the locations of the centers of rigidity will be load independent are thus determined. Similar treatment can be applied to the centers of twist.

The x coordinates of the centers of twist are given by

$$\{X_T\} = [\delta_\theta]^{-1}[K_{yy}]^{-1}[K_{y\theta}]\{\delta_\theta\} \tag{2.37a}$$

Using eqns. (2.38) and (2.39), the above equation can be written as

$$\{X_T\} = [\delta_\theta]^{-1}[a]^T\{\delta_\theta\}$$
$$= [\bar{a}]\{I\} + [\delta_\theta]^{-1}[a^*]^T\{\delta_\theta\} \tag{2.44}$$

Following the same argument as for the centers of rigidity, the condition for the x coordinates of the centers of twist being load independent is

$$[a^*]^T = [0] \tag{2.45}$$

or when [a] is a diagonal matrix. This is the same condition as required for load independency for the centers of rigidity. The proof for load independent condition for the y coordinates of the centers of twist follows along a similar line of reasoning.

In summary, the conditions that the centers of rigidity, and also for the centers of twist, to be load independent are when [a] and [b] are both diagonal matrices. If the centers of rigidity and centers of twist are load independent, they are in fact the same set of points. This fact is evident by comparing eqns. (2.40) and (2.44)

A special class of multistory buildings can be identified having centers of rigidity and centers of twist

being the same set of points and both are load independent. Consider a building that has proportional framing. The stiffnesses of the resisting elements are proportional to one another in each of the global directions for this type of building. In other words, the stiffness matrix of each element can be expressed by the relationship:

$$[K_x]_i = \alpha_i[\bar{K}_x] \tag{2.46}$$

and

$$[K_y]_j = \beta_j[\bar{K}_y] \tag{2.47}$$

where α_i, β_j are some proportional constants and $[\bar{K}_x]$ and $[\bar{K}_y]$ are stiffness matrices characteristic to the resisting elements in the x and y direction, respectively. Using the definitions of the global stiffness matrices as given in eqn. (2.28), one can easily verify that

$$\{Y_L\} = \{Y_T\} = [K_{xx}]^{-1}[K_{x\theta}]\{I\} = \frac{\Sigma\alpha_i Y_i}{\Sigma\alpha_i}\{I\} \tag{2.48a}$$

$$\{X_L\} = \{X_T\} = [K_{yy}]^{-1}[K_{y\theta}]\{I\} = \frac{\Sigma\beta_j X_j}{\Sigma\beta_j}\{I\} \tag{2.48b}$$

In this case, not only the centers of rigidity and centers of twist are load independent, hence representing the same set of points, but they will also lie on a vertical axis. The location of the centers in this case can be determined using the relative stiffness consideration of the elements based on a typical single floor plan of the

building; a fact that is generally recognized by the design professions. For such structures, the centers of rigidity can again be identified as the centers of stiffness or shear centers as for single story buildings. With the building being uniform, the center of mass at each floor will also fall on a vertical line. Thus uniform multistory buildings with proportional framing is one class of buildings to which the torsional provisions of NBCC 1985 are applicable.

2.3.4 A Procedure to Compute Floor Eccentricities

To determine the eccentricities of a multistory eccentric building, it is necessary to locate the center of rigidity at each floor. The locations of the centers of rigidity are given by eqn. (2.32). They can be determined once the lateral load distribution along the height, and the global stiffness of the complete structure are defined. However, such an approach to obtain the locations of centers of rigidity is not particularly useful during preliminary design since the global stiffness matrix of the structure may not be readily available at this stage. An alternative approach is suggested here which does not require the explicit use of the global stiffness matrix of the structure and therefore is more suitable to be used in the design context.

This alternative approach is based on the interpretation of the center of rigidity formula as given by eqn. (2.34). It is shown that the rigidity centers can be interpreted as the "load centers" at floor levels. Therefore, if the loading on each resisting element at each floor is known under the assumption of no rotational deformation, the load center at each floor can be obtained by dividing the first moments of the element loads by the total loading at that floor.

Assuming that the building is restrained from rotating, the lateral floor displacements in the x direction, $\{\delta_x\}$ and the interstory shear of all elements under loading $\{P_x\}$ can readily be obtained by means of a standard plane frame program. The global stiffness matrix $[K_{xx}]$ can be simulated by joining all the resisting elements spanning the x direction by rigid beam elements with hinged ends at floor levels. An example of the computer model for a wall-frame building will be given in the next section. Once the interstory shears in each resisting element are known, one can obtain the floor loads on the individual elements. The y coordinate of the load center at each floor is given by the ratio of the first moments of these floor loads about reference axis z and the total floor load at that floor. One can repeat the same procedure to obtain the x coordinates of the load centers by analyzing the

displacement and interstory shears of elements in the y direction subjected to lateral loads $\{P_y\}$.

2.3.5 Examples

Three examples are presented, representing three different classes of multistory buildings to demonstrate the variation of the rigidity, shear, stiffness and twist centers under given lateral load distribution. Each of these buildings is nine story high, having uniform rectangular floors of dimensions 20 m by 10 m and a uniform floor height of 3 m. The arrangement of the resisting elements are such that each building is symmetric in the x direction and eccentric in the y direction, as shown in Fig. 2.2. Building A has wall elements to resist the lateral loads. The rigidity of each element at the top three floors is reduced to two-thirds that at the base. Therefore, Building A is a building with proportional framing, and the centers of rigidity can be determined on a per floor basis. Building B is similar to Building A in every aspect except for the right edge wall (wall 4). There is no reduction of rigidity for wall 4 along its height for this building. Therefore, Building B represents a building where the framing is non-proportional. Building C represents an eccentric uniform wall-frame building. The lateral

resisting elements in the y direction consist of two identical uniform walls and two identical uniform frames. Further, the beams in the frames are considered very stiff in relation to the columns so that each frame can be treated as a "shear beam" for computational purposes. The rigidities of the walls and frames are chosen such that there is significant wall-frame interaction in the building. Other information concerning the buildings are summarized in Table 2.2. For Building C, it should be noted that although the walls and the frames are uniform, the framing of this structure is non-proportional, as the stiffness matrix of a wall differs from that of a frame.

The buildings are subjected to an uniform distribution and an inverse triangular distribution of lateral loads. The lateral load resultants are assumed to act through the centers of mass of each building.

The locations of the centers of rigidity in each of the three buildings are determined by the procedure as outlined in the last section. A computer model is created for each building to be analysed by the plane frame program. As an example, the computer model for Building C is shown in Fig. 2.3. The centers of stiffness of the resisting elements are also determined, on a per floor basis assuming each floor behaves like a single story building. The

distribution of the rigidity and stiffness centers of the three buildings are shown in Fig. 2.4a and 2.4b for uniform and inverse triangular load distribution respectively. Building A, having a proportional framing arrangement, is shown to have the centers of rigidity lying on a vertical axis, as expected. Despite the fact that Building B differs only in a minor manner from Building A, it nonetheless is a building of non-proportional framing, and there is a considerable scattering of the centers of rigidity. This scattering is a result of compatibility requirement imposed on the resisting elements at each floor due to the rigid floor diaphragms of the building. Finally, the scattering is even larger for the uniform wall-frame building C. It can be seen that only for Building A that the figidity centers can be identified as the centers of stiffness of the building.

Plotted in the same figures are the shear centers and centers of twist distribution for the given loadings. The centers of rigidity and shear centers are different sets of points for Building B and C. Thus measuring the eccentricity with reference to the shear center will be, in general, incorrect for multistory buildings.

The centers of twist may also scatter and do not necessarily fall on a vertical line. Howeyer, the scattering is not as much as the variation of the centers of

rigidity as demonstrated by Building B. The centers of twist lie virtually on a vertical line for both load cases.

Based on the examples studied, it is shown that the centers of rigidity, stiffness centers, shear centers and centers of twist will be different sets of points, in general. Only for buildings with proportional framing that they represent the same set of points.

2.3.6 Uncoupling the Equation of Equilibrium

It has been shown that the center of twist is a convenient point of reference in the analysis of single story buildings for eccentric lateral loads. The centers of twist also play a similar role in the case of multistory buildings.

In this section, it is shown that the set of 3N equations of equilibrium as given by eqn. (2.27) can be uncoupled into three sets of N equations of equilibrium using centers of twist as reference points. The resulting equations will describe the translational deformations in two horizontal directions and the rotational deformation of the system.

Let the coordinates of the load resultants relative to the reference axis z be $\{X_m\}$ and $\{Y_m\}$ respectively. For lateral loads that arise due to the inertial effect of the

floors, as commonly assumed in seismic analysis of multi-story buildings, $\{X_m\}$ and $\{Y_m\}$ will be the coordinates of the mass centers of the building. Instead of referring to the z axis, let one define a new displacement vector $\langle\{\Delta_x\}, \{\Delta_y\}, \{\Delta_\theta\}\rangle$. $\{\Delta_x\}$ and $\{\Delta_y\}$ are displacement vectors referred to the centers of twist of the building. In other words, the reference points for $\{\Delta_x\}$ and $\{\Delta_y\}$ have coordinate vectors $\{X_T\}$ and $\{Y_T\}$ respectively. The relation between this new set of displacement vector $\{\Delta\}$ and the old set of displacement vector $\{\delta\}$ with respect to the z reference axis is given by

$$\{\delta\} = [\Gamma]\{\Delta\} \tag{2.49}$$

where

$$[\Gamma] = \begin{bmatrix} [I] & [0] & [Y_T] \\ [0] & [I] & -[X_T] \\ [0] & [0] & [\ I] \end{bmatrix} \tag{2.50}$$

The equation of equilibrium using the new displacement vector $\{\Delta\}$ can be written as

$$[K^*]\{\Delta\} = \{P^*\} \tag{2.51}$$

The transformed stiffness matrix $[K^*]$ and transformed load vector $\{P^*\}$ can be related to the original stiffness matrix $[K]$ and load vector $\{P\}$ by

$$[K^*] = [\Gamma]^T[K][\Gamma] \tag{2.52a}$$

and

$$\{P^*\} = [\Gamma]^T\{P\} \tag{2.52b}$$

Eqn. (2.52) is obtained from the requirement that the strain energy of the system is invariant under linear transformation. Using eqns. (2.50) and (2.52), the equilibrium equation given by eqn. (2.51) becomes uncoupled into three sets of N equations each, as given below:

$$[K_{xx}]\{\Delta_x\} = \{P_x\} \tag{2.53}$$

$$[K_{yy}]\{\Delta_y\} = \{P_y\} \tag{2.54}$$

$$[K_{\theta\theta}^*] = ([K_{\theta\theta}] - [K_{\theta x}][K_{xx}]^{-1}[K_{x\theta}] - [K_{\theta y}][K_{yy}]^{-1}[K_{y\theta}])\{\Delta_\theta\} = \{P_\theta^*\} \tag{2.55}$$

where

$$\{P_\theta^*\} = -[P_x]\{Y_m\} - [K_{\theta x}][K_{xx}]^{-1}\{P_x\} + [P_y]\{X_m\} - [K_{\theta y}][K_{yy}]^{-1}\{P_y\} \tag{2.56}$$

The second term on the right hand side of eqn. (2.56) can be written, with the use of eqn. (2.32b), as

$$-[K_{\theta x}][K_{xx}]^{-1}\{P_x\} = -[P_x][P_x]^{-1}[K_{\theta x}][K_{xx}]^{-1}\{P_x\} = [P_x]\{Y_L\} \tag{2.57}$$

Similar interpretation can be used for the fourth term in eqn. (2.56). Therefore, eqn. (2.56) can be rewritten in the form

$$\{P_\theta^*\} = -[P_x](\{Y_m\} - \{Y_L\}) + [P_y](\{X_m\} - \{X_L\}) \quad (2.58)$$

Physically, eqn. (2.58) represents the torques generated by the lateral loads if the resultants of the applied loads are transferred to act through the centers of rigidity. Defining the eccentricity at each floor as the distance between the load resultant and the center of rigidity (or load center) at that floor, then

$$\{e_x\} = \{X_m\} - \{X_L\} \quad (2.59a)$$

$$\{e_y\} = \{Y_m\} - \{Y_L\} \quad (2.59b)$$

Using the definition of eccentricity as given by eqn. (2.59), the applied torque vector due to lateral loads on the building takes the familiar form of

$$\{P_\theta^*\} = -[P_x]\{e_y\} + [P_y]\{e_x\} \quad (2.60)$$

Eqns. (2.53) and (2.54) represent the equations of force equilibrium in the x and y direction, with the displacements referred to the centers of twist; while eqn. (2.55) is the torque equilibrium equation. They are uncoupled and can be solved individually. Once the solutions of displacement vectors are obtained, the floor loads acting on individual resisting elements can be determined. The forces in an element are given by the sum

of the lateral and torsional resisting forces. For element i in the x direction,

$$\{F_x\}_i = [K_x]_i(\{\Delta_x\} - ([Y]_i - [Y_T])\{\Delta_\theta\}) \qquad (2.61a)$$

For element j in the y direction, then

$$\{F_y\}_j = [K_y]_j(\{\Delta_y\} + ([X]_j - [X_T])\{\Delta_\theta\}) \qquad (2.61b)$$

Base on eqn. (2.61), it shows that it is difficult to identify those resisting elements of a multistory building being the most susceptible to the torsional load effect. Difficulties arise due to the following reasons:

(i) A scattering of the centers of rigidity on both sides of the mass centers will result in torque loadings not acting in the same direction at the floor levels. Thus some floor torques are counteracting floor torques at other levels. The net torsional effect is difficult to interpret.

(ii) Being an edge element does not guarantee that the element is most critical to torsional effect. The centers of twist can scatter on both sides of an edge element, as demonstrated by Building C under triangular distributed load (Fig. 2.4b). Thus it is difficult to provide a single measure to determine whether an element is furthest away from the centers of twist.

(iii) Wall-frame buildings can have different degrees of lateral and torsional wall-frame interaction. In

such case, the torsional shears in the walls may not always act in the same direction as the lateral shears along the height of the element. In other words, the torsional shears may counteract the lateral shears at certain levels, resulting in a smaller value of shear acting on the element. This situation will be illustrated with the aid of an example later in this section.

To show that the uncoupling procedure has merit, not only to provide a better physical insight, but also in computational sense, a program is prepared, based on the procedure outlined. The computation time for analysing a number of eccentric multistory buildings is compared, using the proposed procedure and also obtaining the solution directly by solving the 3N by 3N matrix formulation (coupled procedure) [35]. For each computation scheme, efficient algorithms are used. Evaluation of the two schemes is made by comparing the CPU time required in (i) solving for the global structural displacement vectors $\{\delta\}$ and $\{\Delta\}$ in the solution phase; and (ii) determining the floor loads on the resisting frames in the backsubstitution phase. The torque vector $\{P_\theta^*\}$ as defined by eqn. (2.56) is used in the computation. A summary of the algorithms employed in each phase of the schemes are given in Table 2.3.

An eight, sixteen and thirty-two story asymmetric

uniform wall-frame building with floor plan shown in Fig. 2.5 will be used as sample structures. Structures with the same floor plan had been used by Glück in multistory building studies [13]. Each building has an uniform floor height of three meters and the lateral resisting elements consist of planar walls and frames spanning the y direction and two identical walls spanning the x direction. The frames are modelled as shear beams with due consideration to account for the flexibility of connecting beams. The properties of the resisting elements are given in Table 2.4. Each building is subjected to a distributed lateral loading of 4×10^4 N/m uniform along its height.

Identical results were obtained using the two analysis schemes. The distribution of the centers of twist and centers of rigidity is shown in Fig. 2.6 for the sixteen story building. Again, the center of twist and center of rigidity are not the same point at each floor. Also, the loci of these centers do not lie on vertical axes. The significant scattering of these centers from vertical axes are due to wall-frame interaction which exists in these example buildings. The shears in the right edge wall (element 9) are plotted in Fig. 2.7. Through the concept of eccentricity, the proposed procedure makes it possible to isolate the torsional load effect from the lateral load effect. At the bottom nine floors, and also the top two

floors, the torsional effect due to the eccentric lateral loads actually reduces the total lateral shears in this element. Thus the edge elements are not necessarily most susceptible to torsional effect in the case of eccentric wall-frame structures. This finding, contrary to common expectation, is a consequence of the complex wall-frame interaction effect existing in the example buildings considered. A more detail study of eccentric wall-frame buildings will be given in chapter 4.

The CPU seconds required in each phase on a CDC CYBER 815 computer are listed in Table 2.5. It can be seen that the proposed procedure has an advantage over the coupled scheme, requiring only about half of the computation time in the solution phase. In the backsubstitution phase, the proposed procedure is more mathematically involved thereby requiring more computation effort. However, such draw back is offset by the gain in the solution phase which consumes the major portion of computation time in the overall analysis process. The overall advantage of the present scheme over the coupled scheme is 66%, 96% and 116% respectively for the eight, sixteen and thirty-two story building. With increasing number of stories, the amount of computation time saved can be significant.

2.3.7 Torsional Provisions in Seismic Codes as Applied to Multistory Buildings

With the proposed procedure based on the use of standard plane frame programs, the centers of rigidity can conveniently be located for a multistory building. With the rigidity centers determined, the structural eccentricities will also be defined. However, complications can arise in applying the computed values of floor eccentricities to the torsional provisions in building codes. This is because of the possible scattering of the rigidity centers along the height of the building [8,9]. For discussion purposes, Building A, B and C (Fig. 2.2) will again be used in this section as example structures. Building A has proportional framing and the mass and rigidity centers fall on two vertical lines. For this type of buildings, there would be no problem of interpretation and the code would provide adequate provisions to allow for the seismic torsional effects. Once deviated from proportional framing, the rigidity centers no longer lie on a vertical axis, as demonstrated by Building B and C. It is observed that the centers of rigidity can be located on either side of the centers of mass of the floors. Since the floor eccentricity is defined as the distance measured from the center of rigidity to the center of mass at that floor, one would therefore encounter both positive and negative values of

floor eccentricities for Building B and C, which in turn makes the interpretation of the code provisions difficult.

To simplify the interpretation, one simple, but not strictly correct way is to treat the center of rigidity at each floor to be the stiffness center at that floor. The locations of the centers of rigidity determined in this manner were shown as solid lines in Fig. 2.4. The floor eccentricity based on such locations of the centers of rigidity is denoted as e^*, in contrast to the true floor eccentricity "e".

The seismic shears in some elements of these buildings will be determined next, assuming each building is located in Vancouver, Canada. The acceleration related and velocity related seismic zone (Za and Zv respectively) are both zone four in this case. The buildings have a fundamental period of 0.6 seconds and will be subjected to seismic ground excitation in the y direction. The base shear is determined according to the base shear formula of NBCC 1985. The distribution of the design base shear as lateral loadings at floor levels is computed based on two approaches. The first approach relies on the static equivalent loading distribution as suggested by NBCC 1985. In the second approach, a dynamic modal response analysis is carried out for each building. To make the comparison

meaningful, the base shear as determined by dynamic analysis is normalized to the static base shear value. The interstory shear distribution is obtained by combining the first five modes of modal contributions to interstory shears in a square-root-sum-square (SRSS) manner. For ease of identification, any quantity obtained by combining the first five modal responses is labelled as "dynamic" in this section.

Shown in Fig. 2.8 is the comparison of the interstory shear force envelopes based on NBCC 1985 and dynamic analysis. The results based on dynamic analysis is larger than those based on NBCC 1985 at the top portion of the buildings. This can be expected since there is no correction for the higher modal contributions in the static code computation for these buildings (F_t = 0, [3]). However, the difference between the static and dynamic results is small, and both approaches give a similar pattern of load distribution.

One of the most important effects due to torsional response is the additional interstory shears, commonly referred to as the torsional shears, on certain resisting elements of the building. It is usual to consider the resisting element that is furthest away from the centers of twist and is located on the same side as the centers of mass as the element most susceptible to this torsional shear

effect. For this reason, the interstory shear envelopes are calculated for element 4 of each of the three buildings. Shown in Fig. 2.9a are the shear envelopes of wall 4 of Building A. Three curves are shown in the figure. They are calculated based on (i) dynamic modal analysis including first five modal contributions; (ii) the code design eccentricity formula according to NBCC 1985, namely $e_n = 1.5e + 0.10D_n$; and (iii) when the effect of torsion is neglected. On one hand, the shear envelope determined by dynamic analysis represents the best estimate of the interstory shear in that element. The shear envelopes obtained based on code provisions is an attempt to approximate the dynamic shear envelope. On the other hand, the difference between the shear envelopes determined by static analysis and that with torsion ignored represents the torsional shears on the resisting element as predicted by the code.

From Fig. 2.9a, it is seen that the torsional shears on the edge wall are in fact significant. Also, the code procedures lead to results which are in good agreement with that from dynamic analysis. Since Building A has proportional framing and the centers of rigidity and centers of mass lie on two vertical straight lines, such an agreement could have been anticipated.

Shown in Fig. 2.9b are the shear envelopes for wall 4 of Building B. The computation of the shear envelope based on the code procedures is carried out using the approximate floor eccentricity value e^*. Despite the crude nature by which e^* is determined, the shear envelope using the code procedures and taking e^* as the structural eccentricity did provide a good estimation of the interstory shears for wall 4. Similar to Building A, the torsional shears are significant for the design of this element, as evident from the total shear and lateral shear (torsion ignored) envelopes shown.

The interstory shears in frame 4 of the eccentric wall-frame building C are shown in Fig. 2.10. To be able to apply the design eccentricity equations, it is assumed that the centers of twist coincide with the centers of stiffness of this building. Further, the floor eccentricity is again taken to be e^* for use in code procedure computation. Two observations can be made in this figure. First, the torsional shears in this frame is in general small. For certain locations along the height of the frame, the lateral shears become larger than the total shears, suggesting that torsion has in fact a beneficial effect at these locations of the frame. Second, the code procedures provide a resonable estimate of the dynamic shears, at least for this frame.

However, due to the complexity of wall-frame interaction in Building C, the conventional notion that frame 4 will be the resisting element most susceptible to torsional effect is no longer valid. This can be seen by examining the shear envelopes of wall 1 in Building C, as shown in Fig. 2.10. The design eccentricity used for this frame is $e_n = 0.5e^* - 0.10D_n$. One can see that over most of the wall torsional shears are substantial.

Based on the examples studied, it is shown that NBCC 1985 provides a good estimate of the torsional shears for Building A. It is the class of regular eccentric structures to which the code provisions are applicable. For other buildings with scattering of the rigidity centers, the distribution of torsional effect can be complicated. The code provisions may (as in the case of Building B) or may not (as in the case of Building C) provide reasonable estimates of the torsional shears. Therefore, the most reliable way to estimate the torsional effect is by means of dynamic analysis.

2.3.8 Summary

In this chapter, the eccentricity concept is extended from single story structures to multistory structures. It is shown that the center of rigidity at each

floor can be interpreted as the center of the lateral resisting loads in the elements. The centers of rigidity of a multistory building will both be a function of the stiffness distribution and lateral load distribution of the building. With the rigidity centers located, the structural eccentricities at the floor levels are also defined.

A practical procedure is suggested to determine the locations of the centers of rigidity for multistory buildings. Despite the complexity of the structural framing, the suggested procedure involves only the use of standard plane frame program and is a procedure well suited for design office use. Since an explicit statement is given in NBCC 1985 that the seismic torsional provisions are applicable to eccentric buildings with locations of centers of mass and centers of rigidity along vertical axes, the procedure is an useful means to determine whether one can apply the codified torsional provisions with confidence.

The centers of twist are a set of convenient points of reference in lateral load analysis of buildings. Formulation of the lateral load problem with respect to the centers of twist will lead to an uncoupling of the equation of equilibrium. The uncoupled analysis procedure has two advantages over the conventional approach in solving the coupled 3N equations of equilibrium. First, by separating the lateral effect from the torsional effect, it provides

better insight into the structural behaviour of the building under eccentric lateral loads. This is particularly valuable during the design phase of the building. Second, the proposed procedure is a more efficient way to obtain numerically the solution to the problem. A factor of two in saving of computation time resulted for the 32 story building example used. The saving increases with increase of the number of stories in a building. In view of these advantages, it is believed that the proposed scheme is a viable procedure to be incorporated in all the standard three-dimensional structural analysis programs.

The conditions under which the centers of rigidity and centers of twist will be load distribution independent are determined. It shows that for multistory buildings with proportional framing, not only the centers of rigidity and centers of twist are load distribution independent, but the two centers are coincident and also lie on a vertical axis. For this class of multistory buildings, the locations of the centers of rigidity can be determined on a per floor basis, treating each floor as a single story building.

The centers of rigidity, centers of stiffness, shear centers and centers of twist are in general different sets of points for multistory buildings. Buildings with proportional framing is one special class of structures that

all four centers will represent the same set of points for such buildings.

By means of examples, the locations of the centers of rigidity and the ability of the codified torsional procedure to estimate the interstory shear envelope in three eccentric buildings are presented. It is shown that for buildings with centers of rigidity located along a vertical axis, the code procedures provide a good estimate of the torsional shear distribution. For buildings with centers of rigidity scattered from a vertical axis, the code procedures may or may not provide a good estimate of the torsional effect. Therefore, one should interpret that the condition of centers of rigidity located along a vertical axis to be a sufficient, but not a necessary condition for the NBCC 1985 torsional provisions to be applicable. Further, the second example (Building B) showed that even with a slight deviation from proportional framing, the rigidity centers showed wide scattering from a vertical axis. It would be reasonable to expect such scattering will exist in most buildings where non-proportional framing is the rule rather than the exception. Therefore, requiring the rigidity centers to be on a vertical axis may not be the best criterion to determine whether code provisions for torsion are applicable to a particular building. When in doubt, the evaluation of torsional effect is best done by means of

dynamic analysis.

2.4 Notations

D_n = plan dimension of building in the direction of the computed eccentricity

e = structural eccentricity

e_n = design eccentricity at level n

$e_x, \{e_x\}$ = structural eccentricity in the x direction

e^* = structural eccentricity measured with respect to stiffness center

F_t = portion of base shear to be concentrated at top of structure

$(F_x)_i$, $\{F_x\}_i$ = total resisting force(s) in element i

$(f_x^L)_i$, $\{f_x^L\}_i$ = resisting force(s) in element i due to lateral load effect

$(f_x^T)_i$, $\{f_x^T\}_i$ = resisting force(s) in element i due to torsional load effect

$\{I\}, [I]$ = identity vector and identity matrix, respectively

I_p = polar mass of inertia about mass center

i, j = element identifiers

$[K], [K^*]$ = overall, global stiffness matrix of a structure with respect to the z reference axis and twist centers, respectively

$(k_x)_i$, $[K_x]_i$ = stiffness and stiffness matrix of element i, respectively

$[\bar{K}]_x$ = characteristic matrix for elements in the x direction

M_{tn} = design torsional moment at level n

m = floor mass

N = total number of floors

n = floor level identifier

$\{P\}, \{P^*\}$ = load vector with respect to the reference z axis and twist centers, respectively

$P_x, \{P_x\}, [P_x]$ = applied lateral load(s) in the x direction

$P_\theta, \{P_\theta\}, \{P^*_\theta\}$ = applied torque(s)

V = design base shear

V_n = design shear at level n

W = work done by applied loads

$X_j, [X]_j$ = x coordinate position(s) of element j

$\{X_L\}, [X_L]$ = x coordinate positions of the centers of rigidity

$X_m, \{X_m\}$ = x coordinate position(s) of the applied loads

X_R = x coordiante position of the center of rigidity

$X_T, \{X_T\}, [X_T]$ = x coordinate position(s) of the centers of twist

Za, Zv = acceleration and velocity related zone, respectively

$\{0\}, [0]$ = null vector and null matrix, respectively

α_i, β_j = proportional constants

$[\Gamma]$ = transformation matrix

$\delta_x, \{\delta_x\}, \{\Delta_x\}$ = translational displacement(s) in the x direction

δ_{xi} = displacement of element i due to rotation of roof slab

$\delta_\theta, \{\delta_\theta\}, \{\Delta_\theta\}$ = rotational displacement(s)

$\{\delta\}, \{\Delta\}$ = global displacement vector with respect to the z reference axis and twist centers, respectively

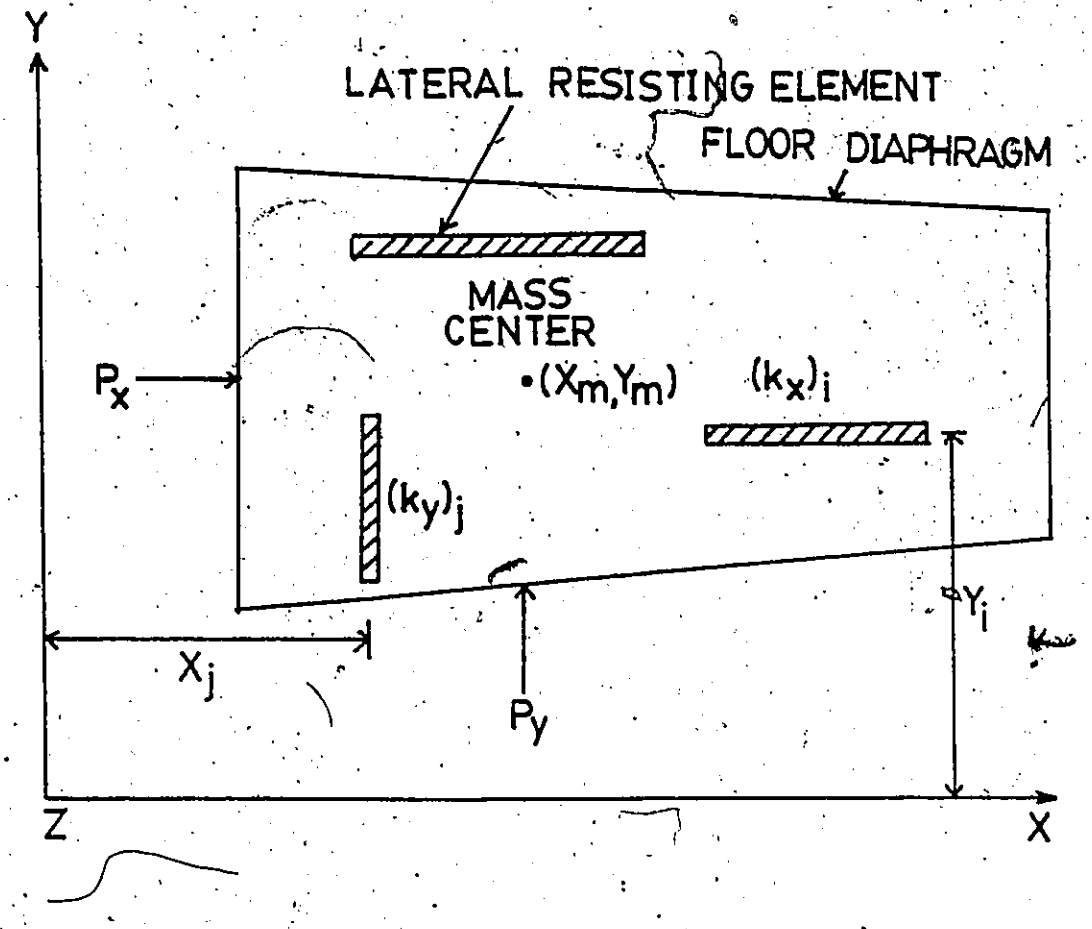

Fig. 2.1 Arrangement of Resisting Elements in Plane of Building

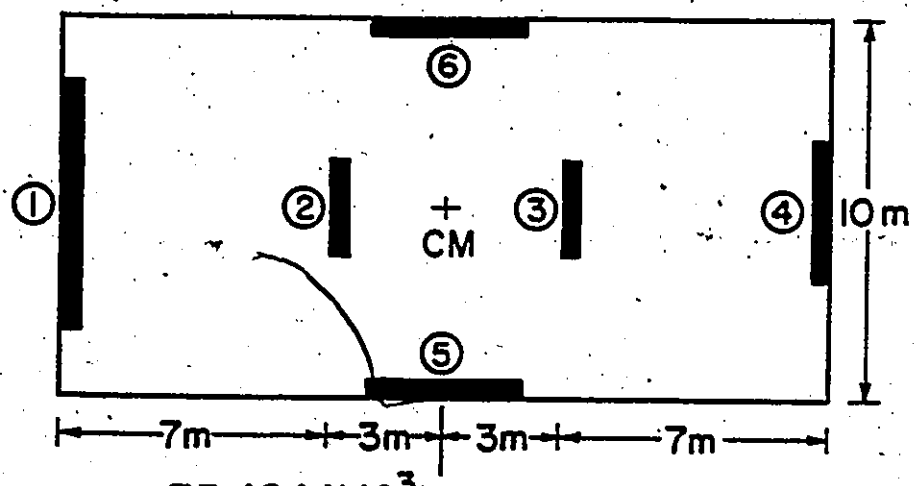

$m = 73.424 \times 10^3 kg$

$I_p = 3.0594 \times 10^6 kg \cdot m^2$

(a) Framing plan of Building A and B

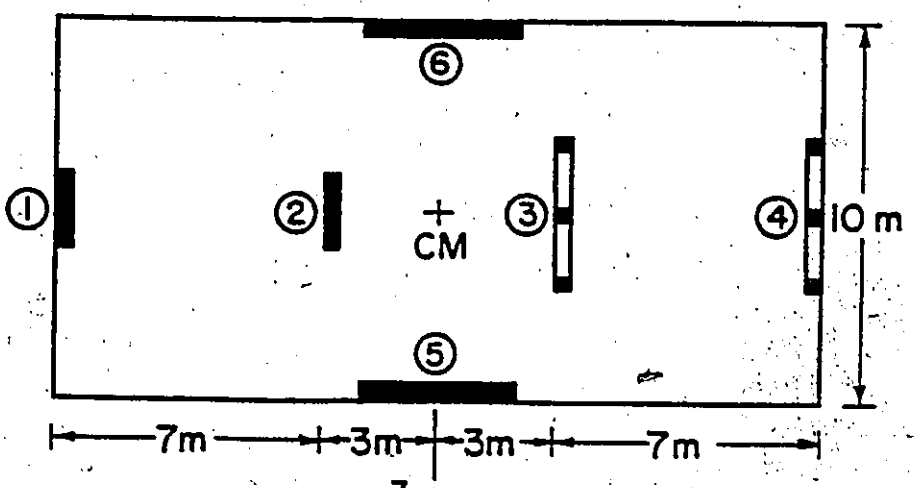

$m = 73.424 \times 10^3 kg$

$I_p = 3.0594 \times 10^6 kg \cdot m^2$

(b) Framing plan of Building C

Fig. 2.2 Framing Plans of Building A, B and C

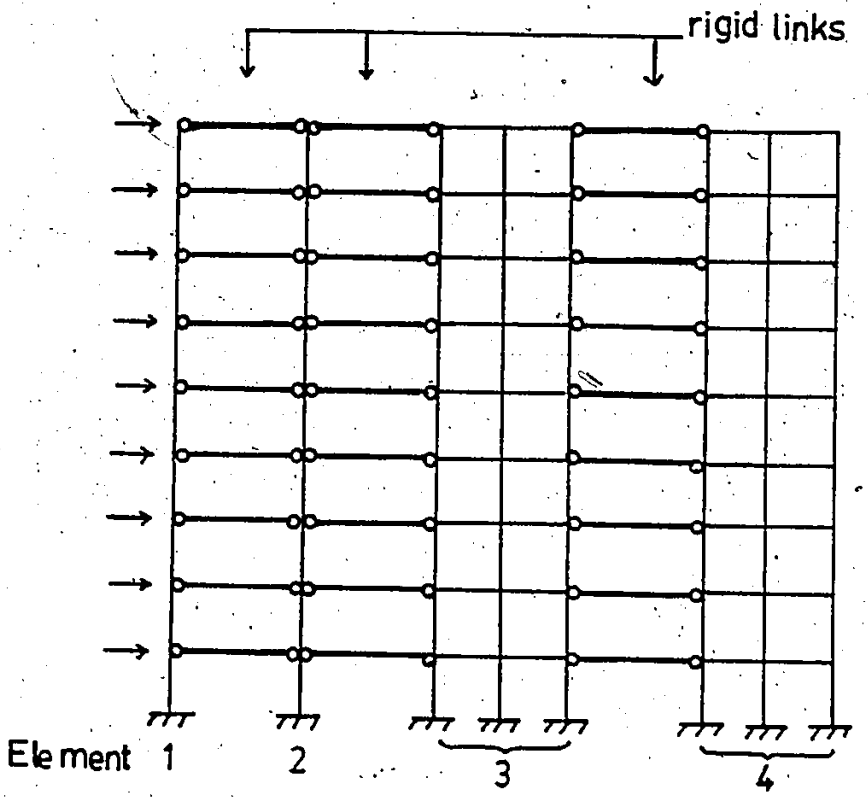

Fig. 2.3 Computer Model for Building C

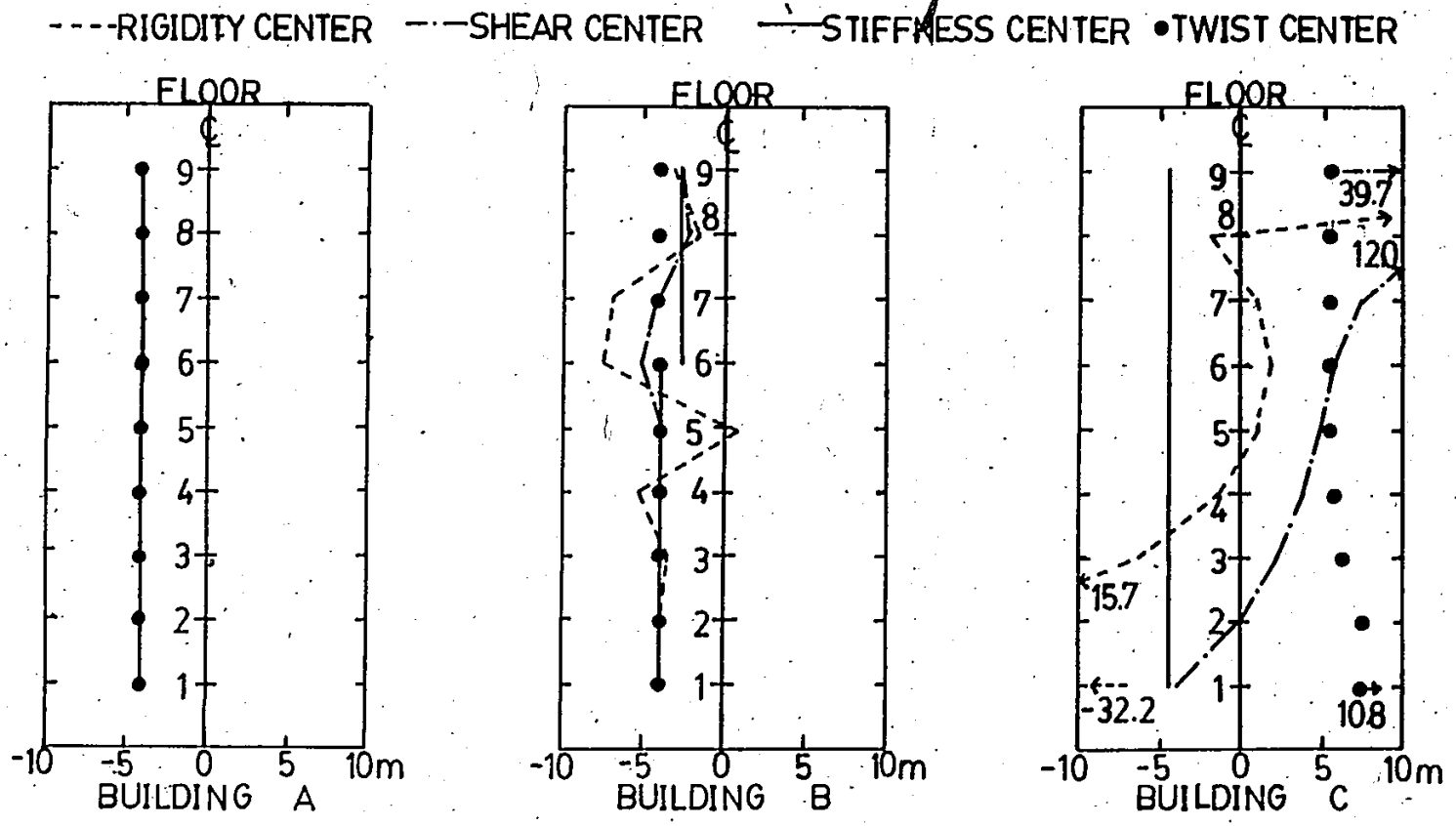

Fig. 2.4a Distribution of Rigidity, Shear, Stiffness and Twist Centers for Building A, B and C under Uniform Distributed Load

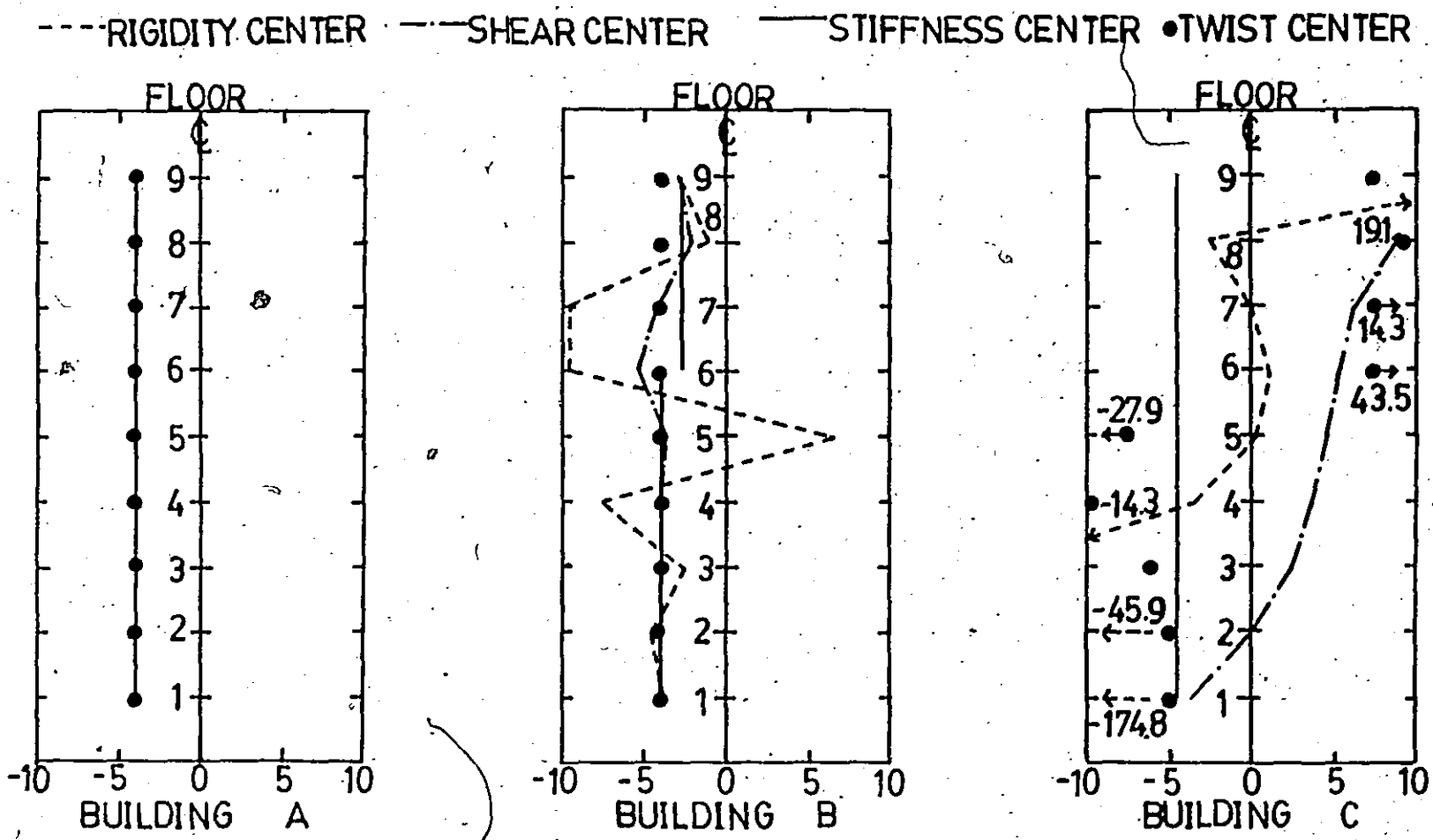

Fig. 2.4b Distribution of Rigidity, Shear, Stiffness and Twist Centers for Building A, B and C under Inverted Triangular Distributed Load

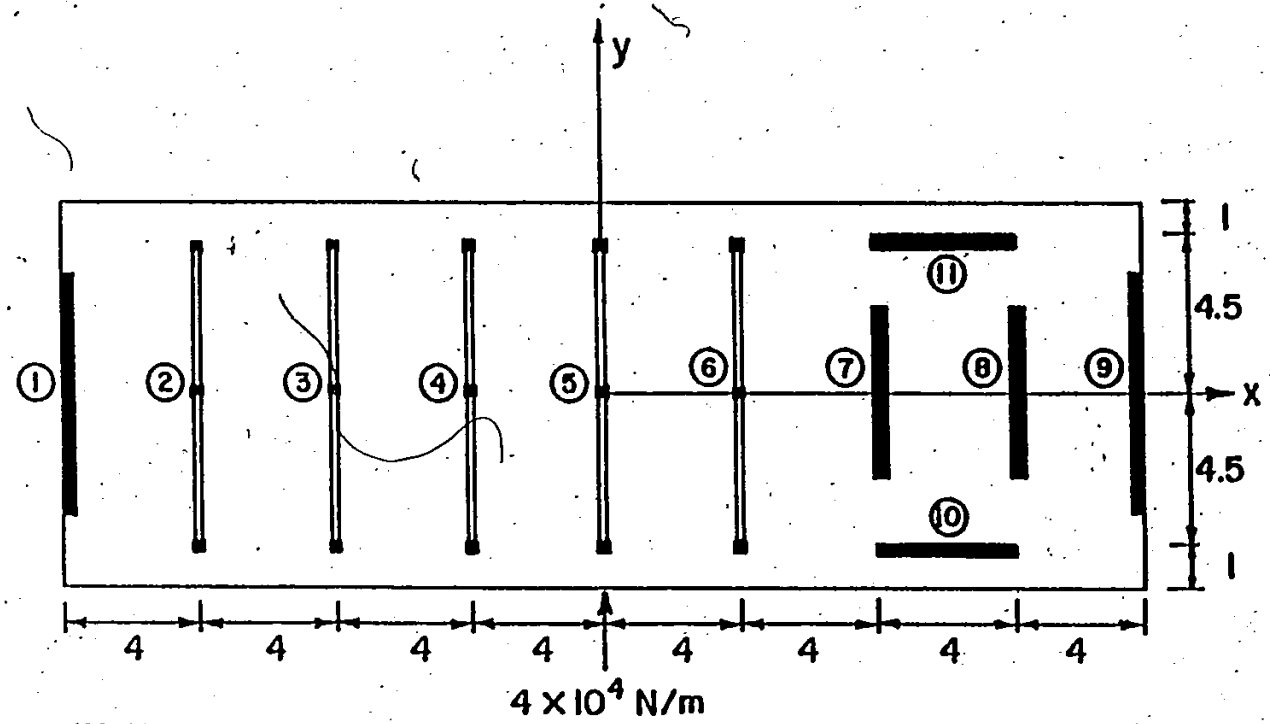

ALL DIMENSIONS IN METERS

Fig. 2.5 Framing Plan of the 8, 16 and 32 story Wall-Frame Building

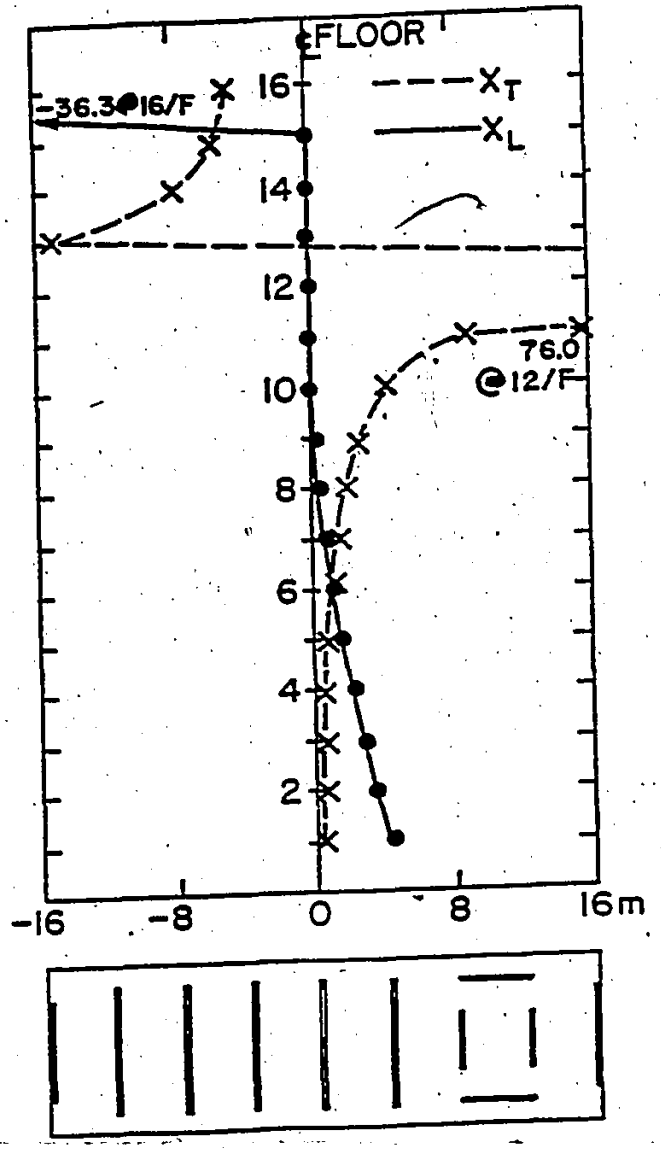

Fig. 2.6 Distribution of Rigidity and Twist Centers for the 16 Story Wall-Frame Building

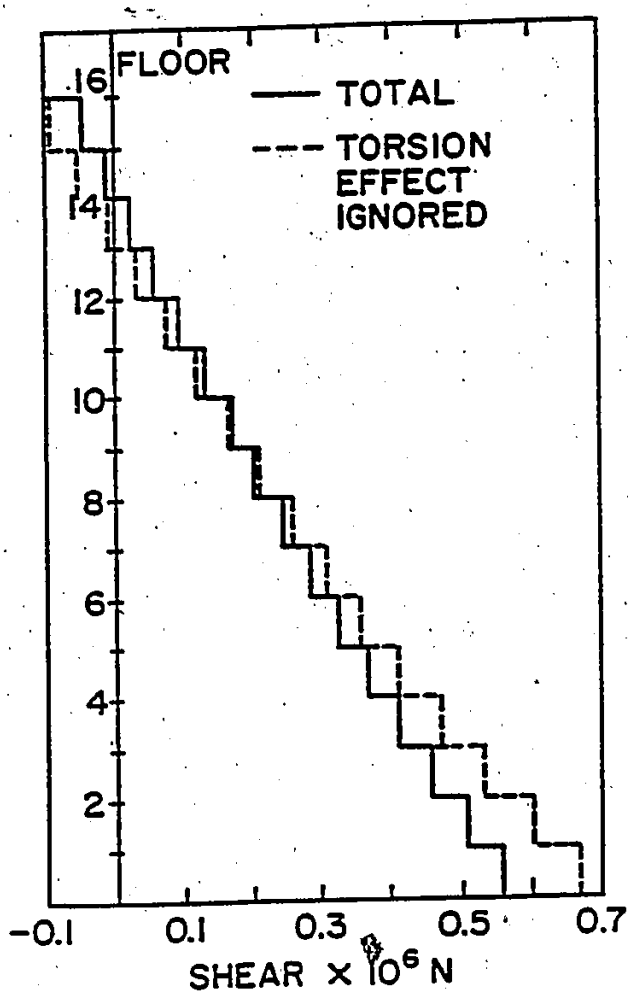

Fig. 2.7 Shear Distribution in Element 9 of the 16 Story Wall-Frame Building

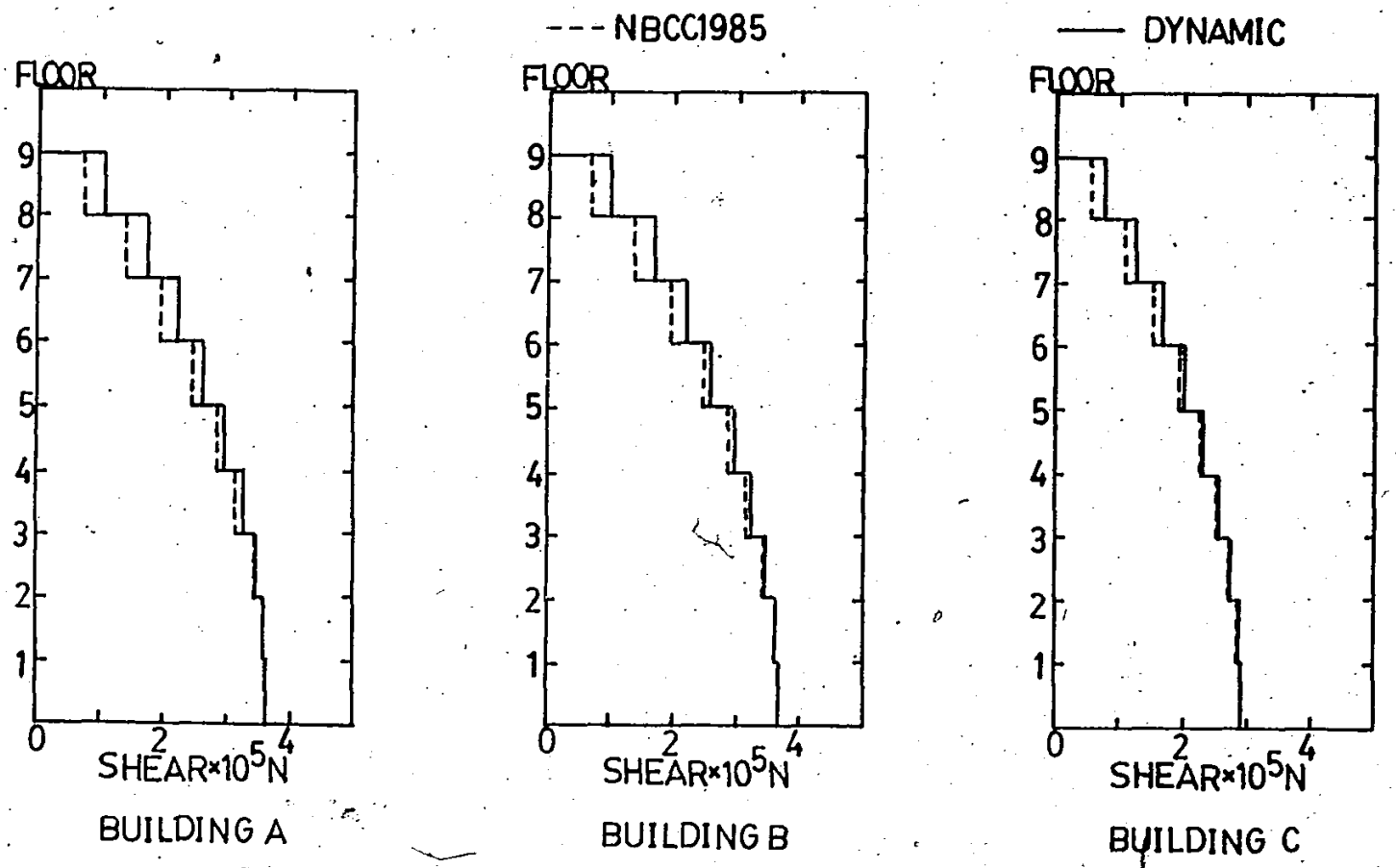

Fig. 2.8 Interstory Shear Envelopes of Building A, B and C

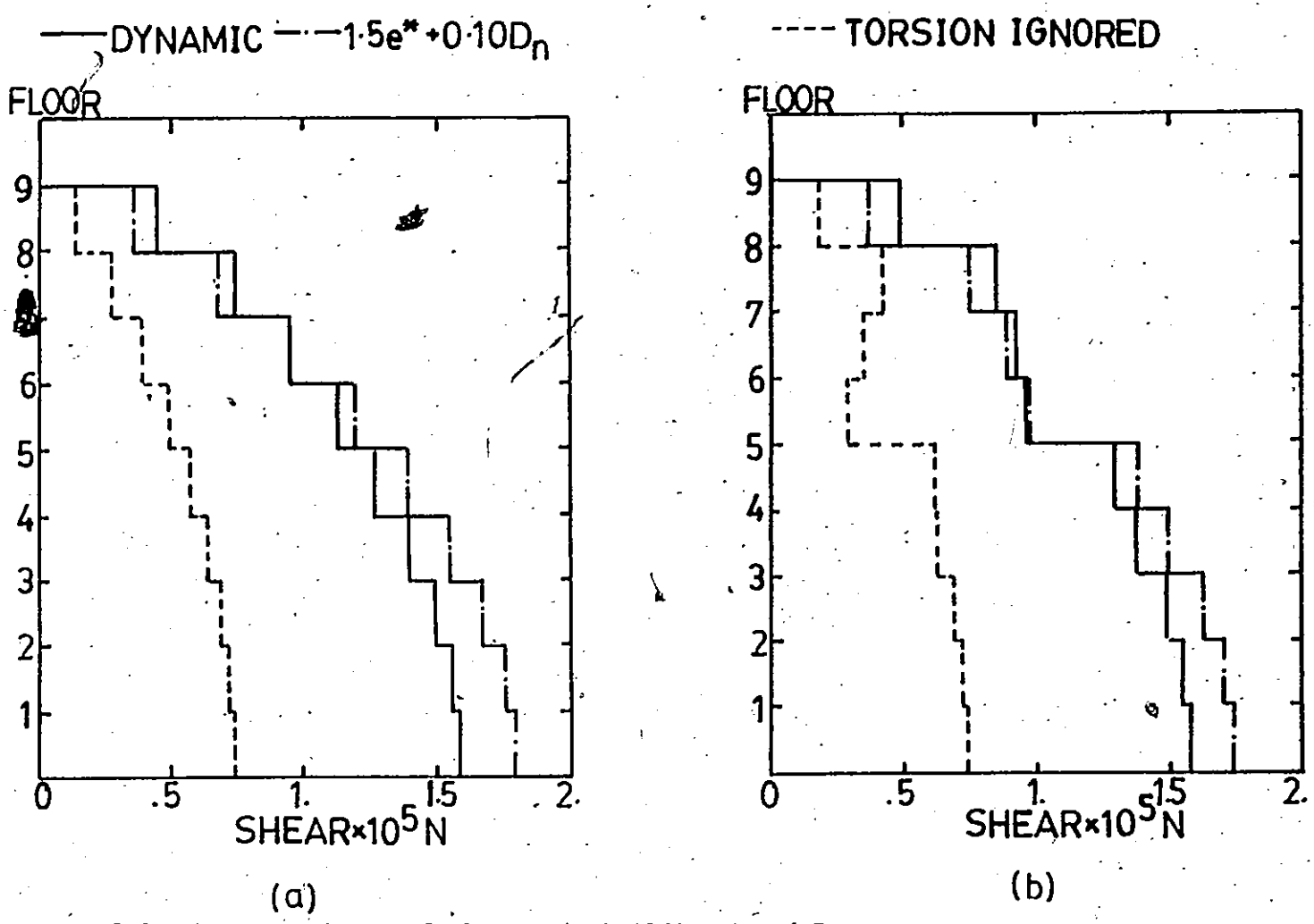

Fig. 2.9 Shear Envelopes of Element 4, Building A and B

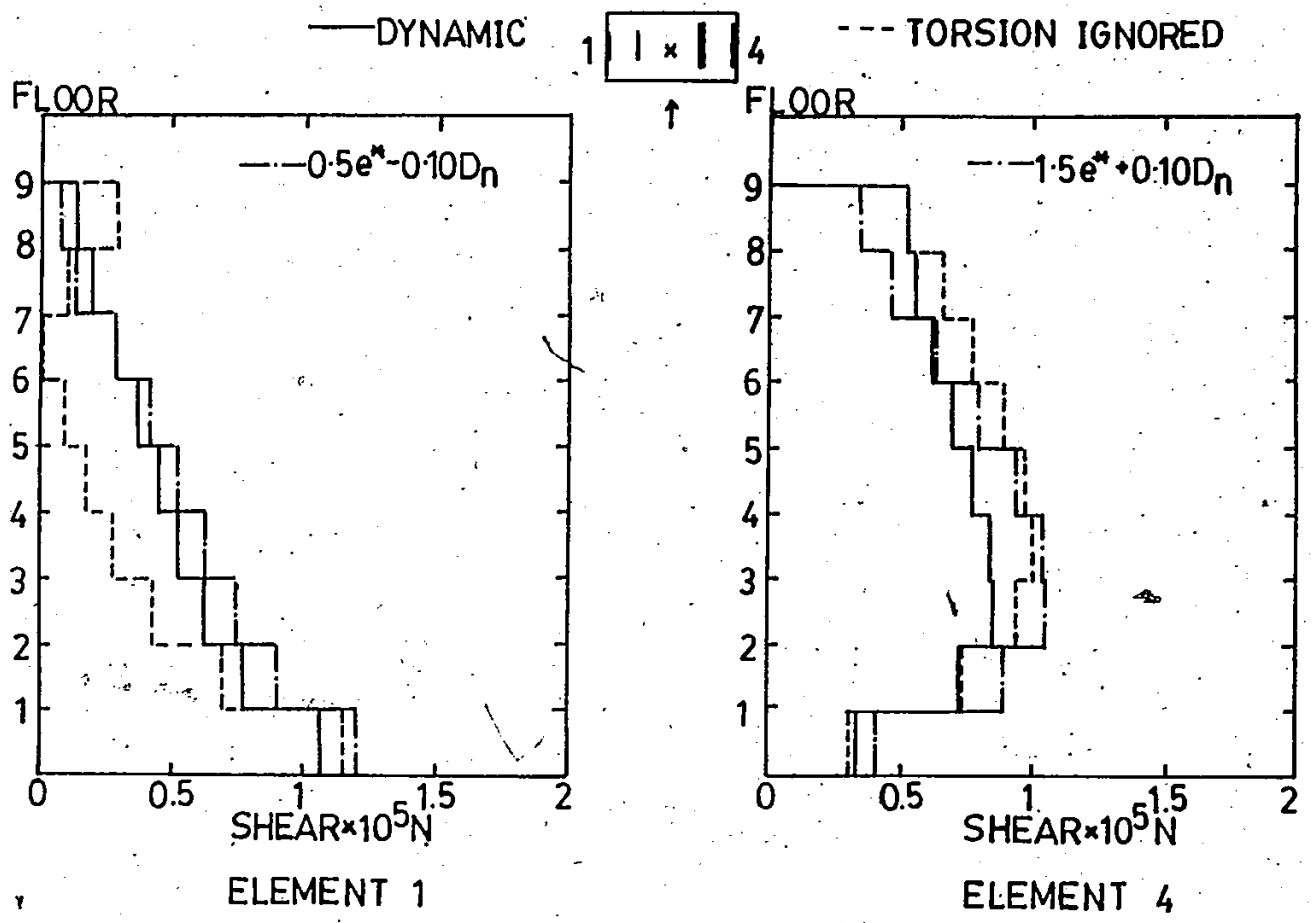

Fig. 2.10 Shear Envelopes of Element 1 and 4, Building C

Table 2.1 DESIGN ECCENTRICITIES FROM SEISMIC CODES OF DIFFERENT COUNTRIES

Country	Design Eccentricity
Canada [3][1,3]	$e_n = 1.5e + 0.10D_n$
	or $e_n = 0.5e - 0.10D_n$
Germany [6][1]	$e_n = e + e_1 + 0.05D_n$
	or $e_n = e - 0.05D_n$
Mexico [27][1]	$e_n = 1.5e + 0.10D_n$
	or $e_n = e - 0.10D_n$
New Zealand [12][1]	$e_n = 1.7e - e^2/D_n + 0.10D_n$
	or $e_n = e - 0.10D_n$
Turkey [21]	$e_n = e + 0.05D_n$
U.S.A. [31][2] (SEAOC)	$e_n = e + 0.05D_n$
U.S.A. [1][1] (ATC 3-06)	$e_n = e + 0.05D_n$
	or $e_n = e - 0.05D_n$

e = structural eccentricity
e_1 = eccentricity factor to allow for sympathetic resonance effect
D_n = plan dimension of floor
1 Torsional shear on member based on worse of two cases
2 Negative torsional shear on member neglected
3 Applicable to buildings with mass and rigidity centers falling on two vertical lines

Table 2.2 FLEXURAL AND SHEAR RIGIDITIES OF RESISTING ELEMENTS IN BUILDING A, B AND C

Building	Floor	Elements					
		1	2	3	4	5	6
A	7/F-9/F	12EI	2EI	2EI	4EI	5EI	5EI
	1/F-6/F	18EI	3EI	3EI	6EI	7.5EI	7.5EI
B	7/F-9/F	12EI	2EI	2EI	6EI	5EI	5EI
	1/F-6/F	18EI	3EI	3EI	6EI	7.5EI	7.5EI
C	1/F-9/F	2.4EI	2.4EI	GA	GA	16.2EI	16.2EI

$EI = 6.4 \times 10^9 N.m^2$

$GA = 0.526 \times 10^9 N$

TABLE 2.3 ALGORITHMS EMPLOYED IN THE COUPLED AND UNCOUPLED ANALYSIS SCHEME

Coupled Scheme	Uncoupled Scheme
1. Solve the equilibrium equation $\begin{bmatrix} [K_{xx}] & [0] & [K_{x\theta}] \\ [0] & [K_{yy}] & [K_{y\theta}] \\ [K_{\theta x}] & [K_{\theta y}] & [K_{\theta\theta}] \end{bmatrix} \begin{Bmatrix} \{\delta_x\} \\ \{\delta_y\} \\ \{\delta_\theta\} \end{Bmatrix} = \begin{Bmatrix} \{P_x\} \\ \{P_y\} \\ \{P_\theta\} \end{Bmatrix}$ by elimination procedures	1. Invert $[K_{xx}]$ and $[K_{yy}]$ 2. Form the products $[A] = [K_{xx}]^{-1}[K_{x\theta}]$ $[B] = [K_{yy}]^{-1}[K_{y\theta}]$ 3. Solve the equilibrium equations (a) $[K_{xx}]\{\Delta_x\}=\{P_x\}$ by inversion making use of $[K_{xx}]^{-1}$ from 1. (b) $[K_{yy}]\{\Delta_y\}=\{P_y\}$ by inversion making use of $[K_{yy}]^{-1}$ from 1. (c) $([K_{\theta\theta}]-[K_{\theta x}][A]-[K_{\theta y}][B])\{\Delta_\theta\} = \{P_\theta\}-[K_{\theta x}]\{\Delta_x\}-[K_{\theta y}]\{\Delta_y\}$ by elimination

(a) Solution Phase

Coupled Scheme	Uncoupled Scheme
1. Determine member forces $\{F_x\}_i=[K_x]_i(\{\delta_x\}-[Y]_i\{\delta_\theta\})$ $\{F_y\}_j=[K_y]_j(\{\delta_y\}+[X]_j\{\delta_\theta\})$	1. Locate the twist centers $\{X_T\}= [\Delta_\theta]^{-1}[B]\{\Delta_\theta\}$ $\{Y_T\}=-[\Delta_\theta]^{-1}[A]\{\Delta_\theta\}$ 2. Determine member forces $\{F_x\}_i=[K_x]_i(\{\Delta_x\}-([Y]_i-[Y_T])\{\Delta_\theta\})$ $\{F_y\}_j=[K_y]_j(\{\Delta_y\}+([X]_j-[X_T])\{\Delta_\theta\})$.

(b) Solution Phase.

TABLE 2.4 SUMMARY OF PROPERTIES OF ELEMENTS IN THE 8, 16 AND 32 STORY UNIFORM WALL-FRAME BUILDING

Element	Type	Rigidity
1,9	Wall	$EI=0.11433\times10^{12}N.m^2$
2-6	Frame	$GA=0.54536\times10^{8}N$
7,8	Wall	$EI=0.41668\times10^{11}N.m^2$
10,11	Wall	$EI=0.24696\times10^{10}N.m^2$

TABLE 2.5 COMPARISON OF COMPUTATION TIME

Structure	Scheme	CPU seconds		
		Solution Phase	Backsubstitution Phase	Total
8 story	Coupled	0.200	0.021	0.221
	Uncoupled	0.109	0.024	0.133
16 story	Coupled	1.474	0.069	1.543
	Uncoupled	0.695	0.094	0.789
32 story	Coupled	11.599	0.259	11.858
	Uncoupled	5.147	0.353	5.500

CHAPTER 3

LATERAL LOAD ANALYSIS OF BUILDINGS WITH SETBACK

3.1 Introduction

By means of the eccentricity concept, one can identify the translational and torsional response of multistory buildings under lateral loads. Each of the translational and torsional response component can be computed by matrix manipulation with the help of computers. However, such an approach is not particularly useful during preliminary design. Details in the configuration of the lateral load resisting system may not be readily available at this stage. For preliminary design purposes, it is preferable to have a hand calculation procedure to get an estimate of the load distribution in the different elements. Such an analysis will usually be performed on an idealized structural model of the building. The results are treated as a first iteration in the design process.

In highrise design, buildings can be classified, in general, as regular and irregular structures. Regular structures are defined as having no variation in geometry of the floor plan along its height. The lateral load resisting system of the regular structures will be of the

same type (i.e. either all frames or all walls). If the resisting elements were not uniform, the change in rigidity of each element needs to follow the same rule of variation along its height so that the framing is proportional. Proportional framing buildings have been defined in chapter 2. For such buildings, the distribution of lateral and torsional loads among resisting elements can be determined on a floor by floor basis. Such a distribution process can easily be carried out using hand calculation procedures.

The floor by floor treatment of load distribution can not be extended to irregular buildings since the resisting elements no longer bear the same ratio of rigidity along their heights. Buildings with setback is a class of irregular structures in which both the floor area and lateral stiffnesses are reduced at upper floors. As a result, it is generally not amenable to be analysed by hand calculation procedures. However, in this chapter, a hand method is presented to analyse the lateral load distribution on multistory buildings with setback occurring at one level. For buildings with lateral resisting elements that satisfy the assumptions in the theory, the procedure will lead to the exact solution of the problem. It is shown by example that even if the restrictions imposed are not satisfied exactly, the proposed procedure can still give an useful estimation of the load distribution among the

resisting elements for design purposes. The proposed method makes direct use of the eccentricity concept for multistory buildings as discussed in chapter 2, and can be considered as a nontrivial example of using this concept on asymmetrical multistory building design.

3.2 Buildings with Setback

Multistory buildings are designed with setbacks for architectural reasons or restrictions imposed by local by-laws [2]. In its simplest form, a building with setback can be considered to be made up of two portions - a tower and a base. The part of the structure above the setback level is identified as the tower and the part below as the base. To provide a tapering effect along the height, a building may have multiple setbacks, each starts at a different level. Depending on the location of the tower relative to the base, one can also classify setback structures into structures with symmetric setbacks and eccentric setbacks.

Due to the sudden change in stiffness at the setback, the load distribution is often complex in the neighbourhood of the setback level. When the setback is eccentrically located, further complication will arise due to the torsional effect.

Before proceeding to eccentric setback structures,

it will be useful to first understand the behaviour of symmetric setback structures. In the following section, the behaviour of symmetric setback structures under lateral loads will first be studied by employing the "displacement compatible load " concept [11].

3.3 Buildings with Symmetric Setback

Consider a multistory building with uniform floor height h and having a single setback along the X direction as shown in Fig. 3.1. For ease of reference, the complete building is divided into two parts, a highrise wing with N stories and a total height of Nh, and a lowrise wing of n stories with a height of nh. Lateral loads $2P_i$ (i=1,2,...,N) along the Y direction are assumed to be acting through the mass center of the floors. Making use of the symmetric nature of the problem, only one half of the building needs be considered, subjected to lateral loads P_i as shown in Fig. 3.1a. This half-building will be referred to as the reduced structure in this section. For simplicity, the lateral load resisting elements are taken to be flexural walls. Within the reduced structure there are a total of B walls in the building spanning the Y direction, with b walls (b<B) in the highrise wing. The walls are numbered consecutively starting from the left inner wall of the highrise wing. Therefore, wall j (j=1,2,...,b) are

walls within the highrise wing while wall j (J=b+1,b+2,...,B) are walls within the lowrise wing. The location of wall J relative to the YZ plane (taken to be the origin) is denoted by coordinate X_j. It is assumed that each wall is uniform with flexural rigidity $(EI)_j$ and floor slabs act as rigid diaphragms, capable of mobilizing the lateral resistance of all the walls.

Conceptually, one can view the highrise wing part of the reduced structure as being equivalent to a cantilever of length Nh and with bending rigidity given by EI^* where EI^* is the combined rigidity of the walls within the highrise wing. Similarly, the lowrise wing portion can be treated as another cantilever of length nh and bending rigidity EI^{**} where EI^{**} is the combined rigidity of the walls within the lowrise wing. These two cantilevers are connected at regular intervals of h up to the setback level via the diaphragm action of the floors. Since there will not be any rotational deformation of the structure when subjected to the lateral loadings, the lateral deflections in the Y direction of these two cantilevers have to be equal at floor levels for each floor up to the setback level. The conceptual model described is shown in Fig. 3.2.

The complication in distributing the lateral loads among the two cantilevers of unequal height is caused by

loadings above the setback level. If there were no load applied above the setback, the loadings at and below the setback can be distributed to the cantilevers in proportion to their relative stiffnesses. This way of load proportioning ensures that both the conditions of equilibrium and compatibility are satisfied at each floor level. However, with applied loads existed above the setback level, and being taken by the highrise cantilever, additional deflections of the highrise cantilever at floors below the setback level will occur. As a result, proportioning the applied loads below the setback level according to the relative stiffnesses of the cantilevers would violate the compatibility requirement at floor levels below the setback.

Based on this observation, the technique of "displacement compatible" loadings is used. For this technique, the applied loadings are divided into two parts. The first loading condition consists of the applied loads above the setback level plus a set of "displacement compatible" loads $(P_c)_i$ acting at and below the setback level on the highrise cantilever and no loading on the lowrise cantilever. The set of displacement compatible loads, or compatible loads for short, is such that it will produce deflections which will nullify the deflections at and below the setback level caused by loadings on the

highrise cantilever above the setback. As a result, compatibility conditions are maintained between the two cantilevers under this part of loading. The second loading condition consists of the difference of the total loadings and loadings of the first part. This second loading is applied at and below the setback level only. The distribution of this part of loading can be carried out in proportion to the relative stiffness of the individual cantilever. Such distribution will again maintain the compatibility conditions required between the two cantilevers. The actual loads applied to each of the cantilever will be the sum of the load contributions resulting from the first and second loading condition. This technique is schematically illustrated in Fig. 3.3.

To establish the first loading condition, consider an imaginary cut being made to separate the highrise and lowrise cantilever. Above the setback level, the highrise cantilever takes the entire applied loads P_i $(i>n)$. These loads will cause deflections Δ_i at floor levels. The deflections Δ_i $(i<n)$ at and below the setback level can be computed based on a cantilever of length nh and rigidity EI^* subjected to an end force S and an end moment M. The force S and moment M are the base shear and overturning moment respectively at the setback level caused by the applied

loads P_i $(i>n)$ on the tower portion. These floor deflections can therefore be written as

$$\Delta_i = (\Delta_i)_S + (\Delta_i)_M \qquad (3.1)$$

where subscripts S and M denote quantities associated with end force S and moment M respectively.

The set of compatible loads is determined such that they will produce deflections equal but opposite to those defined by eqn.(3.1). Application of a force equals but opposite to the shear force at the setback level will produce deflections that cancels $(\Delta_i)_S$. To obtain the compatible loads which will cancel the deflections $(\Delta_i)_M$ as defined in eqn. (3.1), the superposition principle can be used. One can consider the load effect of a cantilever subjected to an end moment M being the combined effect of two loading conditions. The first consists of a set of loadings at floor levels and the end moment M. The set of loadings at floor levels are chosen such that there will be no net deflection at these floor levels. The second consists of loadings at floor levels equal in magnitude but opposite to those floor loads of the first loading, as illustrated in Fig. 3.4. The first loading in Fig. 3.4 is equivalent to the case of a cantilever with intermediate rigid supports at regular intervals subjected to end moment M. Therefore, the set of compatible loads that will cancel the deflections $(\Delta_i)_M$ is equal to the reactions at these

supports. The reaction forces R_i can be expressed as

$$R_i = \frac{M}{h} K_i \qquad (i<n) \qquad (3.2)$$

where K_i is a set of numerical coefficients readily obtainable from structural analysis. The values of K_i depend on the height of the setback level above the ground. For a given setback height, K_i decreases rapidly for floors located remote from the setback level. Table 3.1 shows typical values of K_i. For practical purposes, one can ignore the values of K_i for floors beyond three stories down from the setback level. The displacement compatible loads can then be written as

$$(P_c)_i = -S\bar{\delta}_{in} + R_i \qquad (i<n) \qquad (3.3)$$

where $\bar{\delta}_{in}$ is the Kronecker delta.

Substracting the first part of loadings from the applied loadings, the second part of loadings is given by $P_i - (P_c)_i$, $(i<n)$. The second part of loadings can then be distributed between the two cantilevers according to their stiffnesses in the region below the setback level. Thus, the final distribution of loadings on the highrise cantilever F_i^* is as follows:

Above the setback level,

$$F_i^* = P_i \qquad (i>n) \qquad (3.4)$$

At and below the setback level,

$$F_i^* = (P_c)_i + \frac{EI^*}{(EI^* + EI^{**})}[P_i - (P_c)_i] \qquad (3.5)$$

$$= \frac{1}{(EI^* + EI^{**})}[EI^* P_i + EI^{**}(P_c)_i] \qquad (i \leq n)$$

The final loadings on the lowrise cantilever F_i^{**} $(i \leq n)$ are equal to the proportional loads due to the second loading condition. Mathematically,

$$F_i^{**} = \frac{EI^{**}}{(EI^* + EI^{**})}[P_i - (P_c)_i] \qquad (i \leq n) \qquad (3.6)$$

Once F_i^* and F_i^{**} are determined, the loadings on the individual walls can be obtained by the proportional stiffness rule. The loading at the i^{th} floor on the j^{th} wall in the highrise wing is given by

$$(F_j)_i = \frac{(EI)_j}{EI^*} F_i^* \qquad (i \leq N) \qquad (3.7)$$

$$(j=1,2,..,b)$$

The loading on individual walls in the lowrise wing is

$$(F_j)_i = \frac{(EI)_j}{EI^{**}} F_i^{**} \qquad (i \leq n) \qquad (3.8)$$

$$(j=b+1,..,B)$$

3.4 Buildings with Eccentric Setback

The additional complications involved in eccentric setback structures are twofold. First, it is necessary to

establish the torsional loadings, based on the applied loads and the eccentricities of the building caused by the eccentric setback. Second, it is necessary to evaluate the additional loadings on the individual elements due to the overall torsional effect. Therefore, there are three steps involved in the determination of load distribution among resisting elements in buildings with eccentric setback subjected to lateral loads. These are: (i) evaluation of load distribution on elements due to the lateral loadings, assuming no rotational deformation of the building will take place, (ii) evaluation of the torsional loadings on the structure and (iii) determination of the load distribution on different resisting elements under the torsional loads. The final loadings on each element will be the combination of results from steps (i) and (iii).

Consider a N story building with uniform floor height h having a single eccentric setback along the X direction only. The building is subjected to lateral loads P_i (i = 1,2,...,N) along the Y direction. The load resultant at each floor is assumed to be located at a distance $(X_p)_i$ from the origin, as shown in Fig. 3.5. The structural configuration analysed is similar to that of the reduced structure shown in Fig. 3.1a. The essential difference is that torsional response is expected in the

current analysis.

Let the location of the center of rigidity at each floor be denoted as $(X_L)_i$. Then, one can replace the original applied lateral loads by an equivalent loading consisting of a set of lateral load resultants acting through the center of rigidity at each floor together with a set of floor torques T_i (Fig. 3.6). The magnitude of the floor torques are given by

$$T_i = P_i [(X_p)_i - (X_L)_i] \qquad (3.9)$$

The first set of loadings produces translational displacements only and will be referred to as the translational loadings. The distribution of these translational loadings to the different wall elements can be treated using the procedure as suggested for buildings with symmetric setback; as presented in the previous section. The second set of loadings will produce torsional deformations and are referred to as torsional loadings. As defined in eqn.(3.9), the torsional loadings can be determined if the location of the center of rigidity $(X_L)_i$ at each floor is known. It has been shown in chapter 2 that for a multistory building, the center of rigidity at each floor can be identified as the load center at that floor. In other words, if the loadings on each resisting element at all floors are found based on the assumption that there is no rotation of the floor slabs, then the center of rigidity

at any floor can be obtained by dividing the first moment of the forces on the resisting elements by the total loading at that floor. From eqns.(3.7) and (3.8), the loading on wall J at the i^{th} floor due to translational loadings is given by $(F_J)_i$. Then the location of the center of rigidity can be found as follws:

$$(X_L)_i = \sum_{J=1}^{b} (F_J)_i X_J / P_i \qquad (i>n) \qquad (3.10)$$

For the floors at and below the setback level

$$(X_L)_i = \sum_{J=1}^{B} (F_J)_i X_J / P_i \qquad (i\leq n) \qquad (3.11)$$

Eqn.(3.9), together with eqns.(3.10) and (3.11) completely define the torsional loadings, or floor torques T_i.

The loadings on each resisting element caused by the applied torques can be found using a similar approach as for symmetric setback structures. Conceptually, the building is again represented by the highrise wing and lowrise wing connected at floor levels at and below the setback. The compatibility condition requires that both wings should have the same rotation at each of these floor levels. To obtain the load distribution, the torque loadings will be divided into two parts. The first loading condition consists of the applied torques above the setback level, together with a set of "displacement compatible"

torques $(T_c)_i$ acting at and below the setback level on the highrise wing. No loading will be applied on the lowrise wing in this first loading condition. The "displacement compatible" torques, or compatible torques for short, acting on the highrise wing are such that together with the applied torques above the setback level, there will be no net rotation of floors at and below the setback level. As a result, compatibility is maintaind under the first torque loading condition. The second torque loading condition consists of the remaining torques and is given by $T_i-(T_c)_i$, $(i<n)$. Compatibility condition at floor levels can again be maintained if the forces on the resisting elements are distributed proportionally according to their relative torsional stiffnesses contributions to the overall torsional stiffness of the entire structure (highrise and lowrise wing) below the setback level. The division of torque loadings into these two parts is schematically illustrated in Fig. 3.7.

To calculate the compatible torques $(T_c)_i$, it is necessary to evaluate the loadings on each resisting element in the highrise wing, as caused by torques above the setback. Since the highrise wing is a proportional framing structure, an applied torque T_i will cause lateral forces to be developed in the walls at level i only. As a result, the force acting on the j^{th} element in the highrise wing at the

i^{th} floor due to torque T_j above the setback level can be written as

$$(f_j^*)_i = \frac{T_i (EI)_j (X_j - X_T^*)}{K_\theta^*} \qquad (i>n) \qquad (3.12)$$

In eqn.(3.12), K_θ^* denotes the torsional rigidity of the highrise wing and is given by

$$K_\theta^* = \sum_{j=1}^{b} (EI)_j (X_j - X_T^*)^2 \qquad (3.13)$$

X_T^* denotes the location of the centers of twist of the highrise wing. Being a structure with proportional framing, the centers of twist can be identified with the centers of stiffness. Thus

$$X_T^* = \sum_{j=1}^{b} (EI)_j X_j / \sum_{j=1}^{b} (EI)_j \qquad (3.14)$$

Therefore, the loadings on element j in the highrise wing due to the applied torques T_i $(i>n)$ will consist of point loads $(f_j^*)_i$, $(i=n+1, n+2, \ldots, N)$. These loadings will cause deflections of the element at and below the setback level. These deflections can be written as

$$\delta_{ij} = (\delta_{ij})_s + (\delta_{ij})_m \qquad (i \leq n) \qquad (3.15)$$

where $(\delta_{ij})_s$ and $\delta_{ij})_m$ are deflections due to a force s_j and a moment m_j respectively applied at the setback level on element j. Force s_j and moment m_j are the shear force and bending moment at the setback level caused by the loadings

$(f_j^*)_i$ (i=n+1,n+2,...,N) above the setback. Let $(f_{cj})_i$ be the set of compatible loads applied to the j^{th} wall so that the net floor deflections of the wall at and below the setback level will be zero. The technique to obtain such loadings is similar to what has been described under section 3.3 in dealing with buildings with symmetric setback. In analogous to eqn.(3.3), the set of compatible loads on wall J can be written as

$$(f_{cj})_i = -s_j\bar{\delta}_{in} + (r_j)_i \qquad (i\leq n) \qquad (3.16)$$
$$(j=1,2,..,b)$$

where $\bar{\delta}_{in}$ denotes the Kronecker delta and $(r_j)_i$ is the set of forces needed to nullify the deflection $(\delta_{ij})_m$. Similar to eqn.(3.2), $(r_j)_i$ is given by

$$(r_j)_i = \frac{m_j}{h}K_i \qquad (i\leq n) \qquad (3.17)$$

where K_i is given in Table 3.1.

These sets of compatible loads on the elements in the highrise wing produce no net resultant forces, but they produce a set of "compatible" torques $(T_c)_i$, as given by

$$(T_c)_i = \sum_{j=1}^{b}(f_{cj})_i X_j \qquad (i\leq n) \qquad (3.18)$$

The first torque loading condition then consists of T_i (i>n) of the applied torque loadings above the setback level and $(T_c)_i$, (i≤n), as given by eqn.(3.18) on the highrise wing, with no loading on the lowrise wing. Since there is no

deflection of any wall at floor levels at and below the setback for both wings, there is no floor rotation for both wings. Therefore, the compatibility requirement is ensured for this part of loading.

The second part of loading consists of the remainder of the applied torques at and below the setback level. Mathematically, they can be expressed as $T_i-(T_c)_i$, $(i\leq n)$. The distribution of this part of loading on the base structure (the first n stories of the complete structure) can be obtained by proportioning according to contribution of the torsional stiffness of each element to the overall torsional stiffness of the base structure. Being a structure with proportional framing, the center of twist of the base structure can again be identified with the center of stiffness of the base structure and is determined by

$$X_T = \sum_{j=1}^{B}(EI)_j X_j / \sum_{j=1}^{B}(EI)_j \qquad (3.19)$$

For a given applied torque $T_i-(T_c)_i$ at the i^{th} floor, the loads on the resisting walls are given by

$$(f_j)_i = \frac{[T_i-(T_c)_i](EI)_j(X_j-X_T)}{K_\theta} \qquad (i\leq n) \quad (3.20)$$

$$(J=1,2,..,B)$$

where K_θ is the total torsional rigidity of the base structure. Mathematically, it is given by

$$K_\theta = \sum_{j=1}^{B} (EI)_j (X_j - X_T)^2 \qquad (3.21)$$

Therefore, the load distribution to the walls within the highrise wing is given by the following:

Above the setback level,

$$(f_j^*)_i = \frac{T_i (EI)_j (X_j - X_T^*)}{K_\theta^*} \qquad (i>n) \qquad (3.12)$$

At and below the setback level,

$$(f_j^*)_i = -s_j \bar{\delta}_{in} + \frac{m_j K_i}{h} + \frac{[T_i - (T_c)_i](EI)_j (X_j - X_T)}{K_\theta} \qquad (i \leq n) \qquad (3.22)$$

$$(j=1,2,\ldots,b)$$

For walls within the lowrise wing

$$(f_j^{**})_i = \frac{[T_i - (T_c)_i](EI)_j (X_j - X_T)}{K_\theta} \qquad (i \leq n) \qquad (3.23)$$

$$(j=b+1,\ldots,B)$$

The total loadings on each individual wall will be the summation of the contribution from the translational loadings and the torsional loadings. For walls in the highrise wing, the loadings are given by $(F_j)_i + (f_j^*)_i$ where $(F_j)_i$ is given by eqn.(3.7) and $(f_j^*)_i$ is given by eqns.(3.12) or (3.22). For walls in the lowrise wing, the total loadings are given by $(F_j)_i + (f_j^{**})_i$ where $(F_j)_i$ is given by eqn.(3.8) and $(f_j^{**})_i$ by eqn.(3.23).

Two simplifying assumptions were made in the development of the procedure to facilitate understanding. First, the resisting elements are assumed to be uniform

walls. But, in general, the procedure will apply if the flexural rigidities of the walls vary along the height of the building provided that the rigidities of the walls in the highrise wing as a group remain proportional and the rigidities of the walls within the base structure also remain proportional.

Recognizing the lateral behaviour of the frames is similar to that of a shear beam, the procedure outlined is also applicable to setback buildings with frames instead of walls as lateral load resisting elements with the following modifications. First, the flexural rigidity $(EI)_j$ of the resisting walls should be replaced by the equivalent shear beam rigidity $(GA)_j$, [15]. Second, since the deflection of a shear beam is not governed by bending, the quantities $(\Delta_i)_M$ and $(\delta_{ij})_m$ representing deflections caused by overturning moments at the setback level do not exist. As a result, to apply the procedure to setback-frame structures, the quantities R_i and $(r_j)_i$ as given in eqns.(3.3) and (3.16) should be taken to be zero.

As a second simplifying assumption, the influence of the resisting elements spanning perpendicular to the load direction is neglected in the formulation. These elements will not provide resistance to the translational part of loadings and therefore their effects on buildings with

symmetric setback can indeed be ignored. However, these elements will participate in resisting the torsional loadings. Their effects can be taken into account by including their contributions to the torsional stiffness of the highrise wing K_θ^*, as given in eqn.(3.13), and the torsional stiffness of the base structure K_θ, as given in eqn.(3.21).

3.5 Examples

Three examples will be presented to illustrate the proposed procedure of lateral analysis of setback structures. Each of the example buildings (building D, E and F) is a nine story structure (N=9) with a single setback at the seventh floor (n=7). An uniform floor height of 3 m is assumed (h=3). To reduce the complexity of the problem, shear walls spanning the Y direction only are provided as lateral load resisting elements.

Building D is a symmetric setback structure with framing layout as shown in Fig. 3.8. Due to the symmetrical nature of the problem, only one half of the building needs be considered. The reduced structure (Fig. 3.8b) consists of a total of four shear walls (B=4) with two walls located in each of the two wings (b=2). Walls within the base structure are made uniform, and for those extending into the tower, the flexural rigidity is reduced by one half as given

in Table 3.2. The loads acting on the reduced structure, along the axis of symmetry, consist of point loads of 120 kN at floors 1 through 8 and a 60 kN load at the top.

Since the rigidity variation satisfies the assumptions of proportional framing within the highrise wing and also within the base structure, as assumed in the theory, the proposed procedure will lead to an exact solution of the problem. The first set of loadings consists of the applied loads above the setback level together with the compatible loads at and below the setback. With end shear S being 180 kN and end moment M being 720 kN.m, the compatible loads can readily be computed using eqn.(3.3). The second set of loadings will be the applied loadings at and below the setback less the compatible loads. The subdivision of the applied loads is summarized in Table 3.3. The distribution of the second set of loadings among the two cantilevers is obtained by proportioning the loadings according to their relative stiffnesses.

Knowing the forces on the two wings, further distribution of the forces among elements within each wing can be accomplished using the stiffness proportioning rule, as given by eqns.(3.7) and (3.8). The computed results are given in Table 3.4. and checked with those from matrix analysis. The final load distribution in the elements are

plotted in Fig. 3.9. In the figure, the solid lines represent the load distribution if it is obtained by proportioning according to wall stiffnesses. This simple distribution rule leads to agreement with the correct results at regions above the setback and also at regions two floors below the setback level. Underestimation of wall loads occurred in walls in the highrise wing at location one floor below the setback. For walls in the lowrise wing, underestimation of floor loads occurs at the setback level up to a factor of two. This example indicates that the effect of force concentration occurs in the vicinity of the setback.

To demonstrate the proposed method on eccentric setback structures, Building E, a structure identical to the reduced structure of Building D is adopted for illustration purposes. The wall properties are given in Table 3.2. The same set of loadings, as acting on the reduced structure of Building D, is applied along the Z axis which is now no longer an axis of symmetry; and torsional response is expected in the present analysis. The total load effect can be expressed as a combination of the translational and torsional effects. The translational load effect and its distribution has been dealt with in the previous example on symmetric setback structure. To determine the torsional load effect, it is necessary to establish first the

torsional loadings acting on the building and then the distribution of torsional shears among the resisting walls.

To establish the torsional loadings, eqns.(3.10) and (3.11) are used to locate the rigidity centers. With the wall loads given in Table 3.4, the rigidity centers at floor levels can be determined. The locus of the rigidity centers is plotted in Fig. 3.10. The centers of stiffness, as determined based on treating each floor as a single story structure, are represented by the solid lines in the same figure. It can be seen that identifying the rigidity centers as stiffness centers for multistory buildings can be very much in error in buildings with eccentric setback. This will in turn lead to larger errors in the estimation of torsional loadings, particularly in the setback region. For example, the torque at the setback level (7^{th} floor) is 9552 kN.m. However, if the "stiffness center" is considered as the center of rigidity, the torque at the setback level will be 2667 kN.m, an underestimation of more than three times the actual torque in this example.

Using the compatible load concept, the total torque loadings are again segregated into two sets. The first set consists of torques applied to the structure above the setback level together with the compatible torques at and below the setback. The second set will be the applied

torques at and below the setback level less the compatible torques.

As determined by eqn.(3.9), the applied torques above the setback level are given as 960 kN.m. The center of twist for the highrise wing, as given by eqn.(3.14), is found to be located at 8 m from the origin. Forces in walls 1 and 2 within the highrise wing due to torques above the setback can be determined using eqn.(3.12). At the 9^{th} floor, we have $(f_1^*)_9=-(f_2^*)_9=24$ kN. At the 8^{th} floor, $(f_1^*)_8=-(f_2^*)_8=48$kN. With $s_1=-s_2=72$ kN and $m_1=-m_2=288$ kN, the compatible loads, as expressed by eqn.(3.16) can be found. Typically, the compatible loads on walls 1 and 2 at the 7^{th} floor are $(f_{c1})_7=-(f_{c2})_7=193.9$ kN. The resultant compatible torque at this level is given by the moment of the compatible loads about the reference axis as given by eqn.(3.18). Thus, the compatible torque at the 7^{th} floor becomes $(T_c)_7 = 3878$ kN.m. Compatible torques at other floors can be calculated in a similar manner. The division of torsional loadings on the structure is presented in Table 3.5. The first set of torques is to be resisted by walls in the highrise wing while the second set is resisted by elements within the base structure. Forces on the resisting walls due to the torsional load effect is tabulated in Table 3.6. The total loadings on an element can be obtained by combining the translational loads (Table 3.4) with the

torsional loads (Table 3.6). The actual load distribution in the edge walls are plotted in Fig. 3.9. The solid lines represent shears on the wall, computed on a floor by floor basis [19]. Due to the irregularity at the setback level, the two methods produce very different results. In the case of wall 4, the shear force is actually reduced at floor 6 while the floor by floor approach predicts an increase in shear.

In order to evaluate the practicality of the method to apply to buildings where the conditions of proportional framing are not satisfied, another building, Building F is considered. Building F has the same framing as Building E except that the rigidity of walls 3 and 4 are reduced by 25% at floors 5, 6, and 7 (Fig. 3.8 and Table 3.2). The same loadings on Building E are applied to Building F. The load distribution in Building F is calculated in two ways. First, it is calculated by the proposed method, neglecting the 25% rigidity reduction in walls 3 and 4. The results of this computation will be identical to those shown for building E. Second, a three dimensional frame analysis is carried out, using actual framing properties of Building F. The results of both calculations are shown in Fig. 3.11. The closeness of the results between the two calculations indicate that the proposed hand calculation procedure is

capable of estimating the load distribution among resisting elements in buildings with setback, even though the framing of the building is not strictly proportional.

3.6 Summary

A method suitable for preliminary design use is presented to calculate the load distribution among resisting elements in buildings with symmetric or eccentric setback subjected to lateral loads.

This proposed method is a non-trivial application of the concept of eccentricity to evaluate the force distribution in irregular eccentric multistory buildings. One of the complexities in load distribution in structures with setback is due to the abrupt change in stiffness at the setback level. To overcome this difficulty, the concept of "displacement compatible" loading is employed in the proposed method.

For buildings with symmetric setback, the lateral loading is divided into two loadings. The first loading consists of applied loadings acting on the tower structure together with a set of "displacement compatible" loads acting at and below the setback. All such loadings will be resisted by the highrise wing alone. The lowrise wing has zero loading on it and remains undeformed. The second loading will then consist of the applied loads at and below

the setback less the "displacement compatible" loads. This second set of loadings will be resisted by the base structure. The final response can be obtained by summing the responses under each loading condition.

For buildings with eccentric setback, additional computation is necessary to take into account the torsional effect. The lateral loadings are first subdivided into a translational component and a torsional component, using the concept of eccentricity as developed in chapter 2 for irregular multistory buildings. The distribution of the translational component of lateral loadings can be done using the technique for buildings with symmetric setback. To establish the torsional component of lateral loadings, the locations of the center of rigity of the building need to be determined. The locations can be found conveniently based on the results from the translational component load distribution. The distribution of torsional shears to various elements can be done by using the same "displacement compatible" load concept again. The final loadings on each resisting element would then be the sum of loadings due to the translational and the torsional component of lateral loads.

Three numerical examples had been worked out to demonstrate the proposed method of analysis. Force

concentration is observed in the vicinity at and below the setback level where special attention should be paid to the design of such structures. For buildings with stiffness variation which satifies the basic assumptions of the method, the procedure leads to exact solution of the problem. For structures that do not strictly obey the assumptions, the procedure can still provide reasonable estimates of the design loads.

The proposed method not only can be used as a practical tool for assessing the design loads on resisting elements in a setback structure, it also provides some insight into the load transfer mechanism involved in such structures, especially in the region where the setback occurs and complication of behaviour is expected.

3.7 Notations

B, b = number of resisting walls in the reduced structure and in the highrise wing, respectively

EI^{*}, EI^{**} = flexural rigidity of the highrise and lowrise cantilever, respectively

F_i^{*}, F_i^{**} = translational loading acting on the highrise and lowrise cantilever, respectively

$(F_j)_i$ = translational load on the i^{th} floor of wall j

$(f_{cj})_i$ = compatible load associated with the torsional load effect

$(f_j^{*})_i$ = lateral loading acting on the highrise and lowrise walls respectively, as caused by the

$(f_j^{**})_i$ torsional load effect

h = floor height

i = floor identifier

j = wall identifier

K_i = reaction coefficient

K_θ, K_θ^* = torsional rigidity of the base structure and of the highrise wing, respectively

M, m_j = overturning moment acting on the highrise cantilever and on wall j, respectively

N, n = number of floors in the highrise and lowrise wing, respectively

$P_i, (P_c)_i$ = applied lateral load and compatible translational load, respectively

$R_i, (r_j)_i$ = lateral load required to offset the overturing effect

S, s_j = end shear caused by the translational and torsional load effect, respectively

$T_i, (T_c)_i$ = torque loading caused by the eccentric lateral loads and compatible loads, respectively

X_j = x coordinate position of a wall element

$(X_L)_i$, $(X_p)_i$ = x coordinate position of the rigidity center and of the floor load resultant, respectively

X_T, X_T^* = x coordinate position of the twist center of the base and highrise wing, respectively

Δ_i, δ_{ij} = floor deflection of the highrise cantilever and highrise wall, respectively

δ_{in} = Kronecker delta

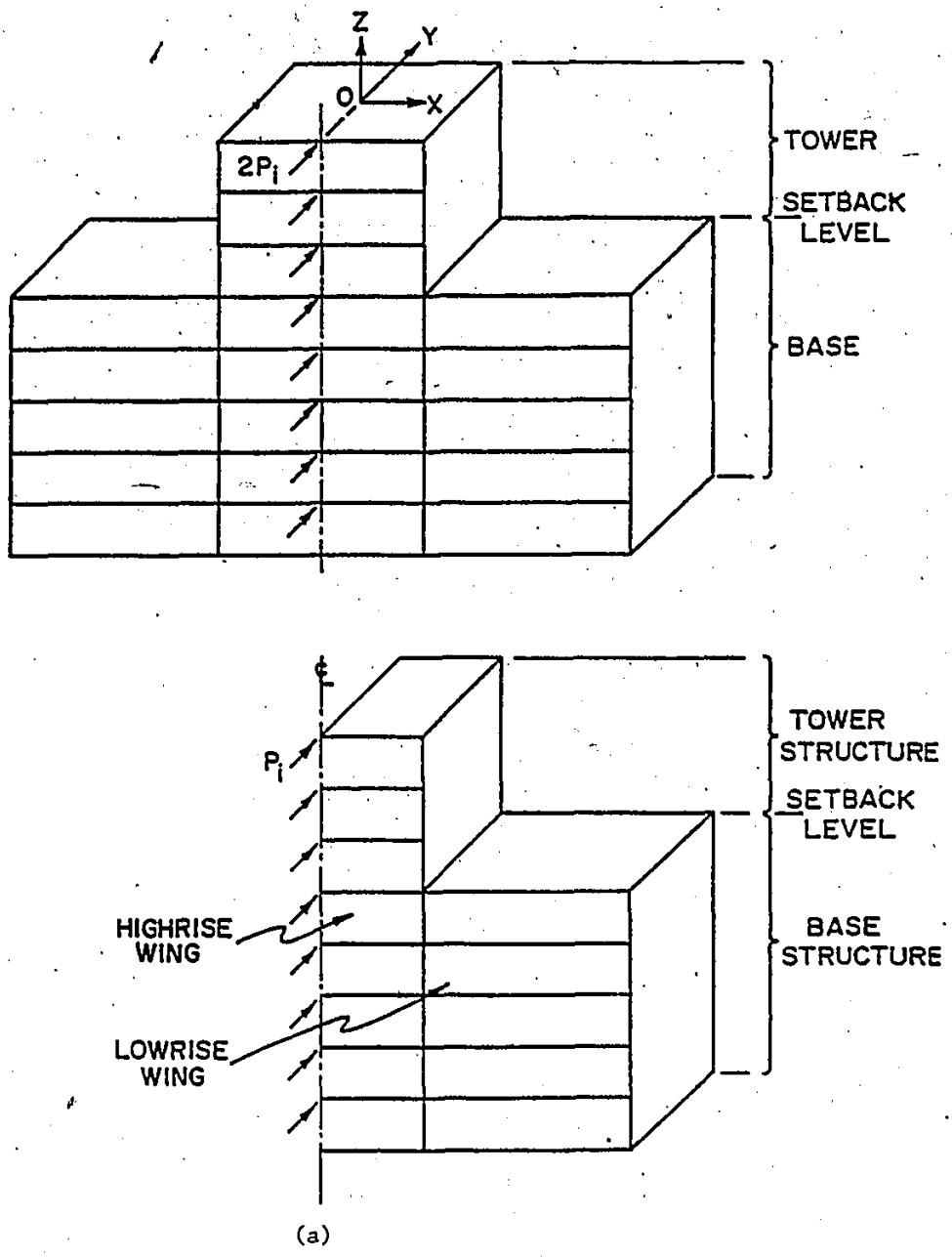

Fig. 3.1 Symmetric Setback Building

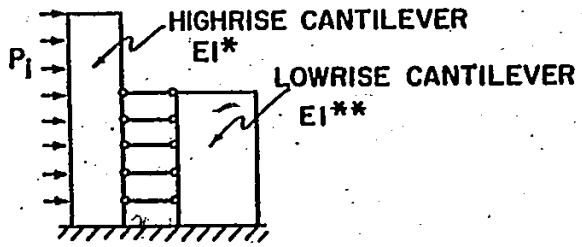

Fig. 3.2 Computer Model for Setback Building

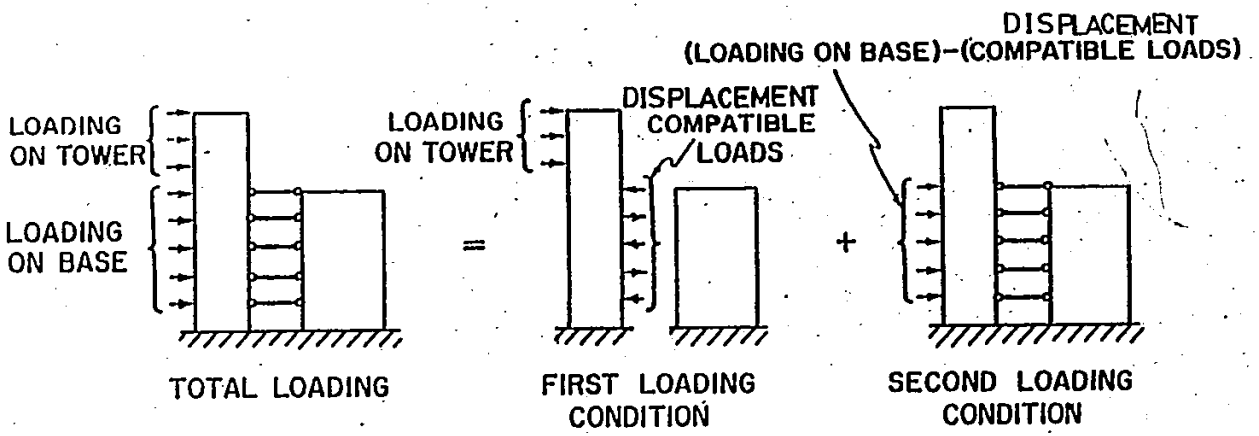

Fig. 3.3 Subdivision of Lateral Loads

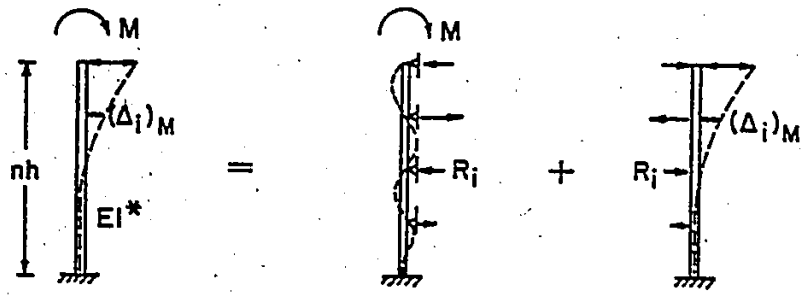

Fig. 3.4 Displacement Compatible Load Effect

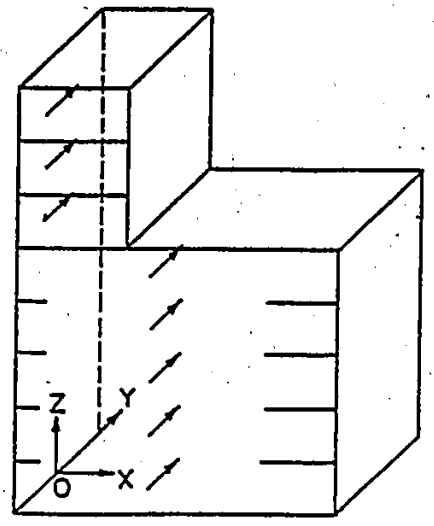

Fig. 3.5 Eccentric Setback Building

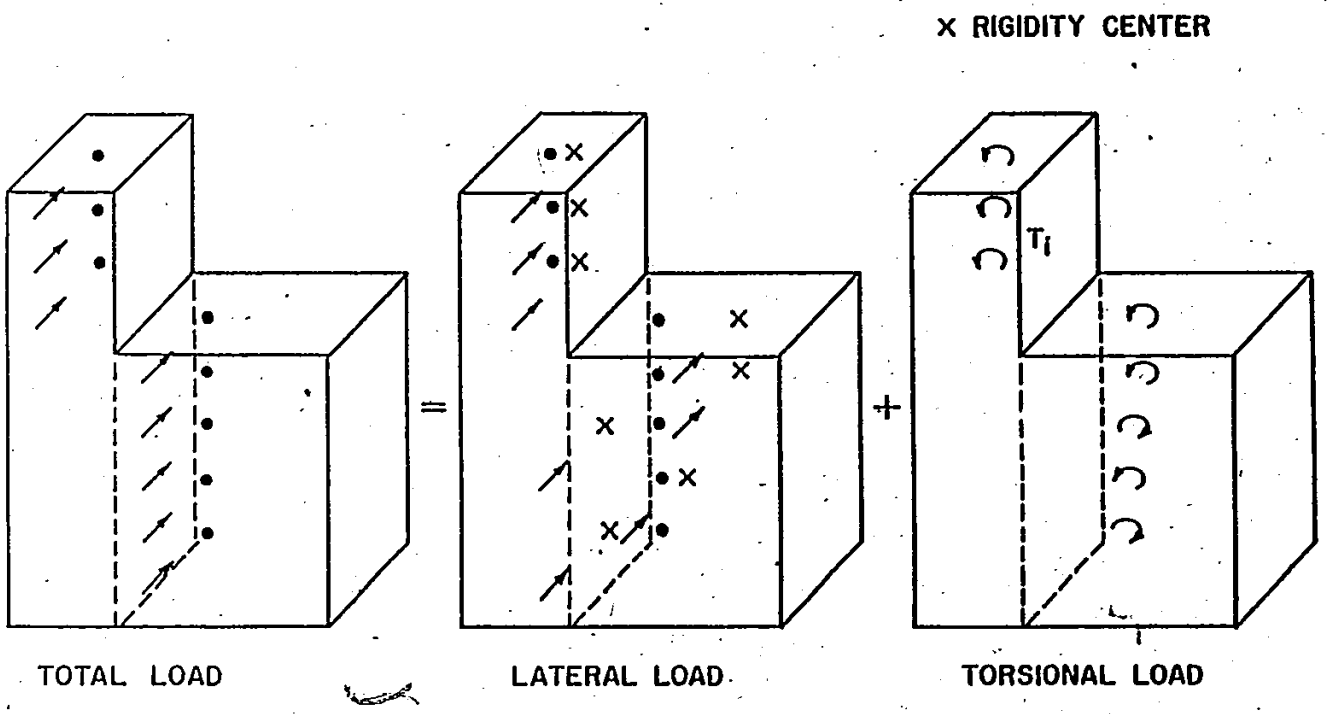

Fig. 3.6 Uncoupling of Total Load Effect

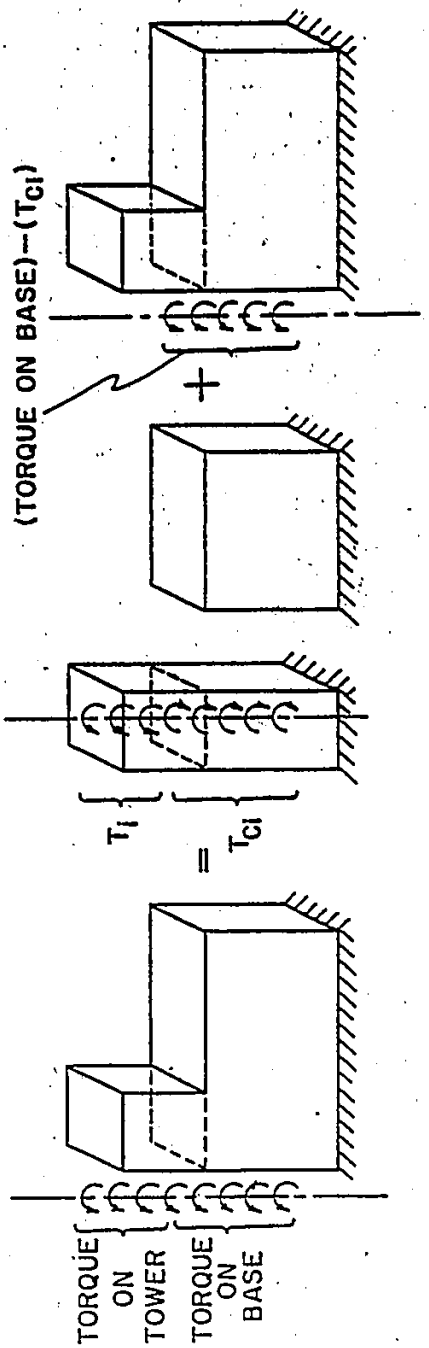

Fig. 3.7 Subdivision of Applied Torques

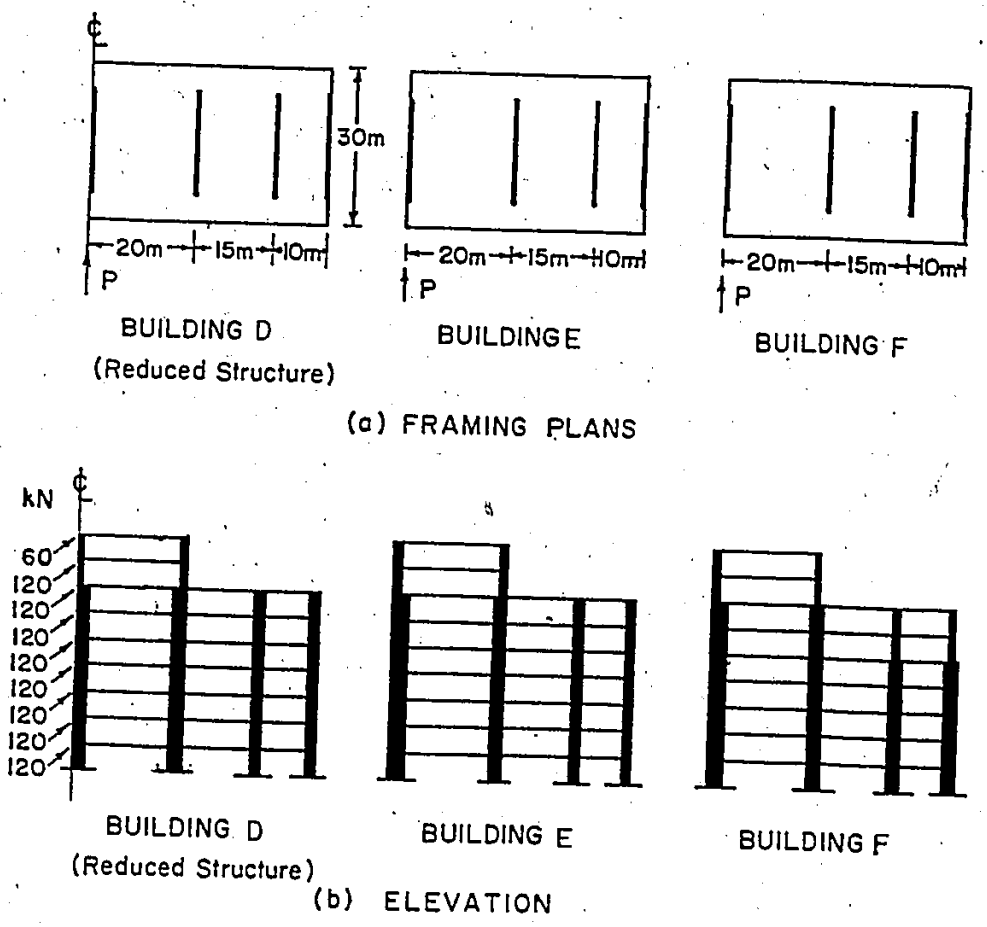

Fig. 3.8 Example Buildings (Building D, E and F)

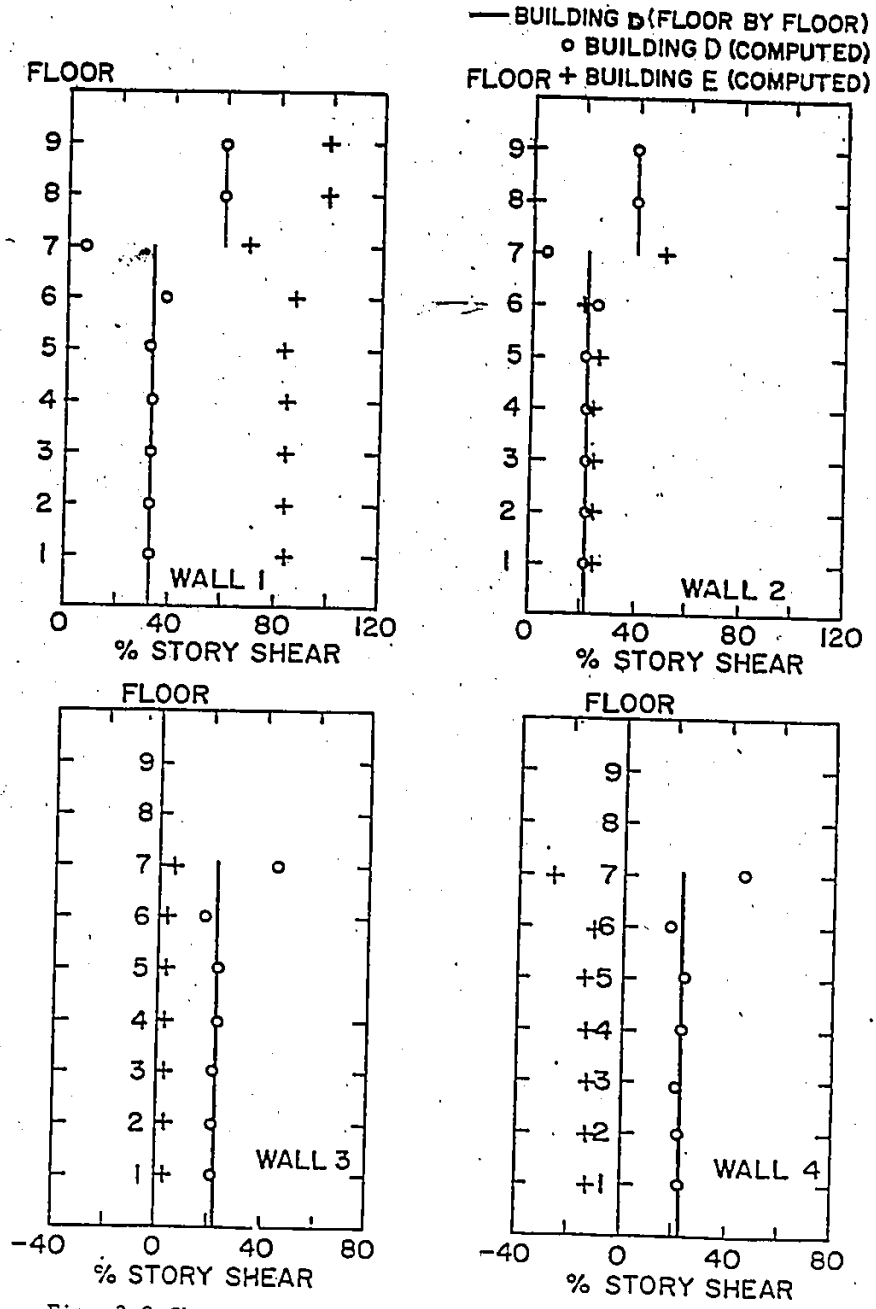

Fig. 3.9 Shear Distribution in Resisting Walls of Building D and E

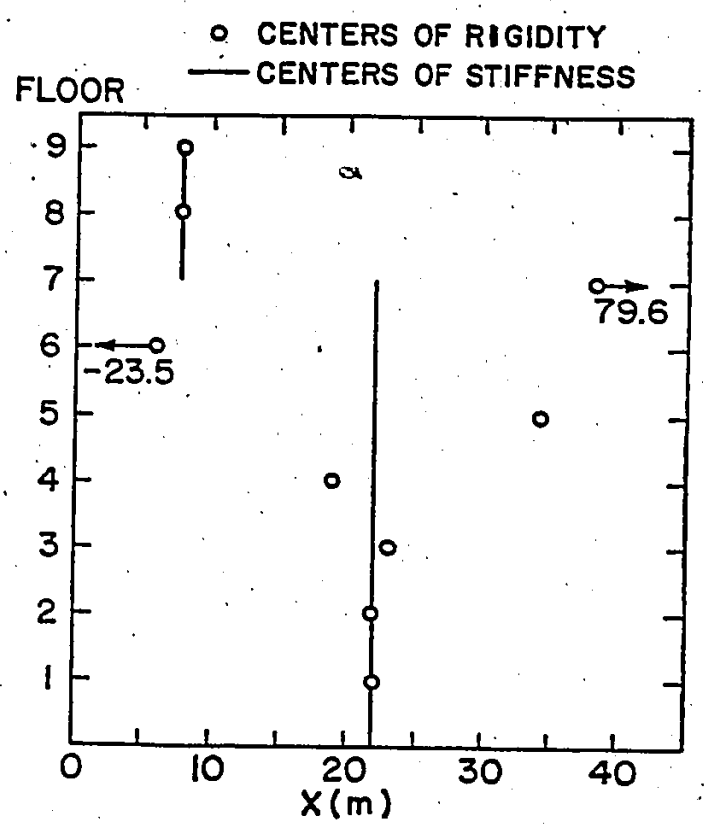

Fig. 3.10 Distribution of Rigidity Centers in Building E

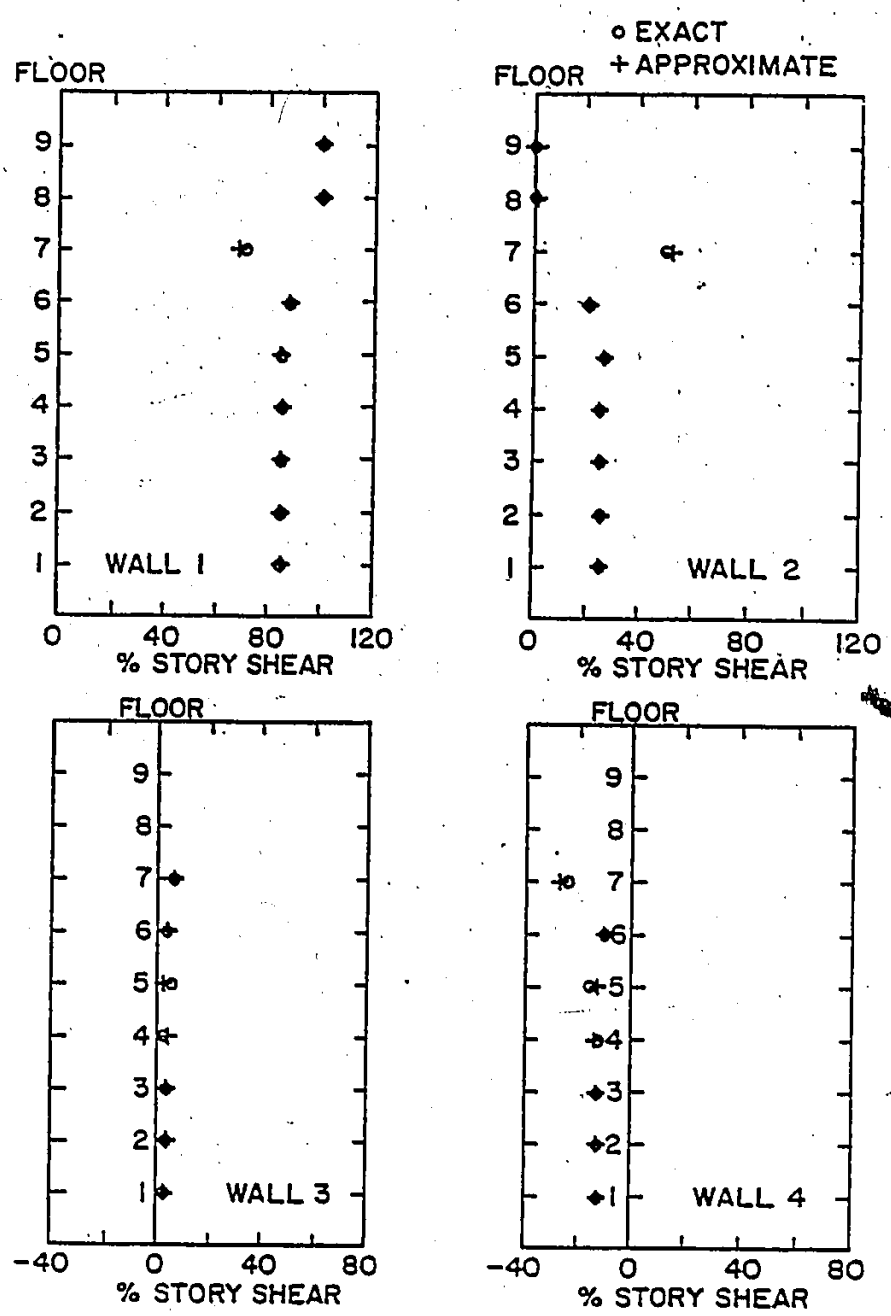

Fig. 3.11 Shear Distribution in Resisting Walls of Building F

TABLE 3.1 NUMERICAL VALUES OF K_i

Level	Setback Level				
	n=2	n=3	n=4	n=5	n≥6
n	-1.27	-1.27	-1.27	-1.27	-1.27
n-1	1.69	1.61	1.61	1.61	1.61
n-2	-	-0.46	-0.43	-0.43	-0.43
n-3	-	-	0.13	0.11	0.11
n-4	-	-	-	-0.04	-0.03
n-5	-	-	-	-	0.01

TABLE 3.2 FLEXURAL RIGIDITIES OF RESISTING WALLS IN BUILDING D, E AND F

Building	Floor	Wall			
		1	2	3	4
D*,E	8/F-9/F	1.5 EI	EI	-	-
	1/F-7/F	3 EI	2 EI	2 EI	2 EI
F	8/F-9/F	1.5 EI	EI	-	-
	6/F-7/F	3 EI	2 EI	1.5 EI	1.5 EI
	1/F-5/F	3 EI	2 EI	2 EI	2 EI

EI= flexural rigidity

* reduced structure

TABLE 3.3 LATERAL LOADINGS ON REDUCED STRUCTURE OF BUILDING D

Floor	Applied Loads (kN)	=	Set 1 (kN)	+	Set 2 (kN)
9	60		60		0
8	120		120		0
7	120		-485*		605
6	120		387*		-267
5	120		-104*		224
4	120		27*		93
3	120		0		120
2	120		0		120
1	120		0		120

* displacement compatible loads

TABLE 3.4 RESISTING FORCES IN ELEMENTS OF REDUCED STRUCTURE OF BUILDING D (kN)

Floor	Wall			
	1* (X_j=0)	2 (X_j=20)	3 (X_j=35)	4 (X_j=45)
9	36	24	0	0
8	72	48	0	0
7	-89	-59	134	134
6	143	95	-59	-59
5	12	8	50	50
4	47	32	21	21
3	38	25	28	28
2	41	27	26	26
1	40	27	27	27

* multiply numbers by 2 to give forces in actual element

TABLE 3.5 TORSIONAL LOADINGS ON BUILDING E

Floor	Applied Torques (kN.m)	=	Set 1 (kN.m)	+	Set 2 (kN.m)
9	-480		-480		0
8	-960		-960		0
7	-9555		3878*		-13433
6	2821		-3097*		5918
5	-4137		829*		-4966
4	-2273		-220*		-2053
3	-2772		0		-2772
2	-2638		0		-2638
1	-2675		0		-2675

* displacement compatible torques

TABLE 3.6 RESISTING FORCES IN ELEMENTS OF BUILDING E DUE TO TORSIONAL EFFECT (kN)

Floor	Wall			
	1	2	3	4
9	24	-24	0	0
8	48	-48	0	0
7	120	215	-120	-214
6	16	-164	53	94
5	75	49	-44	-79
4	59	-8	-18	-33
3	63	7	-25	-45
2	62	3	-24	-42
1	62	4	-24	-43

CHAPTER 4

STATIC AND DYNAMIC BEHAVIOUR OF UNIFORM ECCENTRIC WALL-FRAME BUILDINGS

4.1 Introduction

Shear walls and moment resisting frames are the two most common types of structural systems used in multistory building design. Each can serve both as a gravity and a lateral load resisting system. Moment resisting frames, being more flexible, can be designed to exhibit good ductile behaviour. While for shear walls, though being less ductile, can provide the required stiffness to a building. By the combined use of walls and frames, a better control of interstory drift can be achieved. Therefore, dual systems consisting of a combination of shear walls and frames have become a viable structural system for building design. Such systems also had been recognized by the earthquake design provisions of NBCC 1985 as a desirable form of construction. The code allows lower earthquake design forces to be used for buildings equipped with dual systems, provided that:

"The frames and ductile flexural walls shall resist the lateral force in accordance with their relative rigidities considering the interaction of the flexural walls and frames...".

It is the interaction mechanism of walls and frames

which makes the behaviour more complex than buildings having all walls, or all frames as lateral resisting elements.

This chapter is a study of the behaviour of eccentric wall-frame buildings subjected to lateral loads and the applicability of the seismic torsional provisions of NBCC 1985 to this type of buildings. In studying the behaviour of eccentric wall-frame buildings, not only the wall-frame interaction in lateral deformation, but also wall-frame interaction caused by torsional deformation needs to be taken into account. To make the analysis tractable, only uniform wall-frame buildings will be considered. Specific reference will be made to the class of wall-frame buildings with mass and rigidity centers lying on two vertical lines. Comparison of results will be made between that predicted by the code and results obtained from dynamic spectrum approach in assessing the accuracy of the code provisions for this class of eccentric buildings.

4.2 System Parameter Identification

Before getting involve with the dynamic behaviour, it is useful to have an understanding of the behaviour of such a system under static lateral loads.

4.2.1 Static Lateral Behaviour of Uniform Symmetric Wall Buildings and Uniform Symmetric Frame Buildings

The wall-frame interaction study is most conveniently carried out to base on information of the independent wall and frame system behaviour. Therefore, a short summary of wall behaviour and frame behaviour under lateral loadings will be presented. Rather than referring to specific buildings, a general approach to identify key parameters that affect the overall behaviour will be taken.

A wall building (Fig. 4.1a) deforms mainly by flexure and can conveniently be modelled as a cantilever beam. For a given distribution of lateral loading w(z), the governing differential equation of equilibrium can be expressed as

$$EI_y \frac{d^4y}{dz^4} = w(z) \qquad (4.1a)$$

where EI_y is the total flexural rigidity of the wall system.

On the other hand, moment resisting frames subjected to lateral loadings (Fig. 4.1b) can be modelled as shear beams. For frames, deformation is caused dominantly by shear actions. The corresponding equilibrium equation can be written as

$$GA_y \frac{d^2y}{dz^2} = -w(z) \qquad (4.1b)$$

where GA_y is the shear rigidity of the frame system. For a

given frame system, the shear rigidity GA_y can be evaluated. Study for such evaluation can be found in [15].

For given boundary conditions, the deflection response can be obtained by solving eqn.(4.1). The stress resultants (ie. shears, moments) in the resisting elements can then be computed once the deflection curve is defined.

4.2.2 Static Lateral Behaviour of Uniform Symmetric Wall-Frame Buildings

For a dual system, the walls and frames will both contribute resistance to the applied loads. With walls and frames distributed in parallel and being coupled by floor diaphragm actions, the equilibrium equation of a wall-frame building (Fig. 4.1c) can be written as [15]

$$EI_y \frac{d^4y}{dz^4} - GA_y \frac{d^2y}{dz^2} = w(z) \qquad (4.2)$$

Under uniformly distributed load $w(z) = w$, the deflection curve will be given by

$$y(z) = \frac{wH^4}{EI_y(\alpha H)^4}\left\{\frac{(\alpha H)\sinh(\alpha H)+1}{\cosh(\alpha H)}\left[\cosh\left(\alpha H\frac{z}{H}\right)-1\right]\right.$$

$$\left.-(\alpha H)\sinh\left(\alpha H\frac{z}{H}\right) + (\alpha H)^2\left[-\frac{z}{H} - \frac{1}{2}\left(\frac{z}{H}\right)^2\right]\right\} \qquad (4.3)$$

in which

$$\alpha H = \sqrt{(GA_y/EI_y)}\, H \qquad (4.4)$$

and H is the total height of the building.

It can be seen that the building response is a

function of the non-dimensional parameter αH. αH is a measure of the degree of lateral wall-frame interaction. Eqn.(4.3) is plotted in Fig. 4.2a for different αH values. For small values of αH, a dominant wall system is implied. Large αH values indicate the existence of a dominant frame system. This can be observed in Fig. 4.2a where for extreme αH values, the deflection curves approach that of a wall building or a frame building.

For systems with moderate αH values, a significant degree of wall-frame interaction exists. It can be seen (Fig. 4.2a) that elastic curves of buildings with significant wall-frame interaction will exhibit double curvature characteristics. Such behaviour indicates that wall behaviour dominates at the lower part of the building. Frame behaviour, on the other hand, controls deflections at the top part of the building. The practical range of αH values is from 0 to 6 [15]. A system with αH value of 5 can be considered to have a strong degree of wall-frame interaction.

Knowing the equation of the elastic curve, the stress resultants in individual resisting elements can readily be obtained. The lateral shear distribution in a wall (S_W^L) or a frame (S_F^L) is given by:

$$S_W^L(z) = EI \frac{d^3y}{dz^3} \qquad (4.5a)$$

$$S_F^L(z) = -GA \frac{dy}{dz} \qquad (4.5b)$$

The superscript "L" relates quantities associated with the lateral load effect. EI and GA in eqn.(4.5) is the flexural and shear rigidity of an individual wall and frame respectively. The distribution of lateral shears will thus also be a function of the interaction parameter αH. A plot of eqn.(4.5) with uniform loading is given in Fig. 4.3a. Unlike uniform wall buildings or frame buildings, shear distribution in the resisting elements will no longer be of the same shape as the applied shears. For dual systems with significant wall-frame interaction, shear reversal will occur at the top of the walls. A reverse shear force distribution on the walls are required to limit the interstory drift of the walls to values compatible to the frames. Such reverse shear forces have to be provided by the frame system. As a consequence, the frames have to resist loadings in excess of the total applied loads on the upper part of the building.

In summary, the lateral behaviour of strongly interacting wall-frame systems can be typified by:

(a) a double curvature elastic curve; and

(b) shear reversal in the walls.

4.2.3 Static Torsional Behaviour of Uniform Symmetric Wall-Frame Buildings

Torsional responses result if the building (Fig. 4.1c) is subjected to torque loading T(z). The torsional moment equilibrium equation can be written as

$$EI_W \frac{d^4\theta}{dz^4} - GJ \frac{d^2\theta}{dz^4} = T(z) \qquad (4.6)$$

in which EI_W and GJ are the torsional rigidities of the wall and frame system respectively about the centers of twist of the building. Often it is convenient to express the torsional rigidity as a product of the lateral rigidity and the torsional radius of gyration of the system. Namely:

$$EI_W = EI_y r_W^2 \qquad (4.7)$$

$$GJ = GA_y r_F^2 \qquad (4.8)$$

with r_W and r_F being the torsional radius of gyration of the wall and frame system respectively about the centers of twist. For a given building with walls and frames arranged in a symmetrical manner, the centers of twist and centers of rigidity coincide with the mass centers of the structure.

Under uniform applied torque distribution T(z) = T; the twist distribution is given by:

$$\theta(z) = \frac{TH^4}{EI_W(\beta H)^4}\left\{\frac{(\beta H)\sinh(\beta H)+1}{\cosh(\beta H)}\left[\cosh\left(\beta H\frac{z}{H}\right)-1\right]\right.$$

$$\left.-(\beta H)\sinh\left(\beta H\frac{z}{H}\right) + (\beta H)^2\left[-\frac{z}{H} - \frac{1}{2}\left(\frac{z}{H}\right)^2\right]\right\} \qquad (4.9)$$

where

$$\beta H = \sqrt{(GJ/EI_W)}\, H = \alpha H\, (r_F/r_W) \qquad (4.10)$$

The torsional response will be a function of the non-dimensional parameter βH which measures the degree of torsional wall-frame interaction. Eqn.(4.9) is plotted in Fig. 4.2b alongside the lateral deflection curves. For equal αH and βH values, ie.

$$r_W = r_F = r \qquad (4.11)$$

the lateral and torsional response curves will have identical shapes. The parameter βH has the same effect controlling the torsional behaviour as the parameter αH in controlling lateral responses, namely: for extreme βH values, a torsionally dominant wall or frame system implies.

Under the torque loading, torsional shears S_W^T and S_F^T will be induced in the wall and frame elements respectively.

$$S_W^T(z) = EI \times \frac{d^3\theta}{dz^3} \qquad (4.12a)$$

$$S_F^T(z) = -GA \times \frac{d\theta}{dz} \qquad (4.12b)$$

The superscript "T" relates quantities associated with the torsional load effect. In eqn.(4.12), "x" is the distance of the element as measured from the centers of twist.

The torsional shear distribution is plotted in Fig. 4.3b alongside the lateral shear distribution curves.

Torsional shear reversal is also observed in the resisting walls. As pointed out before, shear reversal is characteristic of wall-frame systems when they interact together, and in this instant, to resist the torsional loads.

For a building subjected to lateral and torsional loadings, the total design shears in a resisting element is given by the sum of the lateral and torsional shears. The above study indicates that, in general, torsional shears in a wall are not always additive to the lateral shears along its whole height. It is only when αH equals βH that the two shears will complement each other. Thus, the commonly held view that "an edge resisting element will be the element most susceptable to torsional effect" is not necessarily true for wall-frame buildings. In other words, it is no longer sufficient to study the torsional effect for an edge element only in evaluating the torsional behaviour of such buildings.

4.2.4 Static Behaviour of Uniform Eccentric Wall-Frame Buildings

To study the behaviour of eccentric wall-frame buildings under static lateral loads, a monosymmetric building model will be used (Fig. 4.1d). The equilibrium equation under lateral load w(z) can be written as [28]:

$$EI_y \frac{d^4y}{dz^4} - GA_y \frac{d^2y}{dz^2} - aGA_y \frac{d^2\theta}{dz^2} = w(z) \qquad (4.13a)$$

$$EI_w \frac{d^4\theta}{dz^4} - aGA_y \frac{d^2y}{dz^2} - GJ \frac{d^2\theta}{dz^2} = T(z) = e\, w(z) \qquad (4.13b)$$

"a" denotes the distance between the rigidity center C_w of the wall system and the rigidity center C_f of the frame system. For uniform buildings, the rigidity center of the wall system corresponds to the center of stiffness of the walls. Similarly, the rigidity center of the frame system can be identified as the center of stiffness of the frames. "e" is the distance between the applied load resultants and the rigidity center C_w of the wall system. Eqn.(4.13) is a pair of coupled equations referring to the wall center as origin. The first equation governs the lateral equilibrium while the second equation governs the torsional equilibrium of the building. Due to the interaction of the walls and frames, the twist centers will not be on a vertical line, even for uniform buildings. Thus it will be difficult to make use of the transformation with the twist centers as points of reference (as discussed in chapter 2) to uncouple the differential equations of equilibrium.

Solution to eqn.(4.13) can be achieved through decoupling of the equilibrium equations by eigenvalue technique [28]. However, such a decoupling process does not

physically generate a translational and a torsional load component. Instead, the uncoupled equilibrium equations have to be interpreted as two independent planar wall-frame systems subjected to prescribed loadings. Such a decoupling approach is an useful means of obtaining the solution, but it does not lend itself readily to useful physical interpretation.

4.2.5. Special Class of Uniform Monosymmetric Wall-Frame Buildings

It can be seen that the parameter "a" in eqn.(4.13) is associated with the coupling terms. Uniform wall-frame buildings with arrangement of resisting elements such that "a" being zero represent a special class of wall-frame structures for the following reasons:

(i) The equilibrium eqn.(4.13) will become uncoupled. As a result, solution to the problem will be simpler in the mathematical sense. The lateral and torsional response can be separately identified and then combined to give the total response.

(ii) The origin of reference (ie. the wall center) will become the rigidity center (and also the twist center) of the building (Fig. 4.1e). The building in this case can be treated as having two "proportional framing systems" sharing a common center of rigidity.

(iii) As a direct implication from (ii), the building will have rigidity centers and mass centers falling on two vertical lines. Therefore, the seismic torsional provisions of NBCC 1985 should be applicable to this special class of wall-frame buildings.

In view of the above observations, it is decided to carry out a detail study of this class of wall-frame buildings in this thesis.

The resulting uncoupled equation of equilibrium will adopt the following form:

$$EI_y \frac{d^4y}{dz^4} - GA_y \frac{d^2y}{dz^2} = w(z) \qquad (4.2)$$

$$EI_W \frac{d^4\theta}{dz^4} - GJ \frac{d^2\theta}{dz^2} = e\, w(z) \qquad (4.6)$$

Alternately, the two equations can be written in a form with non-dimensional parameters as

$$\frac{d^4y}{dz^4} - \frac{(\alpha H)^2}{H^2} \frac{d^2y}{dz^2} = \frac{w(z)}{EI_y} \qquad (4.2a)$$

$$\frac{d^4(r_W\theta)}{dz^4} - \frac{(\beta H)^2}{H^2} \frac{d^2(r_W\theta)}{dz^2} = \frac{e}{r_W} \frac{w(z)}{EI_y} \qquad (4.6a)$$

where

$$r_W = \sqrt{(EI_W/EI_y)} \qquad (4.7a)$$

r_W will be the torsional radius of gyration of the wall system about the centers of twist. The different system parameters associated with a monosymmetric uniform wall-

frame building of this class are : αH, βH and e/r_w. Physically, one can interpret these parameters in the following manner:

αH is the lateral interaction parameter;

βH is the torsional interaction parameter; and

e/r_w is the non-dimensional eccentricity of the system associated with the applied load w(z).

The two uncoupled differential equations of equilibrium, as given by eqns.(4.2) and (4.6), are of the same form as that of a symmetric wall-frame building under lateral and torque loadings respectively. Thus the solution for the static responses of the structure under eccentric lateral loads will be equal to the combined lateral and torsional responses of an equivalent symmetric wall-frame building.

4.3 Dynamic Analysis of a Special Class of Uniform Monosymmetric Wall-Frame Buildings (a=0, $\alpha H=\beta H$)

To evalute the adequacy of the torsional code provisions on the class of wall-frame structures with coincident wall and frame centers, the modal spectrum technique is used as a base for comparison. In this approach, one has to know the dynamic characteristics of the building. In static analysis, the rigidity center is a convenient point of reference from a mathematical point of

view. However, in dynamic analysis, the mass center will be a more appropriate point of reference for interpreting the results. Unlike the rigidity center, the mass center is not sensitive to changes on the structural system configuration and is more readily determined. In view of this, the mathematical formulation of the dynamic problem will be conducted with reference to the mass centers of the building, which are assumed to line up along a vertical axis.

The equation of free vibration for such a building is given by [13,18]:

$$\begin{bmatrix} m & 0 \\ 0 & m\rho^2 \end{bmatrix} \begin{Bmatrix} \ddot{Y} \\ \ddot{\theta} \end{Bmatrix} + \begin{bmatrix} k_y & -ek_y \\ -ek_y & k_\theta \end{bmatrix} \begin{Bmatrix} Y \\ \theta \end{Bmatrix} = \begin{Bmatrix} 0 \\ 0 \end{Bmatrix} \qquad (4.14)$$

in which

$Y(z,t)$ is the lateral response function of the building at the mass centers;

$\theta(z,t)$ is the torsional response function of the building;

ρ is the mass radius of gyration about the mass centers;

k_y is the stiffness operator portraying the lateral stiffness of the resisting system; and

k_θ is the stiffness operator portraying the torsional stiffness of the resisting system.

With the parameter "a" equals zero, the stiffness parameters can be expressed as

$$k_y = EI_y D^4 - GA_y D^2 \tag{4.15}$$

$$k_\theta = (EI_W + EI_y e^2)D^4 - (GJ + GA_y e^2)D^2$$

$$= EI_y(r_W^2 + e^2)D^4 - GA_y (r_F^2 + e^2)D^2 \tag{4.16}$$

In eqns. (4.15) and (4.16), D is the differential operator with respect to z. D^n being defined as $\partial^n / \partial z^n$. Due to the inertial load effect in this case, the equation of motion will be coupled, even for this special class of wall-frame buildings. Letting

$$\begin{Bmatrix} Y \\ \theta \end{Bmatrix} = \begin{Bmatrix} \phi_y \\ \phi_\theta \end{Bmatrix} \sin\omega t = \{\phi\}\sin\omega t \tag{4.17}$$

where ω being the circular frequency and substitution of eqn. (4.17) into eqn. (4.14) leads to the eigenvalue problem:

$$\begin{bmatrix} k_y - \omega^2 m & -ek_y \\ -ek_y & k_\theta - \omega^2 m\rho^2 \end{bmatrix} \begin{Bmatrix} \phi_y \\ \phi_\theta \end{Bmatrix} = \begin{Bmatrix} 0 \\ 0 \end{Bmatrix} \tag{4.18}$$

The normal procedure for obtaining the frequencies and mode shapes will be as follows:

(i) Eqn. (4.18) represents a coupled homogeneous system. Solution to the homogeneous system is termed the homogeneous solution. It will contain a number of integration constants and also the frequency of vibration ω.

(ii) The integration constants can be determined by incorporating the boundary conditions into the homogeneous solution. The boundary conditions for a wall-frame building

are:

At the base :- the geometric boundary conditions require zero deformation (deflection, rotation, twisting and warping) at the base, thus

$$\{\phi\} = \{\phi\}' = \{0\} \qquad (4.19a)$$

At the top :- the stress boundary conditions require zero stress resultant (moment, shear, bimoment and torsional moment) at the top, thus

$$\{\phi\}'' = \{0\} \qquad (4.19b)$$

$$\begin{bmatrix} EI_y & -eEI_y \\ 0 & EI_w \end{bmatrix} \{\phi\}''' - \begin{bmatrix} GA_y & -eGA_y \\ 0 & GJ \end{bmatrix} \{\phi\}' = \{0\} \qquad (4.19c)$$

(iii) For non-trivial solution of the integration constants, a single characteristic equation with unknown ω can be obtained from the homogeneous solution. Solving the characteristic equation will yield the frequencies of vibration of the different modes.

(iv) Backsubstitute the frequency of vibration into the homogeneous solution will yield the mode shape of the particular mode.

It can be seen that close form solution to the eigenvalue problem using the continuous approach is very complex and cannot be obtained in general analytical form. However, the dynamic characteristics of a particular class of wall-frame buildings, namely, buildings with αH equals

βH, can be obtained explicitly. A detail development of the theory for this special class of buildings will be given below.

4.3.1 Natural Frequencies and Mode Shapes

The special classs of wall-frame buildings referred to in this section will be those uniform monosymmetric wall-frame buildings with coincident wall and frame stiffness centers ($a=0$) and equal degrees of lateral and torsional wall-frame interaction ($\alpha H = \beta H$).

The eigenvalue problem for this class of wall-frame buildings is given by

$$\begin{bmatrix} k_y-\omega^2 m & -ek_y \\ -ek_y & k_\theta-\omega^2 m\rho^2 \end{bmatrix} \begin{Bmatrix} \phi_y \\ \phi_\theta \end{Bmatrix} = \begin{Bmatrix} 0 \\ 0 \end{Bmatrix} \tag{4.18}$$

Defining the associated uncoupled translational system as

$$(k_y - \omega_y^2 m)\, \psi_y = 0 \tag{4.20a}$$

or

$$(EI_y D^4 - GA_y D^2 - \omega_y^2 m)\, \psi_y = 0 \tag{4.20b}$$

ω_y will be the natural frequency of vibration of the translational system. The mode shape ψ_y is normalized such that

$$\int_0^H m\, \psi_y^2\, dz = 1 \tag{4.21}$$

Similarly, the associated uncoupled torsional system will be

$$(k_\theta - \omega_\theta^2 m\rho^2)\, \psi_\theta = 0 \tag{4.22a}$$

or

$$[EI_y(r_W^2+e^2)D^4 - GA_y(r_F^2+e^2)D^2 - \omega_\theta^2 m\rho^2]\,\psi_\theta = 0 \quad (4.22b)$$

ω_θ will be the natural frequency of vibration of the torsional system. The mode shape ψ_θ is normalized such that

$$\int_0^H m\rho^2\,\psi_\theta^2\,dz = 1 \quad (4.23)$$

When αH equals βH, then

$$r_W = r_F = r \quad (4.11)$$

Eqn. (4.22b) can be simplified to

$$[(r^2+e^2)(EI_yD^4-GA_yD^2)-\omega_\theta^2 m\rho^2]\psi_\theta = 0 \quad (4.22c)$$

The dynamic characteristics of the uncoupled systems can be expressed as a function of the system parameters. The translational uncoupled system is represented by the equation

$$[D^4 - \frac{(\alpha H)^2}{H^2}D^2 - \omega_y^2\frac{m}{EI_y}]\,\psi_y = 0 \quad (4.20c)$$

The homogeneous solution to eqn.(4.20c) as given in [15] is

$$\psi_y(z) = C_1\cos\lambda_1 z+C_2\sin\lambda_1 z+C_3\cosh\lambda_2 z+C_4\sinh\lambda_2 z \quad (4.24)$$

in which

$$\lambda_1^2 = \sqrt{[\,(\frac{\alpha^2}{2})^2 + \omega_y^2\frac{m}{EI_y}]} - \frac{\alpha^2}{2} \quad (4.25)$$

and

$$\lambda_2^2 = \lambda_1^2 + \alpha^2 \quad (4.26)$$

Substituting the boundary conditions

at the base :

$$\psi_y(0) = 0 \tag{4.27}$$

$$\psi_y'(0) = 0 \tag{4.28}$$

at the top :

$$\psi_y''(H) = 0 \tag{4.29}$$

$$\psi_y'''(H) - \alpha^2\psi'(H) = 0 \tag{4.30}$$

into eqn.(4.24) gives the governing characteristic equation

$$2 + (\frac{\lambda_1^2}{\lambda_2^2} + \frac{\lambda_2^2}{\lambda_1^2})\cos\lambda_1 H\cosh\lambda_2 H + (\frac{\lambda_2}{\lambda_1} - \frac{\lambda_1}{\lambda_2})\sin\lambda_1 H\sinh\lambda_2 H = 0 \tag{4.31}$$

The solution to eqn.(4.31) for obtaining the eigenvalues can be obtained by trial and error for given value of αH. Backsubstituting the eigenvalue ω_{yi} of the i^{th} mode into eqn.(4.24) gives the corresponding mode shape. Normalization with respect to the mass according to eqn.(4.21) yields ψ_{yi}.

Similar treatments can be applied to the uncoupled torsional system:

$$[D^4 - \frac{(\alpha H)^2}{H^2} D^2 - \omega_\theta^2 \frac{m}{EI_y} \frac{\rho^2}{r^2+e^2}] \psi_\theta = 0 \tag{4.22d}$$

$$\psi_\theta(z) = C_1\cos\eta_1 z + C_2\sin\eta_1 z + C_3\cosh\eta_2 z + C_4\sinh\eta_2 z \tag{4.32}$$

in which

$$\eta_1^2 = \sqrt{[(\frac{\alpha^2}{2})^2 + \omega_\theta^2 \frac{m}{EI_y} \frac{\rho^2}{r^2+e^2}]} - \frac{\alpha^2}{2} \tag{4.33}$$

and

$$\eta_2^2 = \eta_1^2 + \alpha^2 \tag{4.34}$$

The corresponding boundary conditions are :

$$\psi_\theta(0) = \psi_\theta'(0) = 0 \tag{4.35}$$

$$\psi_\theta''(H) = \psi_\theta'''(H) - \alpha^2\psi_\theta'(H) = 0 \tag{4.36}$$

The governing characteristic equation is given by

$$2+\left(\frac{\eta_1^2}{\eta_2^2} + \frac{\eta_2^2}{\eta_1^2}\right)\cos\eta_1 H\cosh\eta_2 H+\left(\frac{\eta_2}{\eta_1} - \frac{\eta_1}{\eta_2}\right)\sin\eta_1 H\sinh\eta_2 H=0 \tag{4.37}$$

The eigenvalue from solution of eqn. (4.37) is $\omega_{\theta i}$ and the normalized i^{th} mode shape will be $\psi_{\theta i}$.

The translational component ϕ_y and the torsional component ϕ_θ of the coupled mode shape can be expressed in terms of the uncoupled counterparts ψ_y and ψ_θ respectively as [13,18]:

$$\begin{Bmatrix}\phi_y\\ \phi_\theta\end{Bmatrix} = \begin{bmatrix}\psi_y & 0\\ 0 & \psi_\theta\end{bmatrix}\begin{Bmatrix}\mu_y\\ \mu_\theta\end{Bmatrix} = [\psi]\{\mu\} \tag{4.38}$$

in which μ_y and μ_θ being proportional constants. Eqn.(4.38) holds true only when the modes of the uncoupled system ψ_y and ψ_θ have the same shape. This condition is satisfied when αH equals βH.

One can ascribe to this special class of uniform wall-frame buildings the following structural characteristics:

(i) A single torsional stiffness radius of gyration "r" can be defined for both the wall and frame system.

(ii) Defining Ω as the uncoupled torsional to

lateral frequency ratio ω_θ/ω_y, this ratio can be expressed readily in terms of the other system parameters. Using eqns. (4.20c) and (4.22d) yield

$$\Omega = \omega_\theta/\omega_y = \sqrt{[(r^2 + e^2)/\rho^2]} \qquad (4.39)$$

(iii.) The corresponding uncoupled mode shapes will also bear simple ratio to one another, ie.

$$\psi_y = \rho\, \psi_\theta \qquad (4.40)$$

Substituting eqn.(4.38) into eqn.(4.18), premultiplying by $[\psi]^T$ and integrating over the domain z from zero to H yields

$$\begin{bmatrix} \omega_y^2-\omega^2 & -e\omega_y^2/\rho \\ -e\omega_y^2/\rho & \omega_\theta^2-\omega^2 \end{bmatrix} \begin{Bmatrix} \mu_y \\ \mu_\theta \end{Bmatrix} = \begin{Bmatrix} 0 \\ 0 \end{Bmatrix} \qquad (4.41)$$

By substituting the uncoupled first mode frequencies ω_{y1} and $\omega_{\theta 1}$ into eqn.(4.41), the frequency of the first two modes ω_1 and ω_2 of the coupled system can be solved for.

$$\omega_{1,2}^2 = \frac{\omega_{y1}^2}{2}\left[\, 1+\Omega^2 \mp \sqrt{[(1-\Omega^2)^2+4(e/\rho)^2]}\right] \qquad (4.42)$$

Eqn.(4.42) implies that $\omega_1 \leq \omega_2$. The response modes of the coupled system will thus exist in pairs. The vibration frequency will be a function of the two non-dimensional parameters Ω and e/ρ.

To conduct further studies, it is useful to establish the practical ranges for the parameters Ω and e/ρ. It is unlikely that buildings be designed with lateral and torsional stiffnesses drastically different. For most

buildings, Ω assumes values in the practical range from 0.8 to 1.25.

For the parameter e/ρ, consider the floor plan of a rectangular building (Fig. 4.4) having characteristic dimension D_d. The polar mass radius of gyration about the mass center is related to D_d as follows:

$$\rho^2 = D_d^2/12 \tag{4.43}$$

Defining the aspect ratio of the building as

$$R = D_n/B \tag{4.44}$$

in which D_n is the plan dimension of the building in the direction of the computed eccentricity, then the following relation holds

$$\frac{e}{\rho} = \frac{e}{D_n}\sqrt{\left(\frac{12R^2}{1+R^2}\right)} \tag{4.45}$$

Eqn.(4.45) is plotted in Fig. 4.5. For e/D_n values ranging from 0 to 2.5 will correspond to buildings with small to large eccentricity. Thus from Fig. 4.5, the practical range of e/ρ can be taken from 0 to 1.

The frequency ratio ω_2/ω_1 is a parameter of particular significance. Studies [36,37] had shown that when the frequencies of adjacent modes are closed together within 25%, cross modal coupling will occur. From eqn.(4.42), the frequency ratio ω_2/ω_1 is given by

$$\frac{\omega_2}{\omega_1} = \frac{1+\Omega^2+\sqrt{[(1-\Omega^2)^2+4(e/\rho)^2]}}{2\sqrt{[\Omega^2-(e/\rho)^2]}} \tag{4.46}$$

A plot of eqn.(4.46) is given in Fig. 4.6. The frequencies of the first two modes are closed together when ω_2/ω_1 is about unity. This occurs when Ω is close to unity and when e/ρ is small. Such observation is consistent with previous findings. With larger eccentricity, the two frequencies separate further apart reducing the effect of cross modal coupling.

Three examples will be presented to study the variation of vibration frequencies as a function of the parameters Ω and e/ρ. Three uniform wall-frame buildings (Building G, H and I) are used as example structures. Each structure is a nine story building with uniform floor height of 3 m. The framing plans are shown in Fig. 4.7. There will be two frames providing lateral resistance in the x direction. In the y direction, two walls and two frames are used as resisting elements. The rigidities of the resisting elements in each building are listed in Table 4.1. The αH and βH values of all three buildings are both equal to 5. Thus strong degree of wall-frame interaction, both translationally and torsionally, is expected. The fundamental period of vibration of all buildings is 0.6 seconds. The three buildings will have identical coupled mode shapes, the first six of which are shown in Fig. 4.8. It can be seen that the modes of vibration exist in pairs.

For the first mode, the lateral component and the torsional component will always be in phase with one another. However, for the second mode, the torsional component will be 180° out-of-phase with the lateral component. This will have special significance on the torsional behaviour of buildings under seismic loads. A detail discussion in this aspect will be presented at a later stage.

The frequencies and periods of vibration are given in Table 4.2. Building G has an Ω value of 1.0 and an e/ρ value of 0.05. The computed ω_2/ω_1 ratio, according to eqn.(4.46), is 1.05. As observed from Table 4.2, the same frequency ratio applies to other mode pairs of this building. Due to the closeness in frequencies of vibration of adjacent modes, cross modal coupling is expected for this building. Building H has the Ω value increased to 1.25 while e/ρ is maintanied at 0.05. The computed ω_2/ω_1 ratio is 1.26. Since the frequency separation is more than 25%, modal coupling will not be important in this case. For the last structure, Building I, Ω is maintained at 1.0 while the eccentricity is increased by 10 times with e/ρ being equal to 0.5. The frequency ratio ω_2/ω_1 is computed to be 1.73. Modal coupling again will not be important for this building. It can be seen that once Ω is remote from unity or the eccentricity is increased, the natural frequencies will be far apart. As a result, the effect of cross modal

coupling will not be significant under such circumstances. Since cross modal coupling is a dynamic phenomenon, most code provisions do not allow for such effect. Therefore, the recognition when cross modal coupling is likely to be significant is important, particularly when one tries to compare results between code procedure and dynamic analysis.

The mode shapes of the building after normalization can be expressed as:

$$\begin{Bmatrix} \phi_y \\ \phi_\theta \end{Bmatrix}_1 = \begin{Bmatrix} \bar{\mu}_{y1} & \psi_{y1} \\ \bar{\mu}_{\theta 1} & \psi_{\theta 1} \end{Bmatrix} \tag{4.47a}$$

$$\begin{Bmatrix} \phi_y \\ \phi_\theta \end{Bmatrix}_2 = \begin{Bmatrix} \bar{\mu}_{y2} & \psi_{y1} \\ \bar{\mu}_{\theta 2} & \psi_{\theta 1} \end{Bmatrix} \tag{4.47b}$$

in which the number subscript indicates the response mode number. Defining

$$\mu_{\theta 1} = 0.5[1-\Omega^2+\sqrt{[(1-\Omega^2)^2+4(e/\rho)^2}] \tag{4.48a}$$

$$\mu_{\theta 2} = 0.5[1-\Omega^2-\sqrt{[(1-\Omega^2)^2+4(e/\rho)^2}] \tag{4.48b}$$

then

$$\bar{\mu}_{y1} = \frac{e/\rho}{\sqrt{[(e/\rho)^2+\mu_{\theta 1}{}^2]}} \tag{4.49a}$$

$$\bar{\mu}_{\theta 1} = \frac{\mu_{\theta 1}}{\sqrt{[(e/\rho)^2+\mu_{\theta 1}{}^2]}} \tag{4.49b}$$

$$\bar{\mu}_{y2} = \frac{e/\rho}{\sqrt{[(e/\rho)^2+\mu_{\theta 2}{}^2]}} \tag{4.49c}$$

$$\bar{\mu}_{\theta 2} = \frac{\mu_{\theta 2}}{\sqrt{[(e/\rho)^2 + \mu_{\theta 2}^2]}} \qquad (4.49d)$$

The same procedure can be repeated for obtaining the dynamic properties of other higher pairs of modes.

In the development of the above analysis, specific reference is made to uniform wall-frame buildings. However, it must be emphasized that the results apply equally well to proportional framing buildings, whether they are all wall buildings or all frame buildings.

The success of the above analysis relies on two requirements:

(a) A single structural eccentricity "e" can be defined for the building. For wall-frame buildings, this is made possible only when the wall centers coincide with the frame centers. Mathematically, the parameter "a" equals zero.

(b) A single torsional stiffness radius of gyration "r" can be defined for the building. For wall-frame buildings, this requirement is satisfied when αH equals βH.

4.3.2 Seismic Forces Determination

Knowing the dynamic characteristics of the building, modal spectrum analysis [29] can then be carried out to determine the force resultants on the building caused by the different modes. The dynamic lateral forces on uniform

symmetric wall-frame structures were presented in [5]. When an eccentric building is excited by ground shaking, both translational forces and torques will result in each mode. The translational forces will act through the centers of mass of the building. The forces (F_1 and F_2) and torques (T_1 and T_2) obtained from the first two modes of response are given by

$$F_1 = [\bar{\mu}_{y1}{}^2 m^2 Sa(\omega_1,\xi)\int_0^H \psi_{y1}\,dz]\psi_{y1} \qquad (4.50a)$$

$$T_1 = [\rho\bar{\mu}_{y1}\bar{\mu}_{\theta 1} m^2 Sa(\omega_1,\xi)\int_0^H \psi_{y1}\,dz]\psi_{y1} \qquad (4.50b)$$

$$F_2 = [\bar{\mu}_{y2}{}^2 m^2 Sa(\omega_2,\xi)\int_0^H \psi_{y1}\,dz]\psi_{y1} \qquad (4.50c)$$

$$T_2 = [\rho\bar{\mu}_{y2}\bar{\mu}_{\theta 2} m^2 Sa(\omega_2,\xi)\int_0^H \psi_{y1}\,dz]\psi_{y1} \qquad (4.50d)$$

In eqn.(4.50), Sa is the spectral acceleration. It is a function of the frequency and damping ξ of the particular mode. For simplicity, a flat or a hyperbolic design spectrum (Fig. 4.9) are often used to represent the earthquake input. The flat spectrum will be appropriate for stiff buildings. Hyperbolic spectrum, on the other hand, is suitable for buildings with longer period. Also, equal damping for all modes will be assumed.

The total dynamic response of the building is obtained by combining responses of the contributing modes,

often in a square-root-sum-square (SRSS) manner.

4.4 Torsional Shears from Dynamic Analysis Perspective

The nature of the torsional problem as from a dynamic analysis point of view is different from building code approaches. For an eccentric structure, each mode in dynamic analysis is a coupled mode having both a translational and a torsional response component (Fig. 4.8). Thus a single mode response will give rise to both lateral forces (acting at the mass centers) and torque loadings, as represented by eqn. (4.50).

Under most circumstances, a coupled mode shows a preference of action [32]. It can either be a mode with a dominant translational component and with a small rotational component, or the response is mainly rotational with minor translational movement. The former type of modal behaviour will be denoted as lateral predominant. The action of such a mode will give rise to mainly lateral forces. The latter type of modal behaviour is denoted as torsional predominant, with a minimum amount of induced lateral loadings.

Coupled modes can be labelled either as lateral or torsional predominant only if the cross modal coupling effect is not severe. The condition that will lead to severe cross modal coupling has been discussed in section 4.3.1. When the building has uncoupled lateral and torsional

frequencies being close to one another and when the structural eccentricity is small, cross modal coupling effect can be expected [36]. When the cross modal coupling effect is severe, the lateral and rotational component of a response mode will be comparable in magnitude. As a result, a response mode can not be identified as being lateral or torsional predominant. In this thesis, discussion is restricted to those buildings when the cross modal coupling effect is negligible.

Further, due to structural asymmetry, the lateral forces acting at the centers of mass will induce additional torque loadings on the building. Therefore, the total torsional effect in dynamic analysis can be attributed to two sources: (a) torque loadings arose from the translational-torsional coupling of a response mode, referred to as "inertial torques" in this thesis; and (b) static equivalent torque loadings arose from transferring the lateral forces from the centers of mass to the centers of rigidity of the building, referred to as "torques due to the eccentric lateral load effect" in this thesis.

The torque loading induced on the building by each mode is given by a combination of the inertial torques and torques due to the eccentric load effect. Depending on the phasing of the lateral mode shape and the torsional mode

shape in a coupled mode, these two sources of torque loading may reinforce each other, or tend to cancel each other. Consider the first two coupled modes shown in Fig. 4.8. For the first mode, the inertial torques are in phase with the torque loadings due to the eccentric lateral load effect. In other words, the two torques will be additive resulting in larger torque values. Such modal behaviour will be denoted as an in-phase mode in this thesis. For the second mode, however, the inertial torques will counteract the torques due the eccentric lateral load effect thus reducing the overall torsional effect. This kind of modal behaviour will be denoted as out-of-phase mode.

To facilitate discussion later on, the resisting elements on the same side as the mass centers, as measured from the centers of twist (or centers of rigidity) will be identified as elements on the positive side in this thesis. For these elements, an in-phase mode will induce torsional shears which act in the same direction as the lateral shears, resulting in larger shear magnitudes in them. For elements on opposite side of the mass centers (or elements on the negative side), an in-phase mode induces torsional shears which counteract the lateral shears, resulting in a lower shear value on the element. With an out-of-phase mode, the reverse will be true. The torsional shears caused by an out-of-phase mode will reinforce the lateral shears

in elements on the negative side. For elements on the positive side, the shears are reduced.

Finally, in dynamic analysis, the responses from different modes are combined to give the total response of the building. However, many studies had shown that for symmetric buildings of regular proportion and medium height, the main contribution of lateral forces comes from the fundamental mode. However, for eccentric buildings of regular proportion, one has to include contributions from the first pair of modes. Depending on the relative torsional stiffness to lateral stiffness of the building, it is possible for eccentric buildings to have a second mode rather than a first mode which is lateral predominant. As a result, at least a second mode should be included in the determination of total response for eccentric buildings.

Two situations arise when considering the response of the first pair of modes.

(a) One has the situation with mode 1 being lateral predominant and mode 2 torsional predominant. Being lateral predominant, the first mode is the major contributor of lateral shears to the resisting elements. Further, also being an in-phase mode, torsional shears from the first mode will reinforce the lateral shears in the elements on the

positive side. Thus the first mode response governs the behaviour of these elements. The second mode response is less significant for these elements since this torsional predominant mode is also an out-of-phase mode. However, for the elements on the negative side, the second mode contribution can be as significant as the first mode because torsional shears from the first mode counteract the lateral shears while torsional shears from mode 2 reinforce the lateral shears. Thus one can not identify solely mode 1 as the significant mode for checking the torsional shears in elements on the negative side.

(b) One has the case in which the first mode is torsional predominant and the second mode is lateral predominant. Since mode 2 is now the major contributor of lateral shears, the first mode response no longer governs the behaviour of elements on the positive side. However, on the other hand, the second mode, being an out-of-phase mode, will not be a major contributor of <u>total</u> shears to these elements either. Thus, both the first and the second mode response will be equally important for elements on the positive side. Behaviour of elements on the negative side will be governed mainly by the second modal contribution since the total shears come from the second mode. They will now be the elements most susceptible to the torsional effect.

Summarizing, complexity in shear force distribution in different resisting elements of a structure based on dynamic analysis can be attributed to (i) the existence of lateral and torsional predominant modes; and (ii) the existence of in-phase lateral predominant or out-of-phase lateral predominant modes. Mode 1 of an eccentric structure will always be an in-phase mode while mode 2 will be an out-of-phase mode. For the situation when mode 1 is also lateral predominant, the behaviour of the elements on the positive side will be governed by the fundamental mode response. For elements on the negative side, responses from both mode 1 and 2 are important. For situations when mode 2 becomes lateral predominant, the critical elements are those on the negative side and their behaviour will be governed by the response of the second mode. Responses of both mode 1 and 2 are important for the positive side elements in this latter case.

The torsional provisions of most seismic codes can simulate the situation when the seismic forces in the structure come from an in-phase lateral predominant mode. This would be the case if cross modal coupling effect is small, and also the building's fundamental mode is a lateral predominant mode. In the situation when a building has a

lateral predominant second mode, the code provisions would tend to overestimate the shear for the elements on the positive side. The code failed to identify the elements on the negative side as critical torsionally and may underestimate the tosional effect on such elements.

4.5 Seismic Loading Comparison :- Building Code Approach versus Dynamic Analysis

Due to the static nature of the code provisions, it is only effective to represent the situation when the major contribution of seismic loads to a building comes from a lateral predominant mode with in-phase torsional effect. Therefore, in comparison between dynamic analysis and code provisions, emphasis will be placed on the assumption of the presence of a lateral predominant first mode. Mathematical treatment in determining the behaviour of such a lateral predominant fundamental mode will be given below. To be consistent with the spirit of the code, further restrictions are imposed onto the class of structures to which the discussion is directed to. These restrictions are listed as follows: (i) The class of buildings will be limited to those midrise wall-frame buildings to which higher mode contributions are not important. (ii) For midrise buildings, the natural period is usually over 0.5 seconds and a hyperbolic shape spectral curve will be considered appropriate to use as earthquake spectral input. (iii)

Elements on the positive side of the building are identified by the code as most susceptible to the torsional effect. The design eccentricity equation appropriate for these elements is suggested by the code as

$$e_n = 1.5\, e + 0.1\, D_n \tag{4.51}$$

In this thesis, emphasis will be placed in evaluating the accuracy of the above equation to obtain the shears in these elements.

The condition under which a building will have a lateral predominant fundamental mode can be judged by studying the lateral force ratio F_1/F_2. This ratio will be constant along the height of the building but will be a function of the spectrum used. For a hyperbolic spectrum, ie. $Sa(\omega,\xi) \alpha \omega$, then

$$\frac{F_1}{F_2} = \frac{[1-\Omega^2+2(e/\rho)^2-\sqrt{[(1-\Omega^2)^2+4(e/\rho)^2]}]^2}{4[\Omega^2-(e/\rho)^2](e/\rho)^2} \tag{4.52}$$

Eqn.(4.52) is plotted in Fig. 4.10. With the fundamental mode being lateral predominant requires that the force ratio F_1/F_2 to be much larger than unity. The larger the ratio F_1/F_2 is, the high the degree of lateral predominancy of mode one will be over the second mode. From Fig. 4.10, a lateral predominant fundamental mode exists when Ω is larger than unity and when e/ρ is small. Take the case of Ω being 1.25, the F_1/F_2 ratios corresponding to e/ρ values of 0.15, 0.3 and 0.6 are 9.6, 2.7 and 0.8 respectively. Thus for a

given value of Ω, the degree of predominancy decreases with increasing e/ρ values, as the building becomes more torsionally unbalanced. If the first mode is lateral predominant, then relatively speaking, mode 2 can be identified as torsional predominant. The lateral response of the second mode will be smaller than that of the fundamental mode.

It may be assumed that a lateral predominant fundamental mode exists if the first mode gives rise to at least 90 % of the total combined two mode response. Then, mathematically, for mode 1 to be lateral predominant, it requires that

$$\frac{F_1/F_2}{\sqrt{(F_1/F_2)^2 + 1}} > 0.9 \qquad (4.53)$$

or explicitly, F_1/F_2 needs to be larger than 2.2 (Fig. 4.10). For a given Ω value ($\Omega > 1$), the range of e/ρ values over which mode 1 is lateral predominant can be determined from Fig. 4.10. For example, with Ω equals to 1.25, the effective range of e/ρ values are determined to be $0 < e/\rho < 0.34$.

Two uniform nine story wall-frame buildings having different dynamic properties will be used for illustration. The buildings have an uniform floor height of 3 m. The floor plans of the two buildings (Building J and K) are shown in

Fig. 4.11. Two rigid frames provide lateral resistance in the x direction. In the y direction, two walls and two frames are used as resisting elements. The rigidity distribution of the elements are summarized in Table 4.1. The buildings have equal and significant degrees of lateral and torsional wall-frame interaction with αH equals βH and both take on a value of 5. The fundamental period of vibration is chosen to be 0.6 seconds. Building J has an uncoupled frequency ratio of 1.25 and an e/ρ value of 0.15. The frequency ratio of Building K is reduced to 0.8 while the same eccentricity ratio of 0.15 is maintained.

The lateral shear distribution in the two buildings as predicted by NBCC 1985 will be compared to that from dynamic analysis. The two buildings are again assumed to be located in Vancouver, Canada with acceleration and velocity related zone both being 4 in this case. For comparison purposes, the base shear as determined by dynamic analysis is normalized with respect to the design static base shear value. For dynamic analysis, the response of the first five modes are combined in a SRSS manner to give the total response. By comparing the response as predicted by the code with the five mode combined response, the accuracy of the code procedure can be assessed. By comparing the two mode and the five mode combined responses, the effect of higher mode contributions can be studied.

Shown in Fig. 4.12 is a comparison of the interstory shear force envelopes of the two buildings. The distribution based on NBCC 1985 provisions, two mode and five mode dynamic responses show very little difference for both buildings. Thus the code procedures are capable of providing good estimates of interstory shear distribution. Also, higher modal (modes 3 through 5) contributions are not important for these two buildings.

The lateral response of mode 1 alone is computed to be 99.5 % and 7.3 % of the total response for Building J and K respectively. It is obvious that Building J has a lateral predominant first mode while Building K has a lateral predominant second mode.

Regarding torsional effect, the total torque loadings from each mode are given by combining the inertial torques and torques due to the eccentric lateral load effect. For the first two modes, the inertial torques are expressed by eqns. (4.50b) and (4.50d). The torques due to eccentric lateral load effect are given by the product of the lateral loads F_1 and F_2 and the structural eccentricity "e", which is assumed to be constant along the height of the building. The total torque loadings of mode 1 and 2 can then be written as

$$T_1 = F_1 e + T_1 = F_1 e_{d1} \qquad (4.54a)$$

$$T_{II} = F_2 e + T_2 = F_2 e_{d2} \qquad (4.54b)$$

The torque ratio T_I/T_{II} will be spectrum dependent. Using a hyperbolic shape spectrum input, one obtains that $T_I = -T_{II}$. Two implications can be observed from this relationship. First, it implies that the two torques are always 180° out-of-phase with one another. Second, in terms of absolute magnitude, the torque ratio remains constant and is independent of Ω and e/ρ. Thus a torsional predominant mode does not give rise to total torque loadings larger than a lateral predominant mode. The torsional effect from a lateral predominant mode and a torsional predominant mode is equal, but opposite in direction.

It will be convenient to express the torque loadings of each mode as the product of the lateral forces and the dynamic eccentricity of the particular mode. The dynamic eccentricity e_{di} of mode i is defined as "the distance from the center of rigidity that the lateral forces should apply to produce the <u>total</u> seismic torques for the particular mode". In non-dimensional form, the dynamic eccentricity $\bar{e}_{di}$ can be expressed as

$$\bar{e}_{di} = e_{di}/\rho = e/\rho + T_i/(F_i \rho) \qquad (4.55)$$

$\bar{e}_{di}$ will be constant along the height of the building and is independent of the form of spectrum used. The dynamic eccentricity of the first two modes will be given by

$$\bar{e}_{d1} = \frac{e}{\rho} + \frac{\sqrt{[(1-\Omega^2)^2+4(e/\rho)^2]} + (1-\Omega^2)}{2(e/\rho)} \qquad (4.56)$$

$$\bar{e}_{d2} = \frac{e}{\rho} - \frac{\sqrt{[(1-\Omega^2)^2+4(e/\rho)^2]} - (1-\Omega^2)}{2(e/\rho)} \qquad (4.57)$$

To assess the accuracy of the design eccentricity equation, eqn. (4.51) is to be compared to the dynamic eccentricity calculated based on contribution from mode 1 only and mode 1 is assumed to be a lateral predominant mode. For comparison purposes, the design eccentricity is normalized with respect to ρ. By making use of the relationship given by eqn. (4.45), the normalized design eccentricity from the code can be expressed as

$$\frac{e_n}{\rho} = 1.5\,\frac{e}{\rho} + 0.1\,\sqrt{\left(\frac{12R^2}{1+R^2}\right)} \qquad (4.58)$$

in which "R" is the aspect ratio of the floor plan as given by eqn. (4.44). The design and dynamic eccentricities are compared in Fig. 4.13. Two aspect ratio values were assumed, corresponding to 0.5, and 2 in determining the design eccentricity. It can be seen that the code tends to underestimate the torsional effect in some regions. Take the case Ω being 1.25 and e/ρ being 0.3. The normalized design eccentricity for aspect ratio of 0.5 and 2 are 0.6 and 0.76 respectively. The computed $\bar{e}_{d1}$ value is 0.73. Thus the code slightly underestimate the torsional effect

for R equals to 0.5. Similar comparisons can be made for other values of Ω. In general, the design eccentricity equation is adequate for encompassing the seismic torsional effect. It must be emphasized that if Ω is less than 1.25 and when the eccentricity is small, cross modal coupling will occur. The above comparison based on a single mode response will not be strictly valid.

A comparison of the static design shear envelope with that from dynamic analysis for the left and right edge element of Building J is made in Fig. 4.14. The dynamic response is based on the first two mode contributions, since higher mode contribution is not important for this building. For the right edge element, the code provides a good approximation to the shear distribution as compared to dynamic analysis. For the left edge element, design shears tends to be overestimated by code provisions. By comparing the design shears with the lateral shears (labelled as torsion ignored in the figure), the torsional effect predicted by the code can be studied. The torsional effect expected on the right edge element is larger than the left edge element since the right edge element is on the positive side and identified by the code as a torsional critical element.

A comparison of the static design shears with that

from dynamic analysis in Building K is made in Fig. 4.15. For the left edge element, a good estimate of design shears is obtained. For the right edge element, a drastic overestimation of the torsional effect leads to overestimation of the design shears from code provisions. The reason for such estimation of design shears is because Building K belongs to the class of buildings that has a lateral predominant second mode as discussed in section 4.4.

4.6 Other Classes of Uniform Monosymmetric Wall-Frame Buildings

To complete the discussion on uniform wall-frame buildings, it is necessary also to consider the following classes of wall-frame buildings:

(i) Uniform monosymmetric wall-frame buildings with a=0 and αH is approximately equal to βH.

(ii) Uniform monosymmetric wall-frame buildings with a=0 and αH drastically differs from βH; and

(iii) The more general class of uniform monosymmetric wall-frame buildings with "a" being non-zero.

Each of the above classes of uniform wall-frame buildings will be dealt with in the following sections.

4.6.1 Uniform Monosymmetric Wall-Frame Buildings with a=0 and $\alpha H \approx \beta H$

If the interaction parameters αH and βH of the

resisting system are not equal, then the results in section 4.3 are not strictly correct. However, if the two parameters are similar in magnitude, one may use the solution valid for $\alpha H=\beta H$ as a first approximation to the true solution. A correction or improvement to this first approximation can be established by means of perturbation analysis [23].

When αH is approximately equal to βH, then one can write the torsional radius of gyration r_W and r_F of the wall and frame system respectively as:

$$r_W = r \tag{4.59a}$$

$$r_F = r + r^* \tag{4.59b}$$

in which r^* is the difference between r_F and r_W. It is assumed that r^* is small in this analysis. The eigenvalue problem is now represented by

$$\begin{bmatrix} k_y & -ek_y \\ -ek_y & k_\theta \end{bmatrix} \begin{Bmatrix} \phi_y \\ \phi_\theta \end{Bmatrix} - \varepsilon \begin{bmatrix} 0 & 0 \\ 0 & k'_\theta \end{bmatrix} \begin{Bmatrix} \phi_y \\ \phi_\theta \end{Bmatrix} - \omega^2 \begin{bmatrix} m & 0 \\ 0 & m\rho^2 \end{bmatrix} \begin{Bmatrix} \phi_y \\ \phi_\theta \end{Bmatrix} = \begin{Bmatrix} 0 \\ 0 \end{Bmatrix} \tag{4.60a}$$

or

$$[k_1]\{\phi\} - \varepsilon[k_2]\{\phi\} - \omega^2[m^*]\{\phi\} = \{0\} \tag{4.60b}$$

in which

$$k'_\theta = 2r^* r\, GA_y D^2 \tag{4.61}$$

The perturbation index ε is introduced in eqn.(4.60) to facilitate the grouping of terms of comparable order of magnitude. The eigenvalue and the corresponding eigenfunction of the given system will be denoted by ω_i and

$\{\phi\}_i$ respectively. Expressing the eigenvalue and eigenfunction in powers of ε, then

$$\omega_i = \omega_i^0 + \varepsilon\omega_i^1 + O(\varepsilon^2) \tag{4.62}$$

$$\{\phi\}_i = \{\phi^0\}_i + \varepsilon\{\phi^1\}_i + O(\varepsilon^2) \tag{4.63}$$

The unperturbed solutions ω_i^0 and $\{\phi^0\}_i = <(\phi_y^0)_i \ (\phi_\theta^0)_i>^T$ are obtained in section 4.3.1 in solving the eigenvalue problem given by eqn. (4.18). Substituting eqns.(4.62) and (4.63) into eqn. (4.60b) and equating like powers of ε, the first order perturbation equation is given by

$$[k_1]\{\phi^1\}_i - (\omega_i^0)^2[m^*]\{\phi^1\}_i = [k_2]\{\phi^0\}_i + 2\omega_i^0\omega_i^1[m^*]\{\phi^0\}_i \tag{4.64}$$

Expressing the first order correction of the eigenfunction as a linear combination of the unperturbed eigenfunctions, then

$$\{\phi^1\}_i = \sum_{k=1}^{\infty} a_{ik}\{\phi^0\}_k \tag{4.65}$$

Substitute eqn. (4.65) into eqn. (4.64), multiplying by $\{\phi^0\}_j^T$, integrating over the domain z and making use of the orthogonality properties of the normal modes, then

$$\omega_i^1 = -\frac{\int_0^H [k_\theta'(\phi_\theta^0)_i](\phi_\theta^0)_i dz}{2\omega_i^0} \tag{4.66}$$

$$a_{ij} = \frac{\int_0^H [k_\theta'(\phi_\theta^0)_i](\phi_\theta^0)_j dz}{(\omega_j^0)^2 - (\omega_i^0)^2} \qquad i \neq j \tag{4.67}$$

Coefficient a_{ii} can be determined in the final solution of

eqn. (4.60) in the normalization of the eigenvector $\{\phi\}_i$.

The corrections to the eigenvalue and eigenfunction are given in eqn. (4.66) and (4.67) respectively. Two observations can be made:

(i) The correction to the eigenvalue as represented by eqn. (4.66) is small since r^* is small.

(ii) In eqn. (4.67), the coefficient a_{ij} can take on large values when the natural frequencies of the i^{th} and j^{th} mode, (ω_i^0) and (ω_j^0), are approximately equal. Such a situation will occur when the phenomenon of strong cross modal coupling takes place with mode i and j. In other words, large correction to the unperturbed mode shape can be expected when there is cross modal coupling.

To avoid such a situation, it requires that either Ω be remote from unity or the eccentricity e/ρ be relatively large. This can be demonstrated with three of the example structures used earlier. Building G (Fig. 4.7) has an Ω value equal to unity and with eccentricity being small ($e/\rho = 0.05$). Closeness in vibration frequencies (Table 4.2) of adjacent modes leads to strong cross modal coupling. Once Ω is remote from unity (Building H, Ω=1.25, e/ρ=0.05) or the eccentricity is increased (Building I, Ω=1.0, e/ρ=0.5), the vibration frequencies of adjacent modes will be separated further apart. Cross modal coupling effect will not be important under such circumstances.

4.6.2 Uniform Monosymmetric Wall-Frame Buildings with:
(i) a=0 and αH drastically differs from βH
(ii) a≠0

For these latter two classes of uniform wall-frame buildings, close form solution to the eigenvalue problem using the continuous approach cannot be obtained. As a result, one has to resort to the use of discrete approaches. In matrix form, the equation of motion of a free vibrating structure taking the mass centers as origin will be

$$\begin{bmatrix} [M] & [0] \\ [0] & [M]\rho^2 \end{bmatrix} \begin{Bmatrix} \{\ddot{Y}\} \\ \{\ddot{\theta}\} \end{Bmatrix} + \begin{bmatrix} [K_{yy}] & [K_{y\theta}] \\ [K_{\theta y}] & [K_{\theta\theta}] \end{bmatrix} \begin{Bmatrix} \{Y\} \\ \{\theta\} \end{Bmatrix} = \begin{Bmatrix} 0 \\ 0 \end{Bmatrix} \quad (4.68)$$

in which

[M] is the diagonal mass matrix with diagonal elements being equal to the floor mass $\bar{m}$ of an uniform building;

$[K_{yy}], [K_{y\theta}], [K_{\theta y}], [K_{\theta\theta}]$ are stiffness matrices as defined in eqn. (2.28) of chapter 2 for buildings with orthogonal framing; and

{Y} and {θ} are respectively the lateral and rotational displacement vector of the mass centers.

Assuming

$$\begin{Bmatrix} \{Y\} \\ \{\theta\} \end{Bmatrix} = \{\Phi\} \sin\omega t \quad (4.69)$$

leads to the eigenvalue problem

$$\begin{bmatrix} [K_{yy}]-\omega^2[M] & [K_{y\theta}] \\ [K_{\theta y}] & [K_{\theta\theta}]-\omega^2[M]\rho^2 \end{bmatrix} \{\Phi\} = \{0\} \quad (4.70)$$

Solving the eigenvalue problem of eqn. (4.70) using numerical scheme will yield the natural frequency ω_i and mode shape $\{\Phi\}_i$ of the i^{th} mode of vibration. For a N story monosymmetric building, i will range from 1 to 2N for a total of 2N modes. Substitute eqn. (4.69) into eqn. (4.68), premultiply by $\{\Phi\}^T$ and by making use of the orthogonal properties of the eigenvectors, eqn. (4.68) can be uncoupled into a set of 2N equations. If the mode shapes are normalized with respect to the mass matrix then the uncoupled equations of motion will assume the following form:

$$\begin{aligned}
&\ddot{\Phi}_1 + \omega_1^2 \Phi_1 = 0 \\
&\vdots \\
&\ddot{\Phi}_i + \omega_i^2 \Phi_i = 0 \\
&\vdots \\
&\ddot{\Phi}_{2N} + \omega_{2N}^2 \Phi_{2N} = 0
\end{aligned} \tag{4.71}$$

Each of eqn. (4.71) represents the equation of motion of a free vibrating single degree of freedom system. The modal forces $\langle\{F\}\ \{T\}\rangle_i^T$ of mode i will be given as

$$\begin{Bmatrix}\{F\}\\ \{T\}\end{Bmatrix}_i = \bar{m} S_a(\omega_i, \xi)\{\Phi\}_i^T \{I\} \begin{bmatrix}[M] & [0]\\ [0] & [M]\rho^2\end{bmatrix} \{\Phi\}_i \tag{4.72}$$

in which

$\{F\}$ represents the modal lateral forces acting at the mass centers;

{T} represents the modal torques on the structure; and $S_a(\omega_i,\xi)$ is the modal spectral acceleration as given by the design spectrum.

Once the modal forces {F} and {T} are determined, the stress resultants of the resisting elements in each mode can be obtained by treating it as a static problem. Schemes as outlined in chapter 2 can be employed for obtaining the solution. The total dynamic responses (forces, torques, displacements, etc.) can be obtained by combining the modal responses of several contributing modes, often in a SRSS manner.

In the above, the discrete approach to the modal spectrum technique was outlined. This technique is applicable to a wide class of structures and is not as restrictive as the continuous method. The discrete approach will be a convenient tool of analysis. However, it may not be an efficient tool in enhancing the understanding of the dynamic behaviour of buildings.

Two examples will be presented, one for each of these two classes of buildings forementioned. Each example is chosen to demonstrate specific behaviour of these buildings when subjected to seismic loadings.

Two nine story uniform wall-frame buildings (Building L and M) with floor height of 3m will be used as example structures. Building L has coincident wall and

frame stiffness centers (a=0) with framing plan shown in Fig. 4.16. Two walls are used to provide resistance in the x direction. In the y direction, two walls and two frames are used as resisting elements. The lateral wall-frame interaction parameter αH equals 5 while the torsional interaction parameter βH takes on a value of 1. Thus the two interaction parameters are drastically different. The structure has strong wall-frame interaction laterally but torsionally it has a dominant wall system. Building M is identical to Building J except that the frame elements in the y direction are shifted 1 m to the right from their original position (Fig. 4.16). Due to this change in layout, the wall centers no longer coincide with the frame centers. The separation between the two sets of centers will be 1 m (a=1). The frame center now coincides with the mass center at each floor of the building. The rigidity distribution of the resisting elements for both buildings are summarized in Table 4.1. The fundamental period of the two buildings is approximately 0.6 seconds. They are assumed to be located in Vancouver, Canada. The acceleration and velocity zone are both 4 in this case.

Building L has coincident wall and frame centers. As a result, the centers of rigidity lie on a vertical axis and the code provisions should be applicable. For Building

M, even with a slight shift in the frame centers results in a scattering of the rigidity centers on both sides of the mass centers when subjected to an inverted triangular distributed load (Fig. 4.17). However, the stiffness centers, as determined on a floor by floor basis, will fall on a vertical line as represented by the solid line in Fig. 4.17.

The responses as predicted by the code procedures will be compared to that from dynamic analysis for the two buildings. The dynamic responses are obtained by combining 5 mode responses in a SRSS manner. The dynamic results are normalized so that the dynamic base shear equals to the static base shear for comparison purposes.

The interstory shear distributions are compared in Fig. 4.18. Little difference is found between that predicted by the code and that from dynamic analysis. In other words, the code procedures are capable of providing a very good estimate of interstory shear distribution for both buildings.

The design shears in the left and right edge element of Building L are compared in Fig. 4.19. The torsional provisions of NBCC 1985 provide reasonable estimates of the torsional effect for both elements except at the 7th floor. At this level, the design shears are underestimated by the code. This discrepancy can be attributed to the effect of

higher mode contributions in dynamic analysis. The torsional effect for both elements is very small when the design shears are compared to the lateral shears (torsion ignored). This is due to the fact that the two wall elements in the x direction are very rigid (Table 4.1) and resist most of the torsional loads. Because of the difference in the degree of lateral and torsional wall-frame interaction, the lateral shears are slightly larger than the total shears at the top two stories for both elements. Such observation is consistent with previous findings that due to wall-frame interaction, torsional shears in a wall element do not necessary complement the lateral shears.

Because of the scattering of the rigidity centers, it will be difficult to apply the torsional provisions for the design of Building M. If the stiffness centers are used as reference points to determine eccentricities, the structural eccentricity thus determined will be denoted as e^*. The design shear distribution base on e^* is shown in Fig. 4.20. Despite the crude nature by which e^* is determined, the code did provide a good estimation of design shears for both elements. The torsional shears in the right edge element (element 4) is larger than that in the left edge element (element 1). However, such good agreement in this example can be misleading. Building C studied in

chapter 2 is another uniform wall-frame building with non-coincident wall and frame centers (a=13 m). However, the torsional shears in the left edge element (element 1) as determined by the code procedures are larger than that in the right edge element (element 4), as can be seen in Fig. 2.10. Therefore, for the class of wall-frame buildings when the wall centers do not coincide with the frame centers, the torsional provisions in the code cannot provide consistently a reasonable estimation of the torsional effect. Thus, dynamic analysis appears to be the only reliable means to distribute the torsional effect at the present time for this class of eccentric buildings.

4.7 Summary

Analytical investigation into the behaviour of uniform wall-frame buildings under static lateral loads had been conducted. Three parameters had been identified to be associated with the static behaviour of the special class of uniform wall frame buildings with coincident wall and frame centers, namely: αH, βH, and e/r_w. αH can be interpreted as a parameter measuring the degree of lateral wall-frame interaction while βH measures the degree of torsional wall-frame interaction. e/r_w is the non-dimensional eccentricity associated with the applied lateral loads. The torsional responses will be in direct proportion to this parameter. It

is shown that for wall-frame buildings, an edge element is not necessarily the element most susceptible to the torsional effect. Each element can be equally critical under such circumstances.

Analytical investigation into the dynamic behaviour of uniform wall-frame buildings is made possible when the stiffness centers of the wall system coincide with the stiffness centers of the frame system and with αH equals βH. The parameters which affect the dynamic character of such buildings will be Ω and e/ρ. Ω is the torsional to lateral frequency ratio of the associated uncoupled systems. e/ρ is the non-dimensional eccentricity measured with respect to the inertial torsional effect.

For this special class of wall-frame buildings, the provisions of NBCC 1985 are applicable since the rigidity centers lie on a vertical axis. Therefore, the design eccentricity equation ($e_n = 1.5\ e + 0.10\ D_n$) of NBCC 1985 can be evaluated assuming the first mode of the structure being lateral predominant and is the major contributor to total response. Numerical examples were used to substantiate the findings. The analytical results were extended to wall-frame buildings with αH approximately equals to βH through perturbation analysis. The solution assuming αH equals βH can be used as a reasonable first

approximate to the true solution provided cross modal coupling will not occur in the system.

Numerical investigation into the applicability of the seismic torsional provisions to two more classes of wall-frame buildings were also conducted. These are:

(i) Uniform wall-frame buildings with coincident wall and frame stiffness centers but with α_H drastically different from β_H; and

(ii) The more general class of uniform wall-frame buildings with non-coincident wall and frame stiffness centers.

For buildings with coincident wall and frame centers, the code provisions did provide reasonable approximate of shear distribution in the resisting elements. However, for those wall-frame buildings with non-coincident wall and frame centers, because of the complicated wall-frame interaction, the NBCC 1985 code provisions cannot consistently give reliable estimates of the torsional effect. For this latter class of buildings, evaluation of seismic torsional effect is best done by means of dynamic analysis.

4.8 Notations

a = distance between stiffness centers of wall system and stiffness centers of frame system

a_{ik} = proportional constant

B = dimension of building parallel to ground excitation

C_f, C_w = stiffness center of frame and wall system, respectively

C_1, C_2, C_3, C_4 = integration constants

D = differential operator

D_d = diagonal dimension of rectangular floor plan

D_n = dimension of building in direction of computed eccentricity

EI, EI_y = flexural rigidity of wall element and wall system, respectively

EI_w = torsional rigidity of wall system about wall center

e = structural eccentricity

e_{di} = dynamic eccentricity of mode i

$\bar{e}_{di}$ = normalized dynamic eccentricity of mode i

e_n = design eccentricity at floor n

e^* = structural eccentricity measured with respect to stiffness center

F_i = lateral force distribution at mass centers induced by mode i

$\{F\}$ = lateral force vector

GA, GA_y = shear rigidity of frame element and frame system, respectively

GJ = torsional rigidity of frame system about wall center

H = total height of building

$\{I\}, [I]$ = unit vector and unit matrix, respectively

k_y, k_θ, k'_θ = stiffness operators

$[M], [m^*]$ = mass matrices

m = distributed mass per unit height

$\bar{m}$ = floor mass

N = total number of floors in building

R = aspect ratio of floor plan

r = torsional radius of gyration of wall and frame system

r_F, r_W = torsional radius of gyration of the frame and wall system, respectively about the wall centers

S_a = spectral acceleration

S_F^L, S_W^L = lateral shear distribution on frame and wall element, respectively

S_F^T, S_W^T = torsional shear distribution on frame and wall element, respectively

T = uniform torque distribution

T_i = inertial torque distribution induced by mode i

$T(z)$ = applied torque distribution

$\{T\}$ = inertial torque vector

T_I, T_{II} = total torque loadings induced by mode 1 and 2, respectively

w = uniform lateral load distribution

$w(z)$ = applied lateral load distribution

x = distance of resisting element from wall center

$Y, \{Y\}$ = displacement function and displacement vector respectively with respect to mass centers

y = displacement function with respect to wall center

αH = lateral wall-frame interaction parameter

βH = torsional wall-frame interaction parameter

$\eta_1, \eta_2, \lambda_1, \lambda_2$ = integration constants

ρ = mass radius of gyration about mass center

$\theta, \{\theta\}$ = twist function and twist vector respectively, with respect to the mass center

θ = twist function with respect to the wall center

ω_i = vibration frequency of mode i

ω_{yi} = vibration frequency of mode i of the uncoupled lateral system

$\omega_{\theta i}$ = vibration frequency of mode i of the uncoupled torsional system

ω_i^0, ω_i^1 = zeroth and first order approximation of vibration frequency respectively of mode i

$\{\mu\}$ = vector with proportional constants

Ω = torsional to lateral frequency ratio of uncoupled system

ε = perturbation index

$\{\Phi\}_i, \{\phi\}_i$ = eigenvector and eigenfunction respectively of the i^{th} mode

$\{\phi^0\}_i, \{\phi^1\}_i$ = zeroth and first order approximation respectively of the eigenfunction for mode i

$\psi_{yi}, \psi_{\theta i}$ = eigenfunction of the i^{th} mode of the uncoupled lateral and torsional system, respectively

ξ = damping ratio

[0] = null matrix

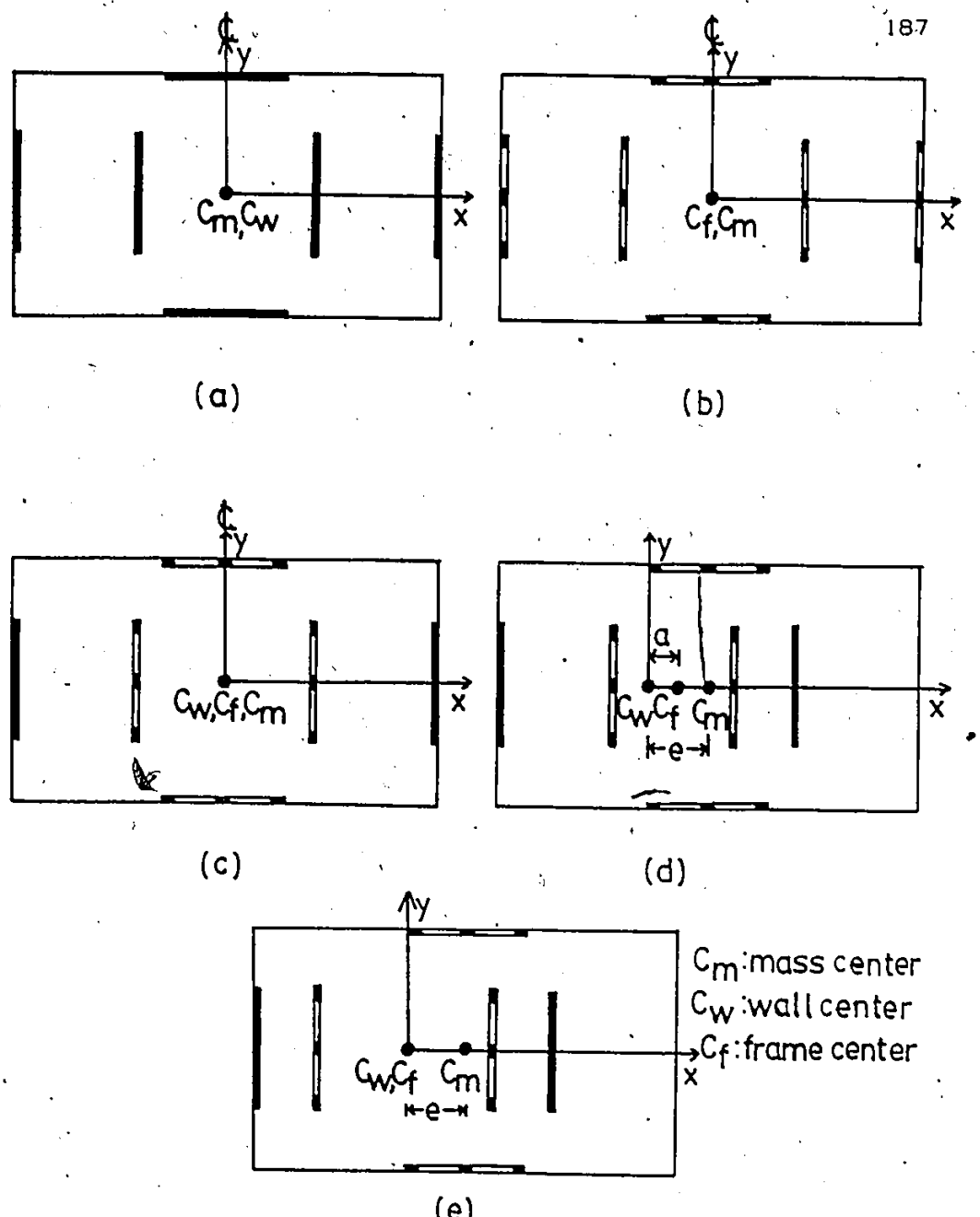

Fig. 4.1 Framing Plans of Wall, Frame and Wall-Frame Buildings
(a) Symmetric Wall Building, (b) Symmetric Frame Building,
(c) Symmetric Wall-Frame Building, (d) Eccentric Wall-Frame
Building ($a \neq 0$), (e) Eccentric Wall-Frame Building ($a=0$)

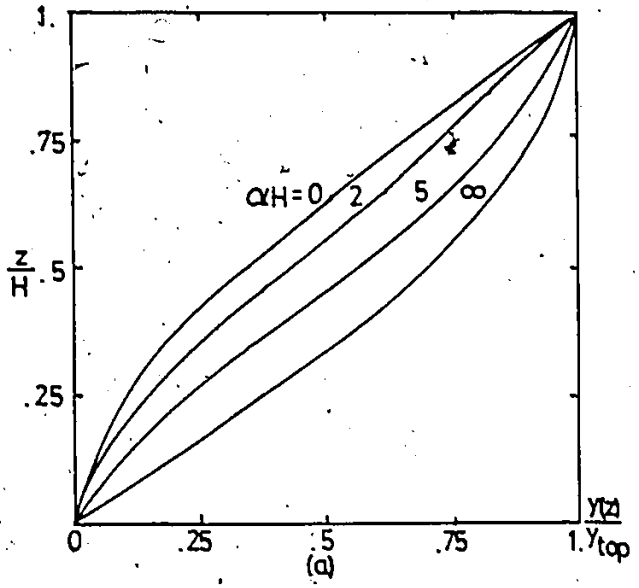

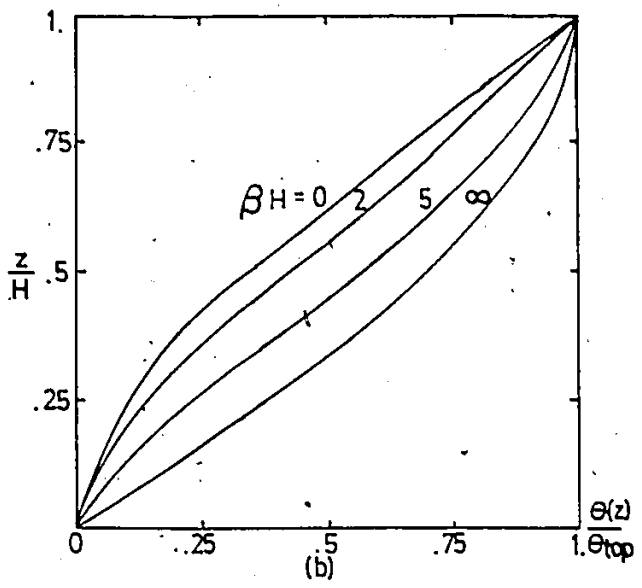

Fig. 4.2 (a) Deflection Curve, (b) Twist Curve of Symmetric Wall-Frame Building Under Uniform Distributed Load

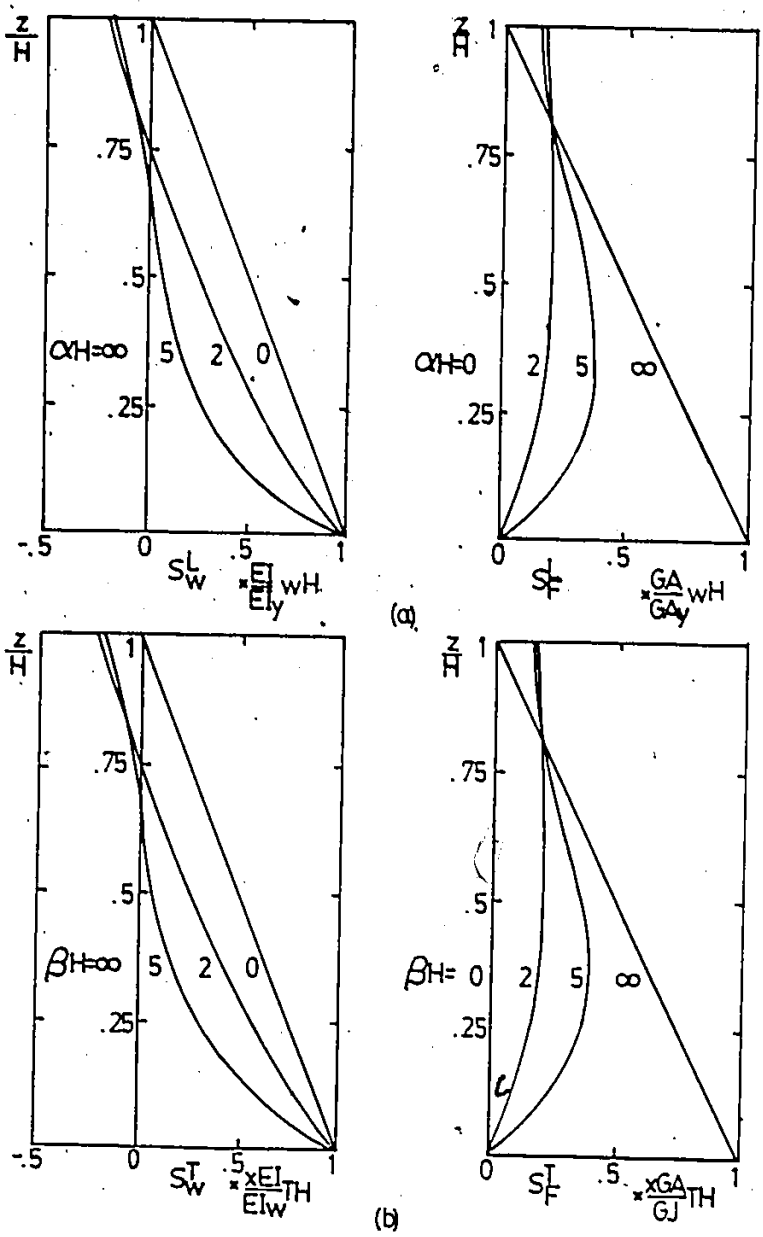

Fig. 4.3 (a) Lateral Shears, (b) Torsional Shears in Wall and Frame Under Uniform Distributed Load

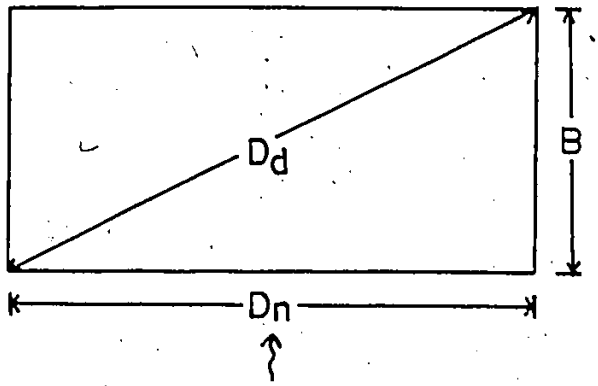

Fig. 4.4 Rectangular Building Floor Plan

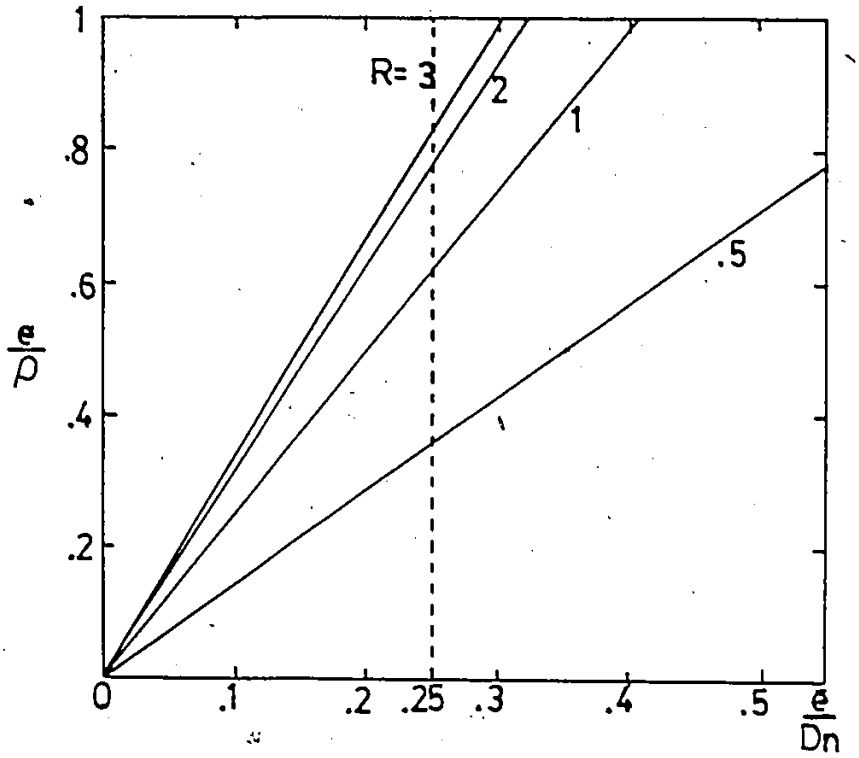

Fig. 4.5 $e/\rho - e/D_n$ Relationship

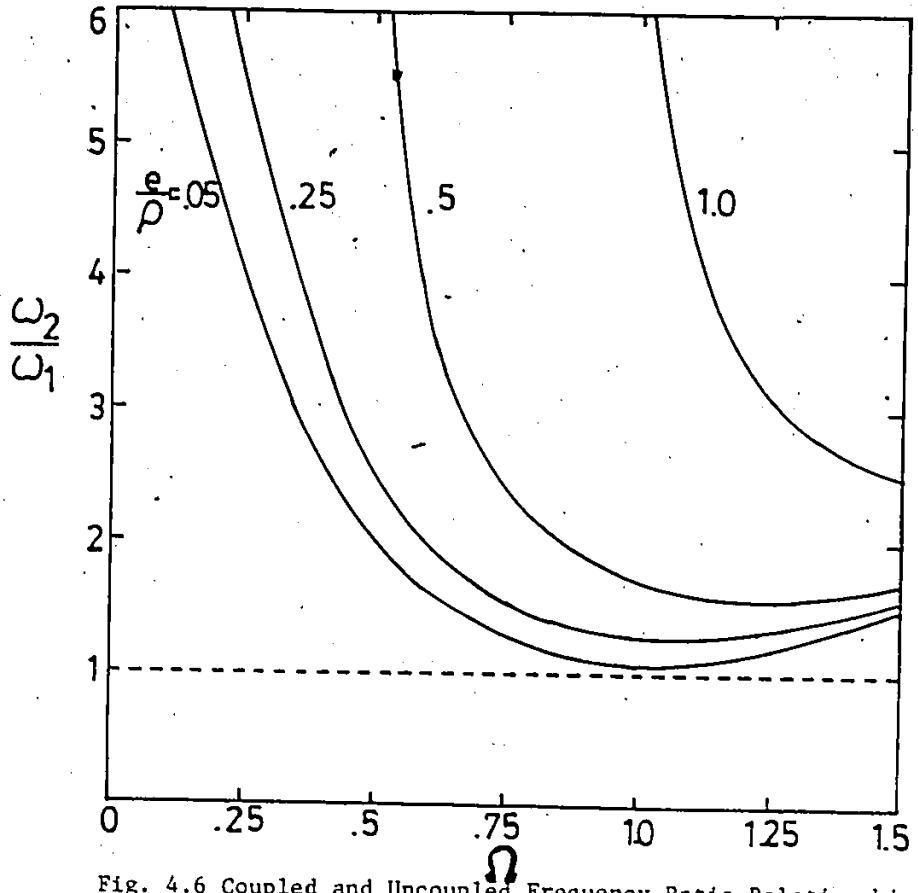

Fig. 4.6 Coupled and Uncoupled Frequency Ratio Relationship

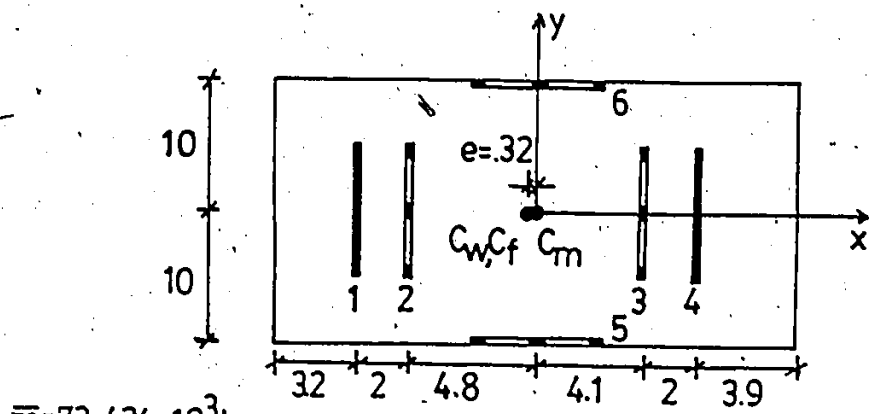

$\bar{m}=73.424\times10^3$ kg

$\bar{m}\rho^2=3.06\times10^6$ kg.m^2

Building G

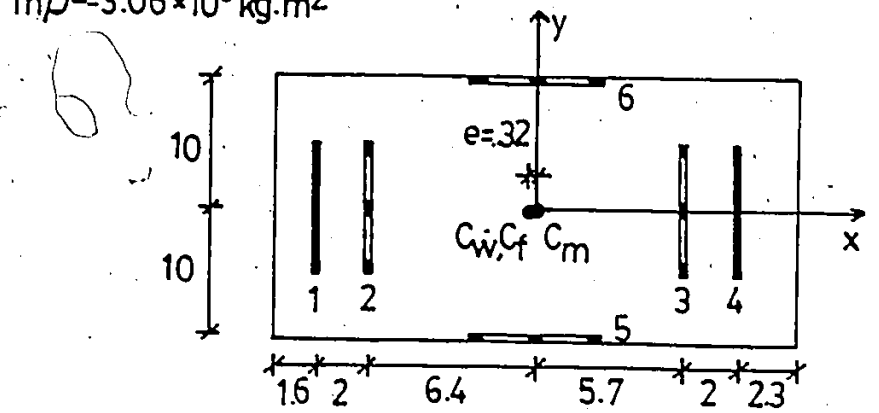

Building H

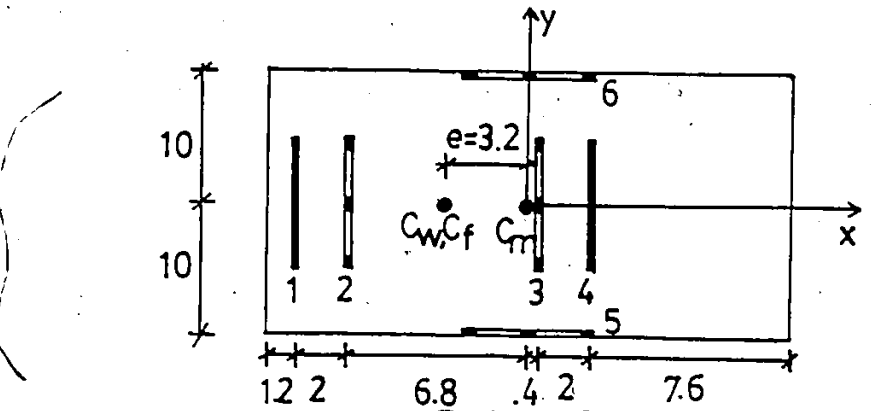

Building I

Fig. 4.7 Framing Plans of Building G, H and I

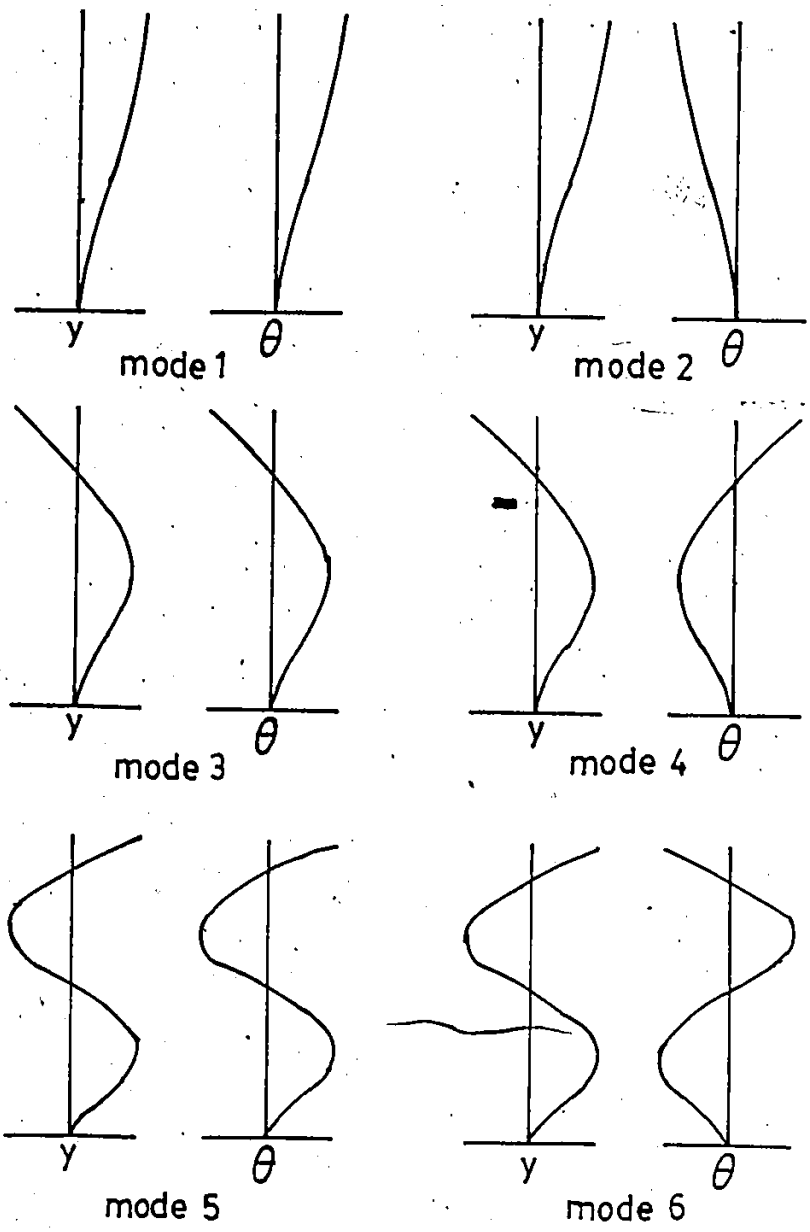

Fig. 4.8 Mode Shapes of Building G, H and I

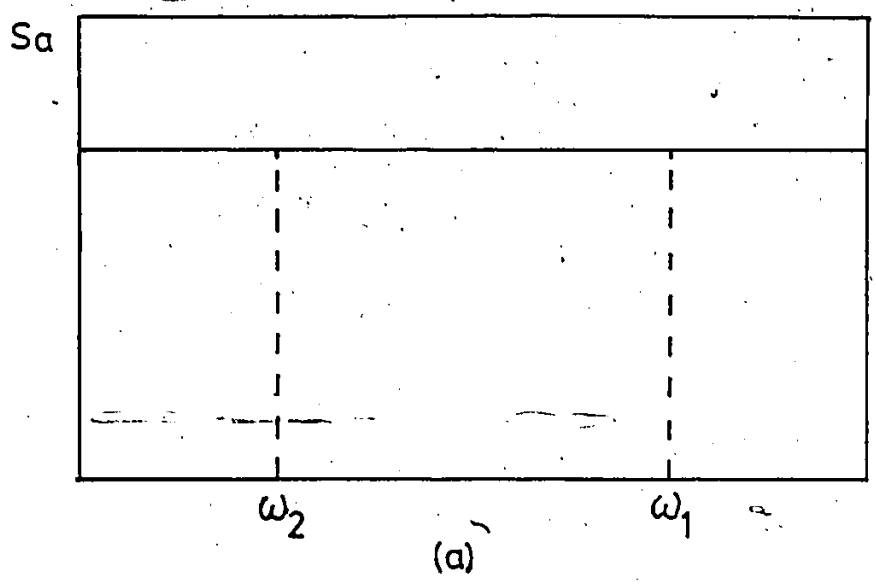

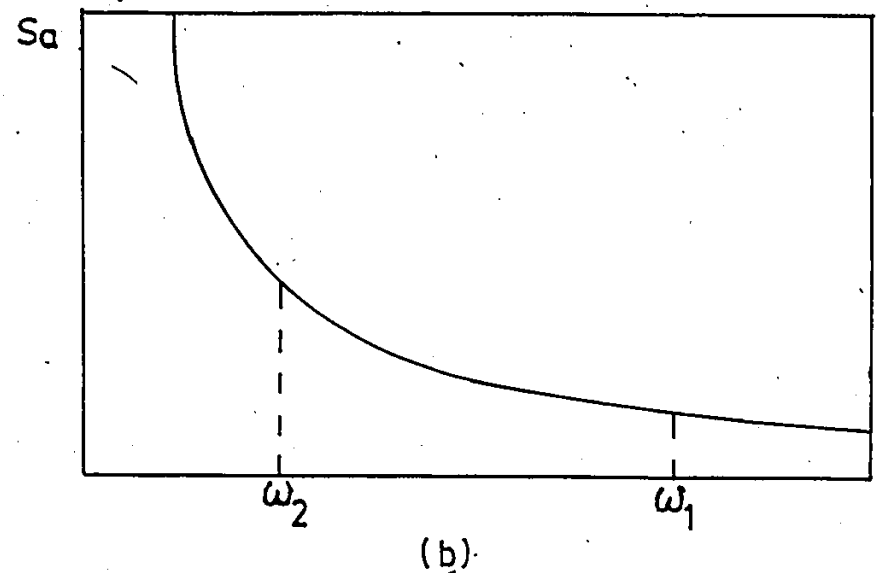

Fig. 4.9 Idealized Acceleration Spectra (a) Flat Spectrum, (b) Hyperbolic Spectrum

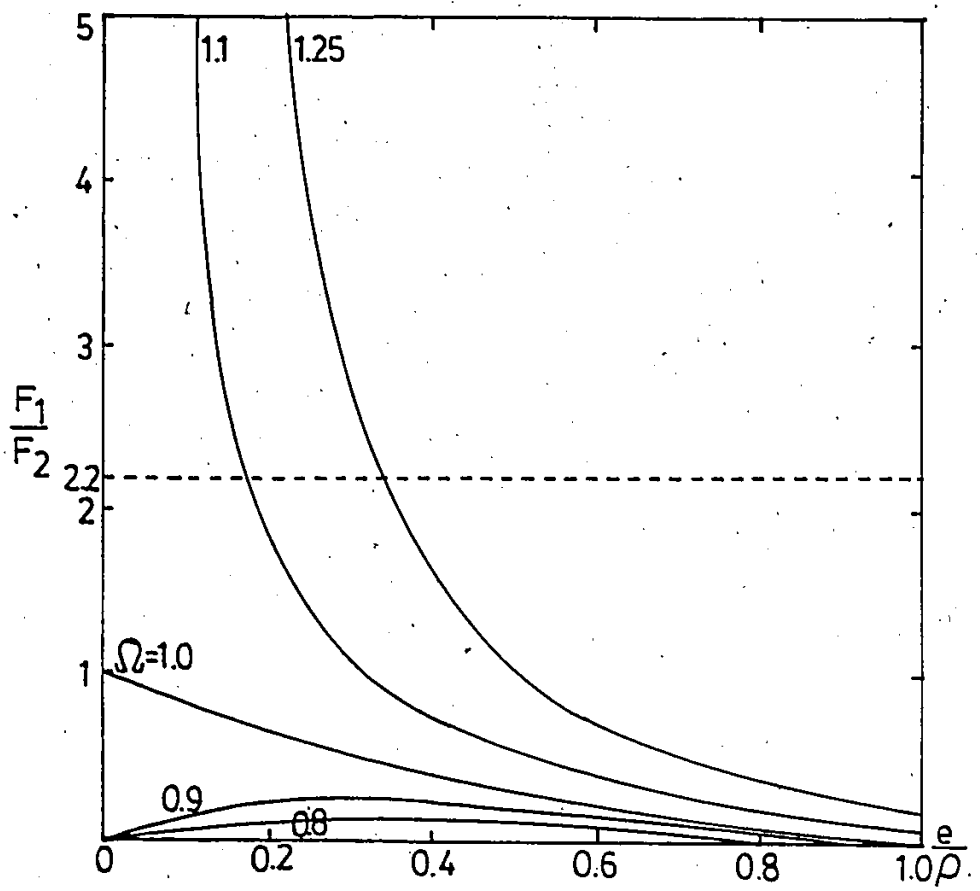

Fig. 4.10 $F_1/F_2 - e/\rho$ Relationship (Hyperbolic Spectrum)

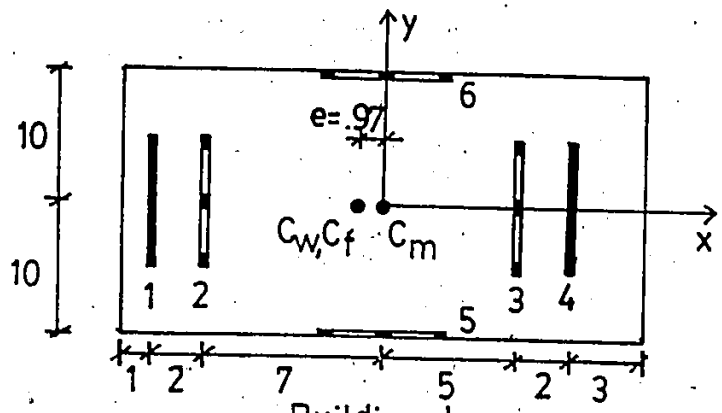

Building J

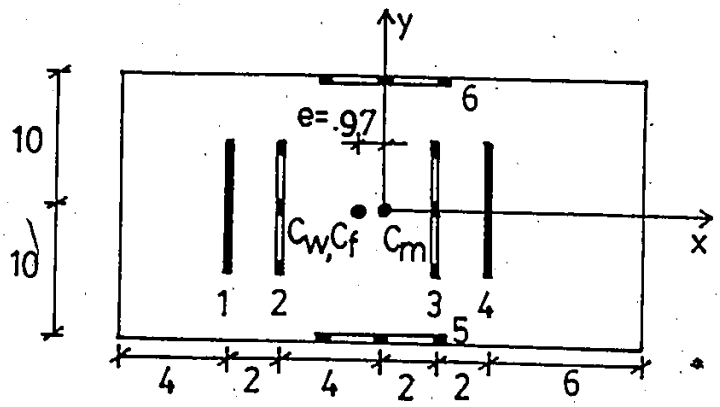

Building K

$\overline{m}=73.424\times10^3 kg$

$\overline{m}\rho^2=3.06\times10^6 kg.m^2$

Fig. 4.11 Framing Plans of Building J and K

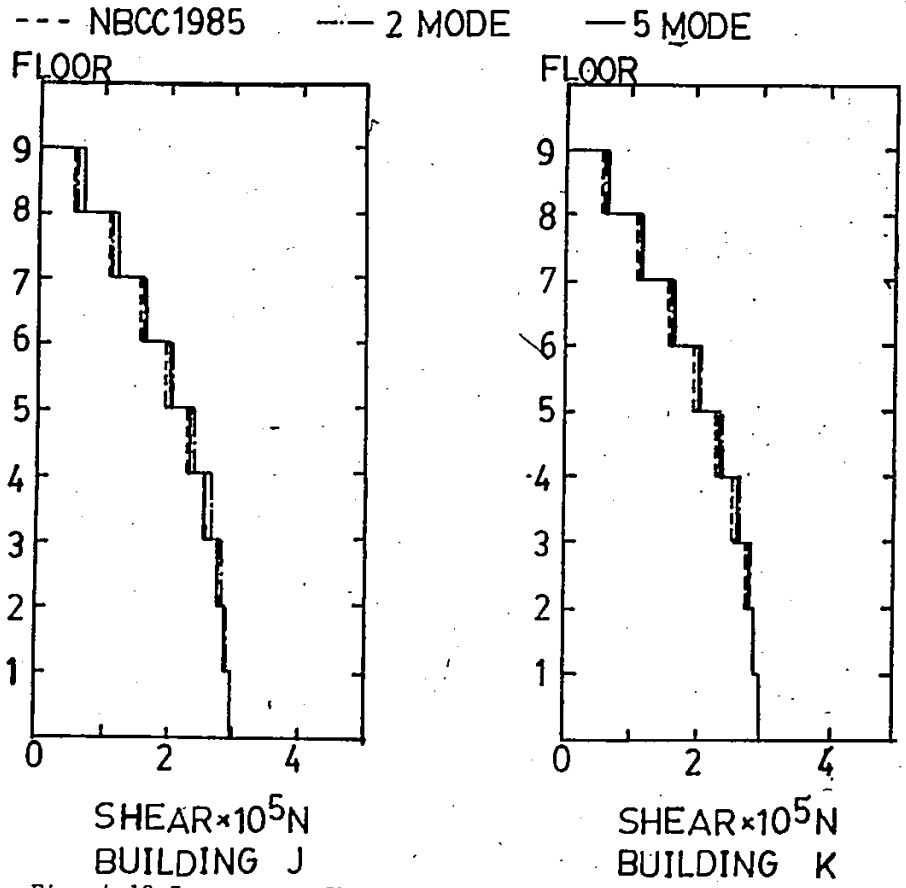

Fig. 4.12 Interstory Shear Envelopes of Building J and K

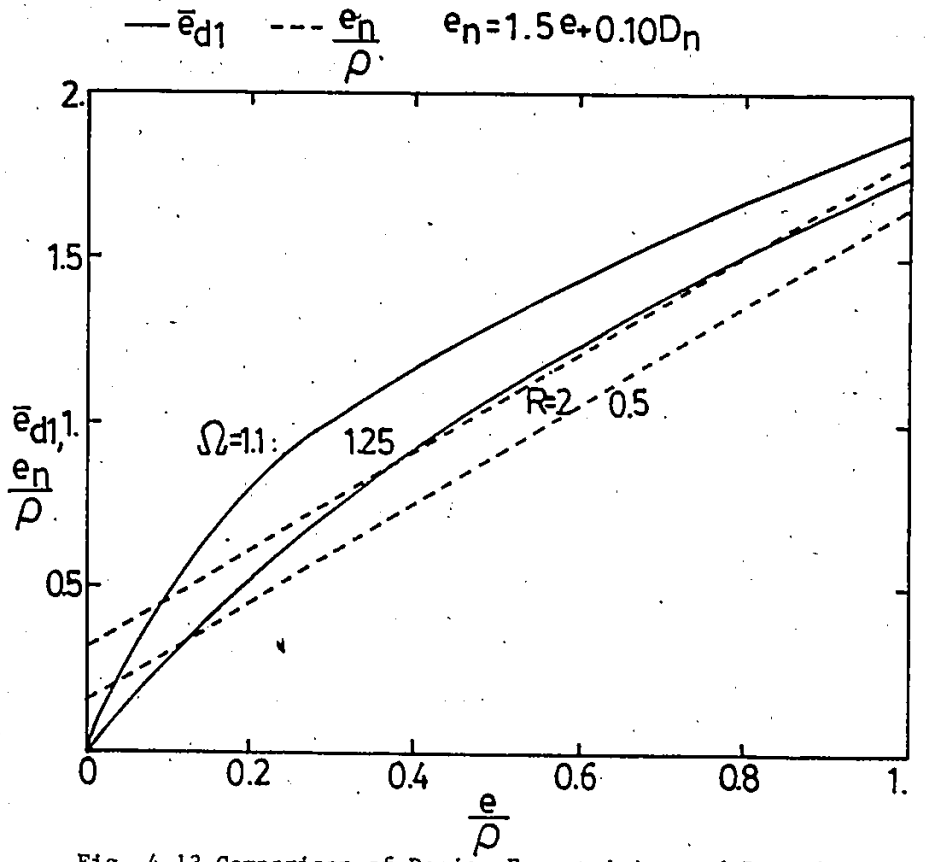

Fig. 4.13 Comparison of Design Eccentricity and Dynamic Eccentricity

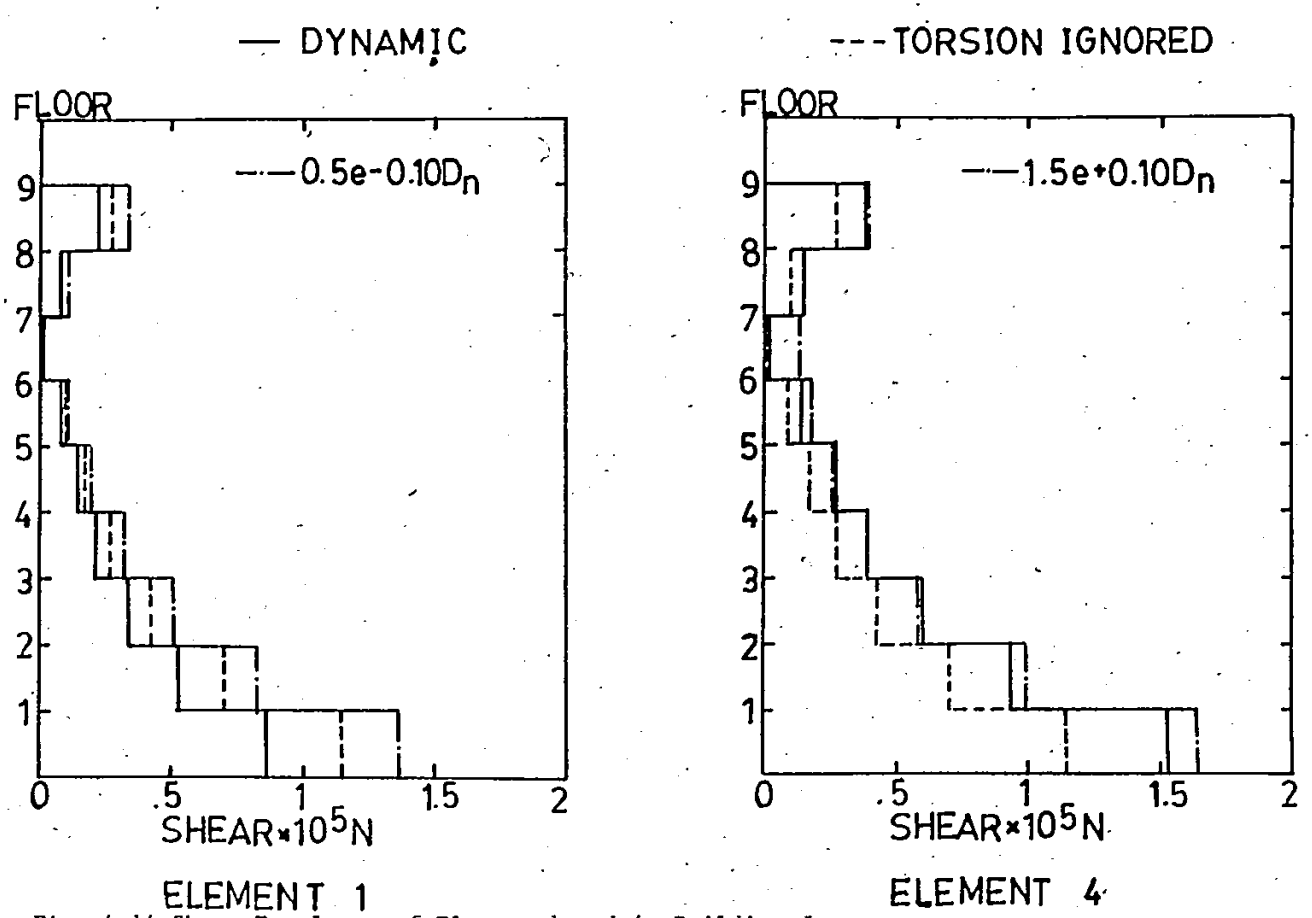

Fig. 4.14 Shear Envelopes of Element 1 and 4, Building J

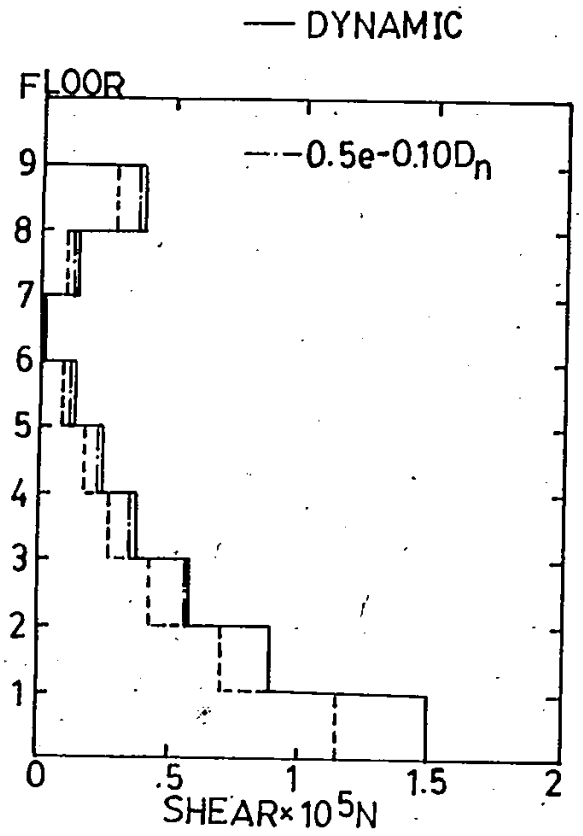

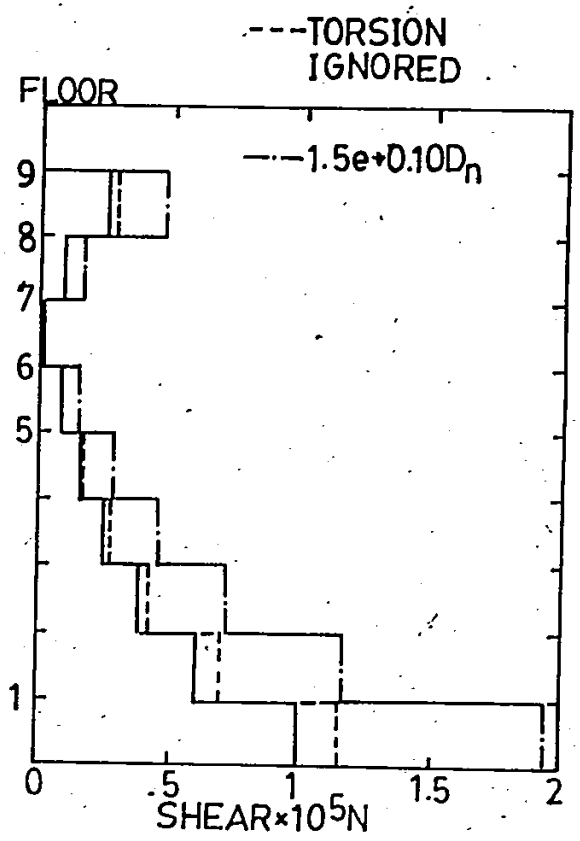

Fig. 4.15 Shear Envelopes of Element 1 and 4, Building K

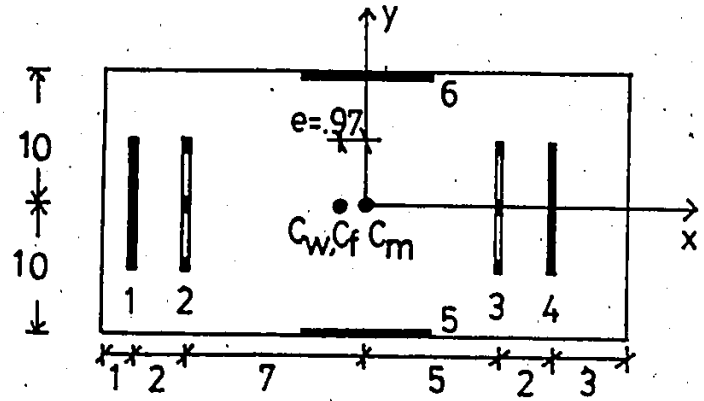

Building L

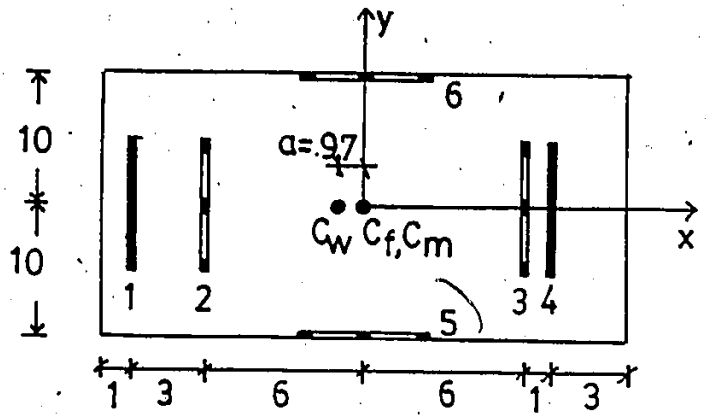

Building M

$\bar{m} = 73.424 \times 10^3 kg$

$\bar{m}\rho^2 = 3.06 \times 10^6 kg.m^2$

Fig. 4.16 Framing Plans of Building L and M

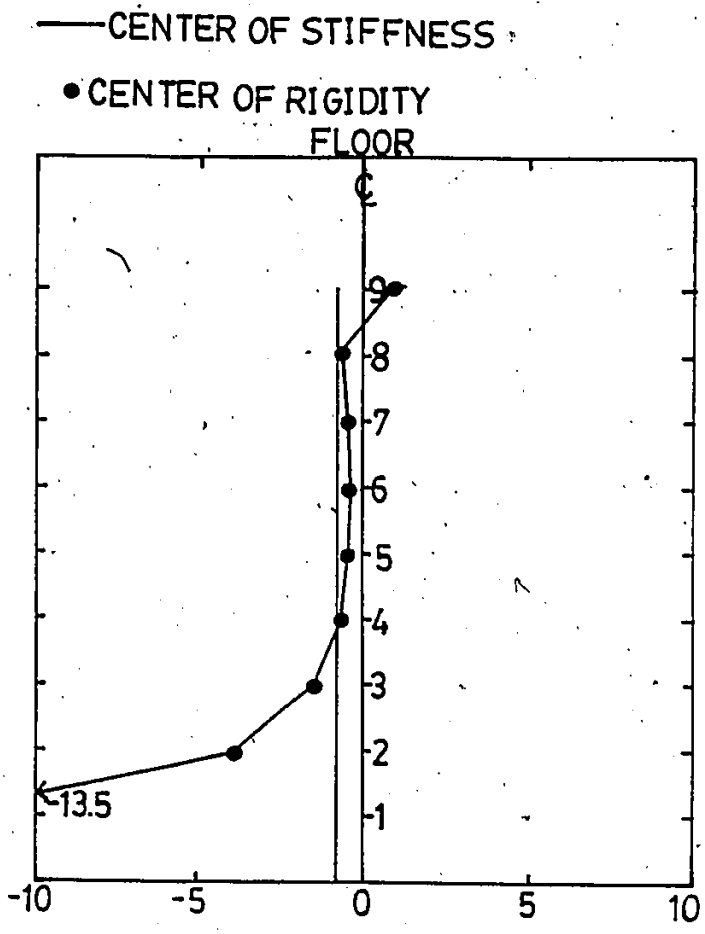

Fig. 4.17 Distribution of Rigidity and Stiffness Centers for Building M Under Inverted Triangular Distributed Load

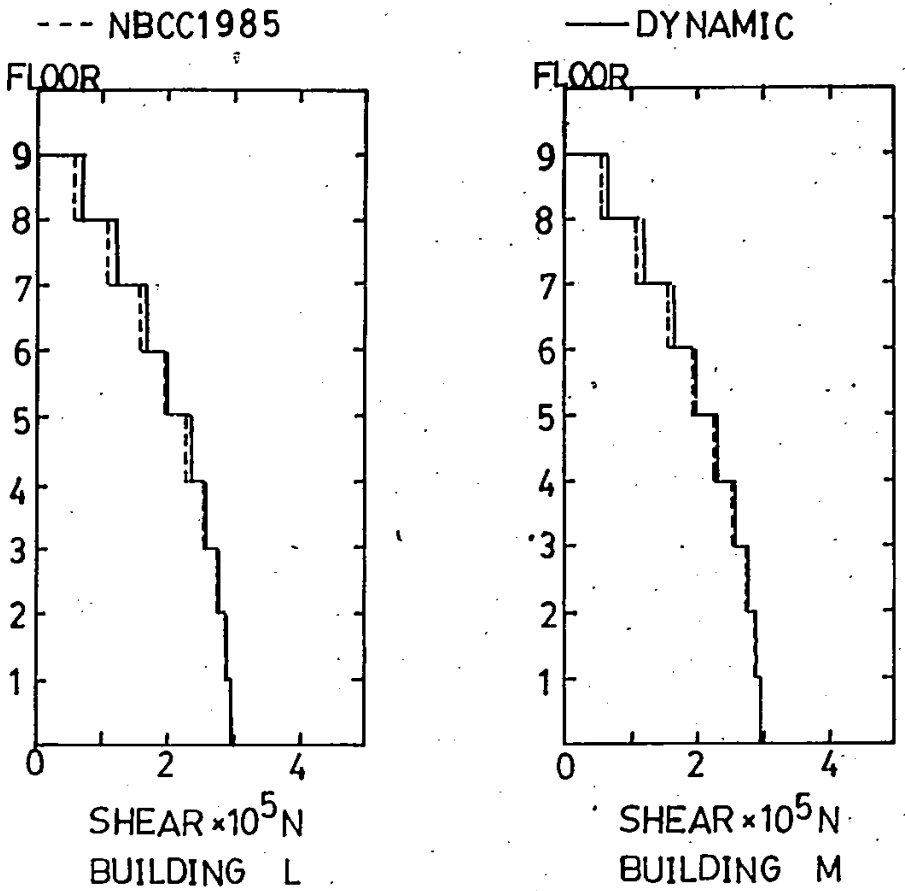

Fig. 4.18 Interstory Shear Envelopes of Building L and M

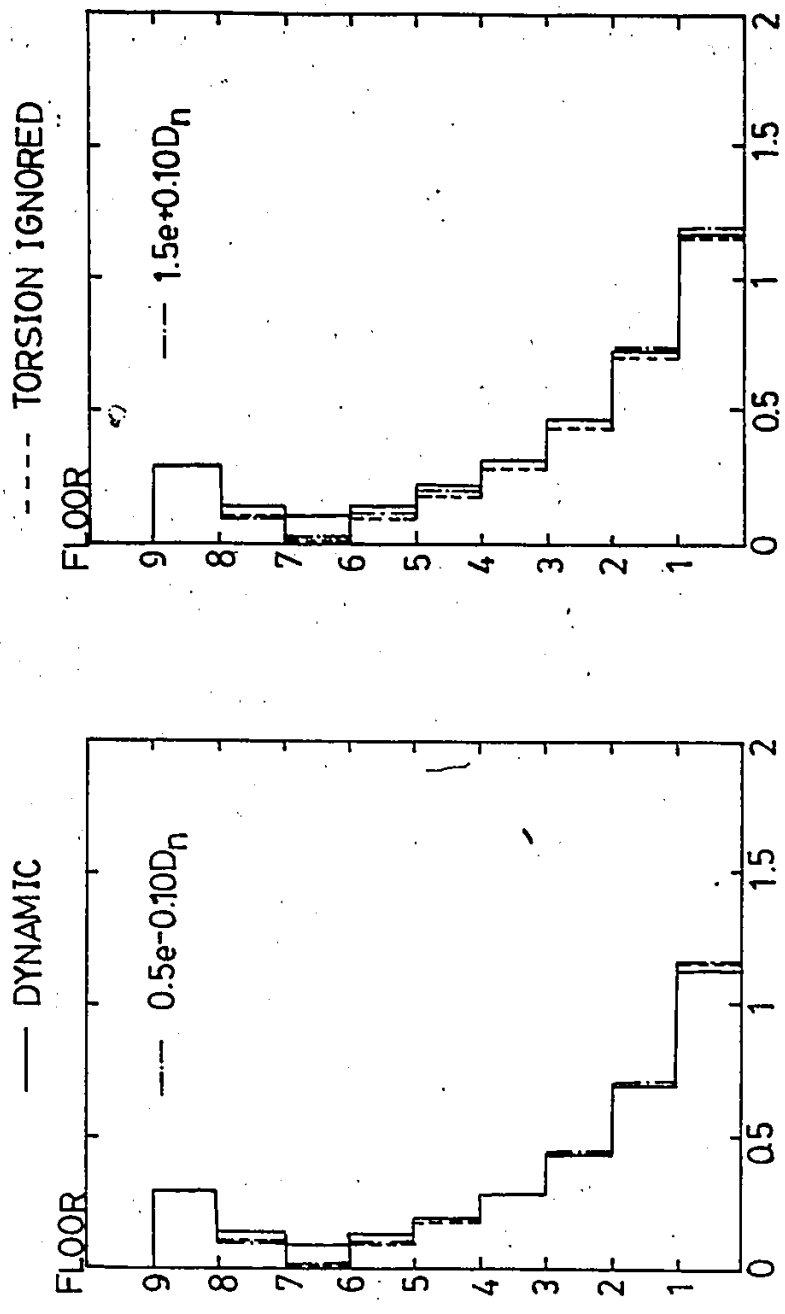

Fig. 4.19 Shear Envelopes of Element 1 and 4, Building L

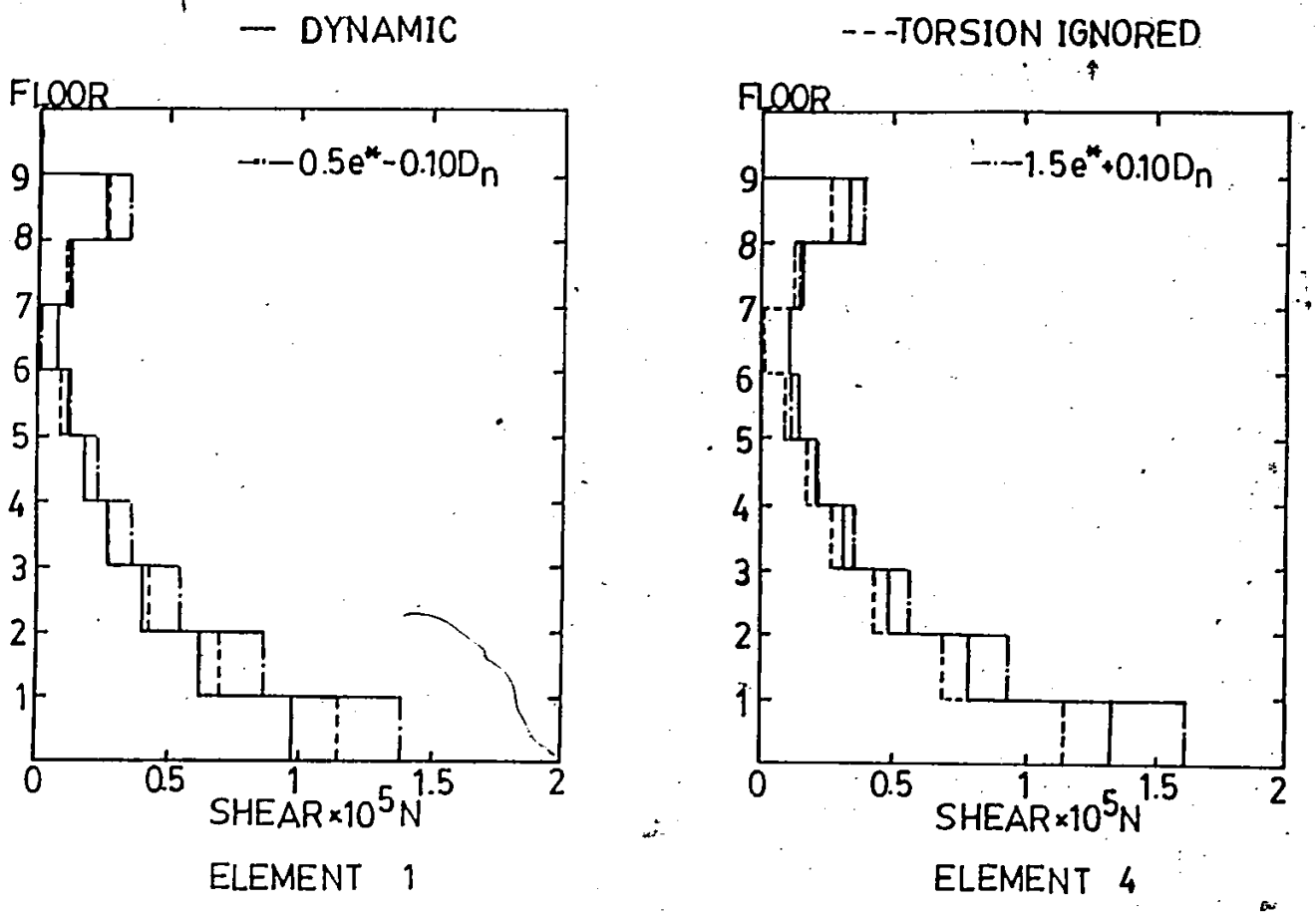

Fig. 4.20 Shear Envelopes of Element 1 and 4, Building M

TABLE 4.1 FLEXURAL AND SHEAR RIGIDITIES OF RESISTING ELEMENTS IN BUILDING G, H, I, J, K, L AND M

Building	Floor	Elements					
		1	2	3	4	5	6
G	1/F-9/F	EI	GA	GA	EI	.87GA	.87GA
H	1/F-9/F	.95EI	.95GA	.95GA	.95EI	1.1GA	1.1GA
I	1/F-9/F	1.9EI	1.9GA	1.9GA	1.9EI	1.4GA	1.4GA
J	1/F-9/F	.99EI	.99GA	.99GA	.99EI	1.1GA	1.1GA
K	1/F-9/F	1.6EI	1.6GA	1.6GA	1.6EI	1.1GA	1.1GA
L	1/F-9/F	.96EI	.96GA	.96GA	.96EI	32EI	32EI
M	1/F-9/F	.99EI	.99GA	.99GA	.99EI	1.1GA	1.1GA

$EI = 8.8 \times 10^9\ N.m^2$

$GA = 0.303 \times 10^9\ N$

TABLE 4.2 FREQUENCIES AND PERIODS OF VIBRATION OF BUILDING G, H AND I

Mode	Frequencies(rad/sec)			Periods(sec)		
	Building			Building		
	G	H	I	G	H	I
1	10.47	10.47	10.47	0.60	0.60	0.60
2	11.01	13.14	18.14	0.57	0.48	0.35
3	35.97	35.97	35.97	0.18	0.18	0.18
4	37.82	45.13	62.30	0.17	0.14	0.10
5	76.88	76.88	76.88	0.08	0.08	0.08
6	80.83	96.45	133.17	0.07	0.06	0.05

CHAPTER 5

CONCLUSIONS

The concept of eccentricity is extended to asymmetrical multistory buildings to study their torsional behaviour under static and dynamic lateral loads.

The definition of centers of rigidity for multistory buildings in this study is taken as "the set of points at floor levels when the resultant lateral loads act through them, no rotational displacement of the building results". The centers of twist for multistory buildings, on the other hand, are defined as "the set of points at floor levels which will not undergo any translational displacement when the building is subjected to applied torques only".

Based on the above definition for each center, mathematical expressions are established and presented. The following findings can be observed based on this study.

(a) The centers of rigidity and centers of twist are in general load distribution dependent, ie., depending on the load variation along the height of the building.

(b) They will be in general two different sets of points.

(c) The centers of rigidity can be interpreted as

the centers of resisting forces in the elements when the building is constrained to deform in a translational mode only. Therefore, the centers of rigidity can be interpreted as the "load centers" for multistory buildings. The rigidity centers will be, in general, different from the shear centers and centers of stiffness of the building.

(d) There is a special class of eccentric multistory buildings generally termed as buildings with proportional framing which will have centers of rigidity, centers of stiffness, shear centers and centers of twist all being the same set of points. Their locations will be load distribution independent, falling on a vertical line and can be determined on a per floor basis.

(e) The centers of rigidity are the set of points to which eccentricity should be measured from. Because of the definition used for rigidity centers, one can identify the lateral and torsional component of the applied loads using eccentricity measures.

(f) By using the centers of twist as the set of reference points to describe the movements of the floor diaphragms, it is possible to obtain, separately and in an efficient manner, the translational and torsional response of the structure.

The eccentricity concept and the "displacement compatible" load concept are employed in the study of the

behaviour of eccentric setback structures under lateral loads. This can be considered as a non-trival application of the eccentricity concept to evaluate force distribution in irregular structures. The eccentricity concept enables the separation of the lateral and torsional load components. The displacement compatible loads are introduced to the highrise wing of a setback building to offset the load effect above the setback level. This enables the remaining applied loads on the base (applied loads less the compatible loads) be distributed according to the relative stiffnesses of the resisting elements. The proposed method is a simple tool of analysis, but it also enables a better understanding of the load transfer mechanism involved in setback structures.

The eccentricity concept plays an important role also in the seismic design of buildings when employing building code procedures. In applying specifically the torsional provisions of the National Building Code of Canada 1985, a knowledge of the rigidity centers of the building is required to:

(a) determine whether the torsional provisions are applicable; and assuming the provisions are applicable, to

(b) determine the structural eccentricities, thus the design eccentricities and finally the design torque at

each story of the building.

For (a) above, the code requires that the following condition be met in order that the torsional provisions are applicable:

"Where the centroids of mass and centers of stiffness of the different floors do not lie approximately on vertical lines, a dynamic analysis shall be carried out to determine the torsional effects.....".

In the above clause, the term "centers of stiffness" is used in place of the term "centers of rigidity". This will have a misleading effect implying that the centers of rigidity can be determined on a per floor basis. To improve the interpretation of the code, formal definition of the centers of rigidity should be given by the code and the centers of rigidity should be the only term used consistently throughout the seismic provisions.

According to the code, the torsional provisions are also applicable to structures with centers of rigidity lying approximately on a vertical axis. However, even for those structures that deviate slightly from structures with rigidity centers falling on a vertical line, they showed considerable scattering of the rigidity centers. Examples of such buildings are (i) near proportional framing buildings (eg. Building B, Fig. 2.2) and (ii) wall-frame buildings with wall center almost coincides with the frame center (eg. Building M, Fig. 4.16). The rigidity centers

are in fact sensitive quantities. Once scattering occurs, the locus of the centers of rigidity will not resemble that of a vertical axis (Fig. 2.4b and Fig. 4.17). So practically it is difficult to identify those actual buildings that fall into the category with rigidity centers falling approximately on a vertical axis and to which the torsional provisions are applicable.

Difficulties arise also in the process of identifying the torsional critical element in design due to the following reasons:

(a) A scattering of the centers of rigidity on both sides of the mass centers will result in torque loadings not acting in the same direction at the floor levels. Thus some floor torques are counteracting floor torques at other levels. The net torsional effect is difficult to visualize.

(b) Being an edge element does not guarantee that the element is critical torsionally. The centers of twist can scatter on both sides of an edge element. Thus an edge element will not be an element located furthest away from the centers of twist at every floor.

(c) Due to the complex nature of wall-frame interactions, the torsional shears in a wall element may counteract the lateral shears resulting in lower design shears. In other words, torsion may have a beneficial effect on wall-frame structures.

Based on the above arguments, it is suggested that clause (4.1.9.24) in NBCC 1985 be rephrased as:
"Where the centroids of mass and centers of rigidity of the different floors do not lie on vertical lines, a dynamic analysis shall be carried out to determine the torsional effects....".

With such strict limitations, the applicability of the torsional provisions will become rather restrictive. However, this should be interpreted as a realization that because of the simplicity of the code procedures, it will not be able to cover a wide class of eccentric buildings in general.

Problems as expressed by (a) and (b) are overcome when requiring the centers of rigidity (thus the centers of twist) to fall on a vertical line. Problem expressed by (c) can be overcome by requiring the torsional shears which counteract the lateral shears (termed as negative torsional shears) be neglected. Such requirement had already been incorporated in some seismic codes [1,31,38].

Base on a strict interpretation on the locations of the rigidity centers, then buildings with proportional framing and uniform wall-frame buildings with coincident wall and frame centers are two classes of structures to which the torsional provisions of NBCC 1985 are applicable.

The code procedures are adequate in encompassing the torsional effect for these two classes of buildngs. For other classes of irregular structures which showed a scattering of rigidity centers, dynamic analysis is the most reliable method for distributing the torsional effect at the present time.

APPENDIX A

CENTERS OF RIGIDITY FOR NON-ORTHOGONAL FRAMING BUILDINGS

Consider a planar element i arranged with its plane of stiffness inclined at an angle with the x reference axis (Fig. A.1). Defining the local stiffness matrix of the given element along the axis of stiffness Y_i as $[\bar{k}]_i$. The contribution of this element to each of the stiffness submatrices appearing in the equilibrium equation

$$\begin{bmatrix} [K_{xx}] & [K_{xy}] & [K_{x\theta}] \\ [K_{yx}] & [K_{yy}] & [K_{y\theta}] \\ [K_{\theta x}] & [K_{\theta y}] & [K_{\theta\theta}] \end{bmatrix} \begin{Bmatrix} \{\delta_x\} \\ \{\delta_y\} \\ \{\delta_\theta\} \end{Bmatrix} = \begin{Bmatrix} \{P_x\} \\ \{P_y\} \\ \{P_\theta\} \end{Bmatrix} \quad \text{(A1)}$$

will be:

$$[K_{xx}]_i = [\bar{k}]_i \sin^2\theta_i \quad \text{(A2)}$$

$$[K_{xy}]_i = [K_{yx}]_i = -[\bar{k}]_i \sin\theta_i \cos\theta_i \quad \text{(A3)}$$

$$[K_{x\theta}]_i = [K_{\theta x}]_i = [K_{xy}]_i x_i - [K_{xx}]_i y_i \quad \text{(A4)}$$

$$[K_{yy}]_i = [\bar{k}]_i \cos^2\theta_i \quad \text{(A5)}$$

$$[K_{y\theta}]_i = [K_{\theta y}]_i = [K_{yy}]_i x_i - [K_{yx}]_i y_i \quad \text{(A6)}$$

$$[K_{\theta\theta}]_i = [\bar{k}]_i (x_i \cos\theta_i + y_i \sin\theta_i)^2 \quad \text{(A7)}$$

in which x_i, y_i and θ_i are defined in Fig. A1. Summing the submatrices as expressed in eqns. (A2) through (A7) for all elements will generate the global stiffness matrix of the structure.

Let the x and y coordinates of the centers of

rigidity be represented by $\{X_L\}$ and $\{Y_L\}$ respectively. When the lateral loads $\{P_x\}$ and $\{P_y\}$ act at the rigidity centers, the structure will undergo no rotational deformation, or $\{\delta_\theta\}$ will be a null vector. Eqn.(A1) can then be expressed as

$$[K_{xx}]\{\delta_x\} + [K_{xy}]\{\delta_y\} = \{P_x\} \quad (A8)$$

$$[K_{yx}]\{\delta_x\} + [K_{yy}]\{\delta_y\} = \{P_y\} \quad (A9)$$

$$[K_{\theta x}]\{\delta_x\} + [K_{\theta y}]\{\delta_y\} = -[P_x]\{Y_L\} + [P_y]\{X_L\} \quad (A10)$$

$[P_x]$ and $[P_y]$ are diagonal matrices with diagonal elements equal to those in vector $\{P_x\}$ and $\{P_y\}$ respectively.

Solving the coupled eqns.(A8) and (A9) gives

$$\{\delta_x\} = [K_1]^{-1}\{P_x\} + [K_2]^{-1}\{P_y\} \quad (A11)$$

$$\{\delta_y\} = [K_4]^{-1}\{P_x\} + [K_3]^{-1}\{P_y\} \quad (A12)$$

in which

$$[K_1]^{-1} = ([K_{xx}]-[K_{xy}][K_{yy}]^{-1}[K_{yx}])^{-1} \quad (A13)$$

$$[K_2]^{-1} = -[K_1]^{-1}[K_{xy}][K_{yy}]^{-1} \quad (A14)$$

$$[K_3]^{-1} = ([K_{yy}]-[K_{yx}][K_{xx}]^{-1}[K_{xy}])^{-1} \quad (A15)$$

$$[K_4]^{-1} = -[K_3]^{-1}[K_{yx}][K_{xx}]^{-1} \quad (A16)$$

Substituting eqns.(A11) and (A12) into eqn.(A10) and making use of the fact that $\{P_x\}$ and $\{P_y\}$ are independent load vectors results in

$$\{X_L\} = [P_y]^{-1}([K_{\theta x}][K_2]^{-1}+[K_{\theta y}][K_3]^{-1})\{P_y\} \quad (A17)$$

$$\{Y_L\} = -[P_x]^{-1}([K_{\theta x}][K_1]^{-1}+[K_{\theta y}][K_4]^{-1})\{P_x\} \quad (A18)$$

Eqns.(A17) and (A18) define the locations of the load centers, and hence the centers of rigidity of any

irregular eccentric multistory building.

Notations

i = element identifier

$[K_{jk}]$ = $\Sigma[K_{jk}]_i$ $(j=x, y, \theta; k=x, y, \theta)$

$[\bar{k}]_i$ = stiffness matrix of planar resisting element

$\{P_x\}, \{P_y\}$ = lateral load vector in the x and y direction, respectively

$\{P_\theta\}$ = torsional load vector

$\{X_L\}, \{Y_L\}$ = x and y coordinate position vector of the load centers

x_i = x coordinate position of the shear center of element with respect to global reference system

y_i = y coordinate position of the shear center of element with respect to global reference system

$\{\delta_x\}, \{\delta_y\}$ = displacement vector of structure in the x and y direction, respectively

$\{\delta_\theta\}$ = rotation displacement vector of structure

θ_i = angle of orientation of element (see Fig. A1)

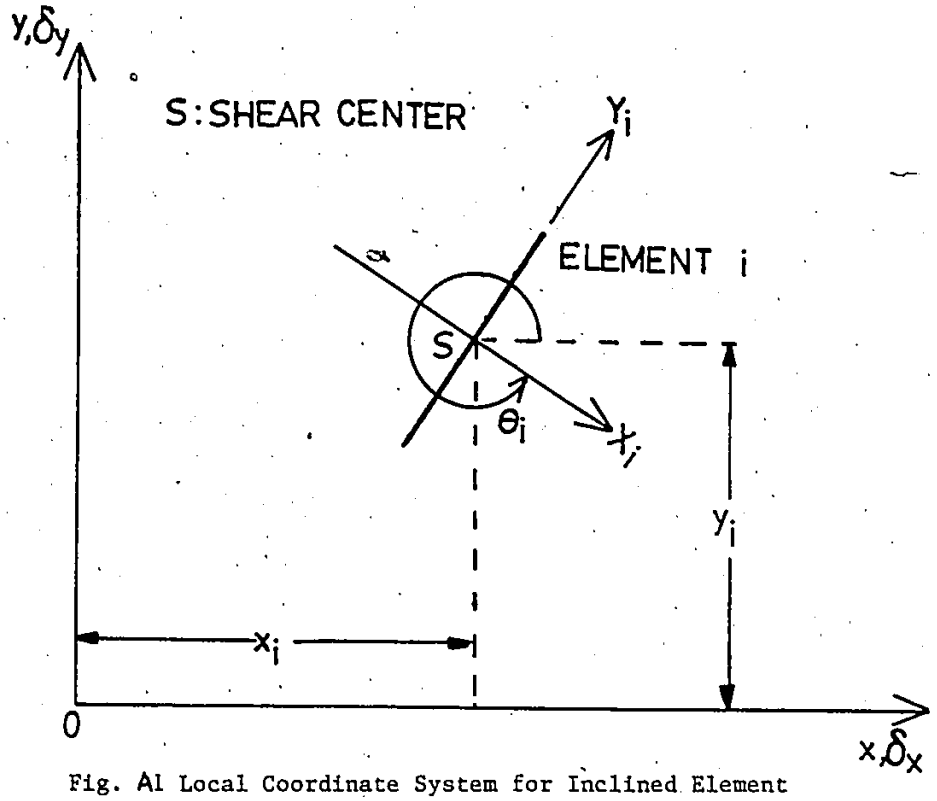

Fig. A1 Local Coordinate System for Inclined Element

REFERENCES

1. Applied Technology Council. Tentative Provisions for the Development of Seismic Regulations for Buildings, ATC3-06. Washington, D.C.: National Bureau of Standards, 1978.

2. Arnolds, C. and Reitherman, R. Building Configuration and Seismic Design. New York: Wiley, 1982.

3. Associate Committee on the National Building Code. National Building Code of Canada 1985. Ottawa, Ontario: National Research Council of Canada, 1985.

4. _____. The Supplement to the National Building Code of Canada 1985. Ottawa, Ontario: National Research Council of Canada, 1985.

5. Basu, A.K., Nagpal, A.K. and Kaul, S. "Charts for Seismic Design of Frame-Wall Systems", Journal of Structural Engineering, ASCE, Vol. 110, No. 1, (January 1984), 31-46.

6. Bauten in deutschen Erdbebengebieten Entwurf DIN 4149. Deutsche Industrie - Normen, 1976.

7. Bustamante, J.I. and Rosenblueth, E. "Building Code Provisions on Torsional Buildings", Proceedings, Second World Conference on Earthquake Engineering, Tokyo, Japan, Vol. 2, (1960), 879-894.

8. Cheung, V. W.-T. and Tso, W. K. "Eccentricity in Irregular Multistory Buildings". Accepted for publication in Canadian Journal of Civil Engineering, Vol.13, (1986).

9. _____. "Eccentricity in Irregular Multistory Buildings", Proceedings, CSCE 1985 Annual Conference, Saskatoon, Saskatchewan, Canada. (May 1985), 283-299.

10. _____. "Lateral Load Analysis for Buildings with Setback". Submitted to Journal of Structural Engineering, ASCE.

11. Cheung, V. W.-T., Tso, W. K. and Rutenberg, A. "Lateral Load Distribution in Structures with Setback", Proceedings, Third International Conference on Tall Buildings, Hong Kong and Guangzhou, (Dec. 1984), 23-27.

12. Code of Practice for General Structural Design and Design Loadings for Buildings NZS 4203:1976, Part 3. Wellington, New Zealand : Standards Association of New Zealand, 1976.

13. Gluck, J., Reinhorn, A. and Rutenberg, A. "Dynamic Torsional Coupling in Tall Building Structures", Proceedings, Institution of Civil Engineers, Part 2, Vol. 67, (1979), 411-424.

14. Heidebrecht, A. C. and Tso, W. K. "Seismic Loading Provision Changes in National Building Code of Canada 1985", Canadian Journal of Civil Engineering, Vol. 12, (1985), 653-660.

15. Heidebrecht, A. C. and Stafford Smith, B. "Approximate Analysis of Tall Wall-Frame Structures", Journal of the Structural Division, ASCE, Vol. 99, No. ST2, (February 1973), 199-221.

16. Humar, J. L. "Design for Seismic Torsional Forces", Canadian Journal of Civil Engineering, Vol. 11, (1984), 150-163.

17. Kan, C. L., and Chopra, A. K. "Effects of Torsional Coupling on Earthquake Forces in Buildings", Journal of the Structural Division, ASCE, Vol. 103, No. ST4, (April 1977), 805-819.

18. _____. "Elastic Earthquake Analysis of a Class of Torsionally Coupled Buildings", Journal of the Structural Division, ASCE, Vol. 103, No. ST4, (April 1977), 821-838.

19. Lin, T. Y. "Lateral Force Distribution in a Concrete Building Story", Journal of the American Concrete Institute, Vol. 12, (1951), 281-296.

20. Mendelson, E. and Baruch, M. "Earthquake Response of Non-Symmetric Multistory Structures", The Structural Engineers, Vol. 51, No. 2 (February 1973), 61-70.

21. Ministry of Reconstruction and Resettlement. Specifications for Structures to be Built in Diaster Areas. Ankara: Earthquake Research Institute of the Turkish Government, 1975.

22. Muller, F. P. and Keintzel, E. "Approximate Analysis of Torsional Effects in the New Seismic Code DIN 4149"; Proceedings, Sixth European Conference on Earthquake Engineering, Dubrovnik, Yugoslavia, Vol. II, (1978), 101-108.

23. Nayfeh, A. H. Perturbation Methods. New York : Wiley, 1973.

24. Newmark, N. M. "Torsion in Symmetrical Buildings", Proceedings, Fourth World Conference on Earthquake Engineering, Santiago, Chile, Vol. 3, (1969), 19-32.

25. Pekau, O. A. and Gordon, H. A. "Coupling of Torsional - Translational Response of Buildings during Earthquake", Canadian Journal of Civil Engineering, Vol. 7, (1980), 282-293.

26. Poole, R. A. "Analysis for Torsion Employing Provisions of NZRS 4203 : 1974", Bulletin of the New Zealand National Society for Earthquake Engineering, Vol. 10, No. 4, (Dec. 1977), 219-223.

27. Rosenblueth, E. "Seismic Design Requirements in the 1976 Mexican Code", International Journal of Earthquake Engineering and Structural Dynamics, Vol. 7, (1979), 49-61.

28. Rutenberg, A. and Heidebrecht, A. C. "Approximate Analysis of Asymmetric Wall-Frame Structures", Building Science, Vol. 10, (1975), 27-35.

29. Rutenberg, A., Hsu, T. I. and Tso, W. K. "Response Spectrum Techniques for Asymmetric Buildings", International Journal of Earthquake Engineering and Structural Dynamics, Vol. 6, (1978), 427-435.

30. Rutenberg, A., Tso, W. K. and Heidebrecht, A. C. "Dynamic Properties of Asymmetric Wall-Frame Structures", International Journal of Earthquake Engineering and Structural Dynamics, Vol. 5, (1977), 41-51.

31. Seismology Committee, SEOAC. Recommended Lateral Force Requirements and Commentary. San Francisco, California : Structural Engineers Association of California, 1975.

32. Shepherd, R. and Donald, R. A. H. "Seismic Response of Torsionally Unbalanced Buildings", Journal of Sound and Vibration, Vol. 6, No. 1, (1967), 20-37.

33. Tso, W. K. "A Proposal to Improve the Static Torsional Provisions for the National Building Code of Canada", Canadian Journal of Civil Engineering, Vol. 10, (1983), 561-565.

34. _____. "Torsions in Multistory Buildings", Proceedings, Third International Conference on Tall Buildings, Hong Kong and Guangzhou, (Dec. 1984), 1-7.

35. Tso, W. K. and Cheung, V. W.-T. "Decoupling of Equations of Equilibrium in Lateral Load Analysis of Multistory Buildings". Accepted for publication in Computers and Structures, Vol. 24, (1986).

36. Tso, W. K. and Dempsey, K. M. "Seismic Torsional Provisions for Dynamic Eccentricity", International Journal of Earthquake Engineering and Structural Dynamics, Vol. 8, (1980), 275-289.

37. Tso, W. K. and Meng, V. "Torsional Provisions in Building Codes", Canadian Journal of Civil Engineering, Vol. 9, (1982), 38-46.

38. Uniform Building Code 1979. International Conference of Building Officials, Whittier, California, 1979.

39. Wilbur, J. B. "Distribution of Wind Loads to the Bents of a Building", Journal of the Boston Society of Civil Engineers, (October , 1935), 253-258.